Auckland University of Technology

Smart Grid Distribution Transformers: Empirical Design and Dynamic Load Management

Michael Bunn

A thesis submitted to Auckland University of Technology
in partial fulfilment of the requirements for the degree of
Doctor of Philosophy

June 2022

School of Engineering, Computer and Mathematical Sciences
Faculty of Design and Creative Technologies
Auckland University of Technology
New Zealand

Attestation of Authorship

I hereby declare that this submission is my own work and that, to the best of my knowledge and belief, it contains no material previously published or written by another person nor material which to a substantial extent has been accepted for the qualification of any other degree or diploma of a university or other institution of higher learning.

Signature of candidate

Abstract

The increasing penetration of electric vehicles and distributed generation into distribution networks gives rise to higher, more volatile and bi-directional energy flows through distribution transformers. Consequently, improved distribution transformer design and monitoring approaches are required to minimise future capital expenditure and maintenance costs over the distribution transformer's lifetime. Traditionally the determination of the health and life of a distribution transformer has relied on modelled rather than measured data, leading to inaccurate assessment of transformer health and non-optimised transformer utilisation. There are many risks associated with overloading transformers, such as increased internal heating to potentially unsafe levels. However, even without reaching unsafe levels, the potential for increased maintenance and reduced distribution transformer lifetime are justifiable causes for concern for utilities operating around a transformer's nameplate rating. The consequence of this approach is that often distribution transformers are used at very low utilisation levels. However, transformers operate more efficiently at utilisation levels at or above 50 %.

This research presents algorithms that support the operation of distribution transformers at higher utilisation levels considering user expectations around required lifetime, manufacturer specifications and limits imposed by the Institute of Electrical and Electronics Engineers (IEEE) and the International Electrotechnical Commission (IEC) standards. Furthermore, it describes possible integration with a close monitoring system for distribution transformers, utilising fibre Bragg Grating (FBG) sensors. Such an

approach can avoid wholesale replacement of existing distribution transformers and limit resource waste over the lifetime of the transformer.

Contents

List of Tables

List of Algorithms

List of Figures

Publications

M. Bunn, B.-C. Seet, C. Baguley and B. Das, "A Smart Supervisory System for Distribution Transformers", *2018 Australasian Universities Power Engineering Conference (AUPEC)*, Auckland, New Zealand, 2018, pp. 1-6, doi: 10.1109/AUPEC.2018.8757994.

M. Bunn, B. P. Das, B.-C. Seet and C. Baguley, "Empirical Design Method for Distribution Transformer Utilization Optimization", *IEEE Transactions on Power Delivery*, vol. 34, no. 4, pp. 1803-1813, Aug. 2019, doi: 10.1109/TPWRD.2019.2926328.

M. Bunn, B.-C. Seet, C. Baguley and D. Martin, "A Thermally-based Dynamic Approach to the Load Management of Distribution Transformers", *IEEE Transactions on Power Delivery*, 2022, doi: 10.1109/TPWRD.2022.3171204.

Acknowledgements

I would like to express my gratitude to my primary supervisor Associate Professor Boon-Chong Seet, who believed in my potential and has guided me so aptly throughout this academic journey. His insight, suggestions and availability have all been contributors in assisting me to this point. I would also like to thank him for trusting that I was still making headway even though there were moments where it felt like the process may have stalled.
I would also like to acknowledge my secondary supervisor Doctor Craig Baguley whose industrial knowledge, enthusiastic support of my research direction and critique of my papers have all been significant factors in seeing this to fruition.
Thanks also to Doctor Bhaba Das, whose previous work with the development of ETEL's Smart Transformer laid the foundation for my current research. His initial support, willingness to let me build on his previous work and belief in my ability created the platform that led to this point.
Thanks to Doctor Daniel Martin whose insights contributed so much to my latest paper and whose insights guided me through the final hurdles to completion.
Thanks also to ETEL who created the project and have backed my research all the way through, and thanks to Callaghan Innovation for sponsoring my study.
Last but not least, I would like to thank and acknowledge my family. Firstly to my parents Richard and Myrle, who made this whole process possible and whose unwavering support has been so invaluable. Finally I would like to thank my sons, Joel and Brandon, who have been so understanding and supportive of their Dad's academic endeavours.

Intellectual Property Rights

All Intellectual Property owned by either party prior to the commencement of this thesis project shall remain the property of that party. All Intellectual Property arising out of the thesis project, the Project IP shall be assigned to the Company. The University/Student Fellow shall have a non-exclusive, non-assignable, royalty free license to the Thesis Project IP for research and education purposes only. The licence does not include any right to sub-licence or to use the Thesis Project IP for any purposes that may result in commercial gain without having first obtained the prior written consent of the Company. The Company will not unreasonably withhold consent to extend the licence to use the Thesis Project IP for commercialisation purposes provided any such commercialisation is not in a market which the Company considers to be a competitive market. The copyright in all scholarly publications and student thesis related to the Project shall rest, in the first instance with the authors.

Confidential Material

Confidentiality The University/Student Fellow has the right to publish research information of general scientific and academic interest in scholarly journals and conference proceedings. The University/Student Fellow will provide the Company with a copy of any proposed publication related to the research at least 30 days prior to submission for publication and a written response must be received within a further 14 days. Should the Company consider that the publication contains information of a commercially sensitive nature it may request that this information is amended or may request the University/Student to delay publication for a maximum of 12 months.

Abbreviations

$\mathbf{\Theta_A}$	Ambient Temperature (°C).
$\mathbf{\Theta_O}$	Top-Oil Temperature (°C).
$\mathbf{\Theta_{HS}}$	Winding Hot-Spot Temperature (°C).
ϕ	Phase.
DP	Degree of Polymerisation.
DT	Distribution Transformer.
EDM	Empirical Design Method.
EV	Electric Vehicle.
LV	Low Voltage.
ONAN	Oil Natural, Air Natural.
OOS	Out Of Scope.
PV	Photovoltaic.

Chapter 1

Introduction

Four distinct epochs have defined the journey of discovery in the modern age of electricity. The first was the era of electrostatic charge, which lasted until the advent of chemically-derived direct current in 1800. The 1820 discovery of the link between electricity and magnetism ensured that this second epoch, utilising continuously flowing direct current derived solely from chemical sources, was the shortest. The third epoch arrived when the generation of direct current from electromagnetic sources was made possible. The fourth epoch, that of alternating current generation and transmission, began with the first practical demonstration of an alternating current distribution system incorporating a transformer in 1885. However, arguably, electrical generation and distribution have entered a new and fifth epoch, the "Smart Grid". It is into this paradigm that this body of research finds its relevance.

1.1 Motivation and Scope

Since the first practical demonstration of transformer-based electrical distribution in Hungary in 1885 [1, 2], the paradigm underpinning distribution transformer use has remained essentially unchanged: Determine the maximum load required and install

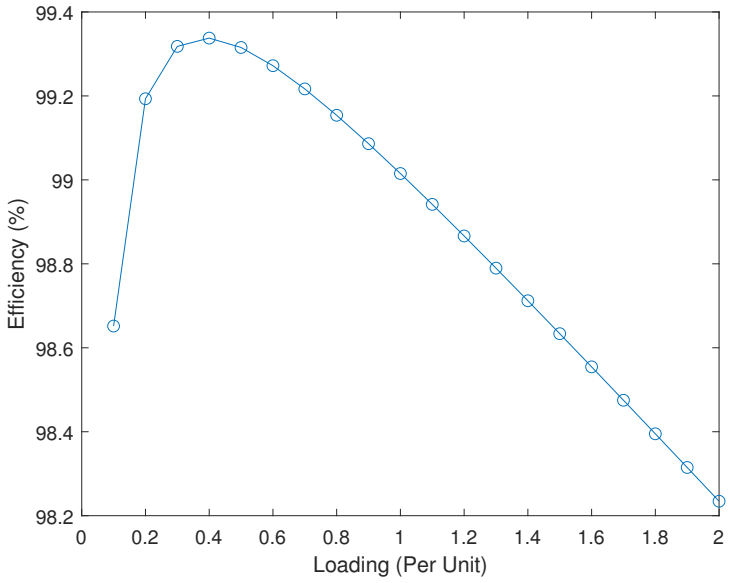

Figure 1.1: Example Efficiency Curve for a 750 kVA 3-Phase Distribution Transformer

a transformer with a nameplate rating typically an order of magnitude greater. The natural effect of such an approach is that transformer utilisation levels are low, and low utilisation leads to lower efficiency (see Fig. 1.1).

The development of transformers has never existed in a vacuum independent of their function supporting the delivery and distribution of electricity. They have always contributed to enhancing the network.

Historically, the distribution system has been designed to support a known load and the rating of transformers has been determined accordingly. However, loads are increasing and becoming more dynamic in nature. In order to address this challenge utilising existing methodologies will result in additional expense, outages and potential over-building. Existing research has predominantly focused on adjusting the load to fit the size of the transformer. This thesis, however, takes a different approach by examining how capable transformers are to accommodate the increasingly dynamic loading expected in the era of the Smart Grid.

Initially conceived in 2001, the rationale behind the Smart Grid is to address the

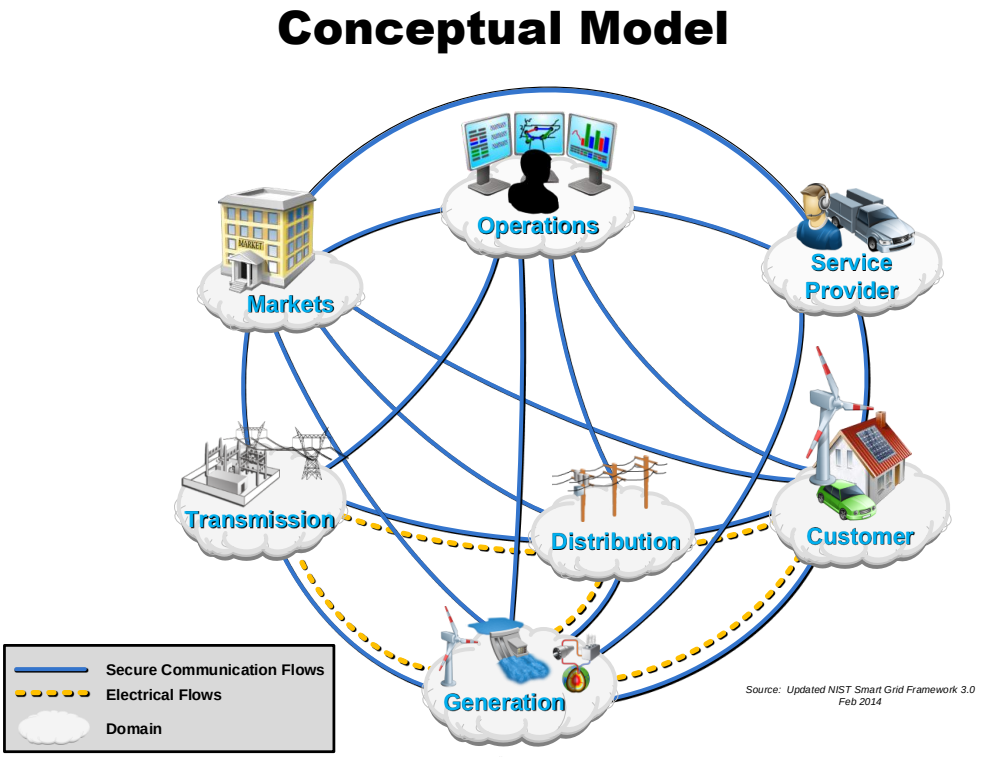

Figure 1.2: Smart Grid Concept Release 3.0 from the National Institute of Standards and Technology (NIST) U.S. Department of Commerce

new paradigms emerging within electrical distribution networks, such as distributed generation sources producing two-way power flow, the intermingling of direct current with alternating current supply and increased network volatility due to high energy loads, such as electric vehicle charging [3]. As of 2021, a search for "Smart Grid" in the International Electrotechnical Commission (IEC) Standards webstore results in 113 active standards. The Smart Grid interoperability model describes a "system of systems" approach to engineering, creating a bridge between conceptual reference models and applications [4]. This approach provides industry with the technical information but not the actual tools to implement Smart Grid. This leaves the impetus for innovation and development within industry.

In 2016, ETEL Limited began a 10-year development programme to develop a "Smart Transformer" for the Smart Grid [5]. A significant motivator for this project

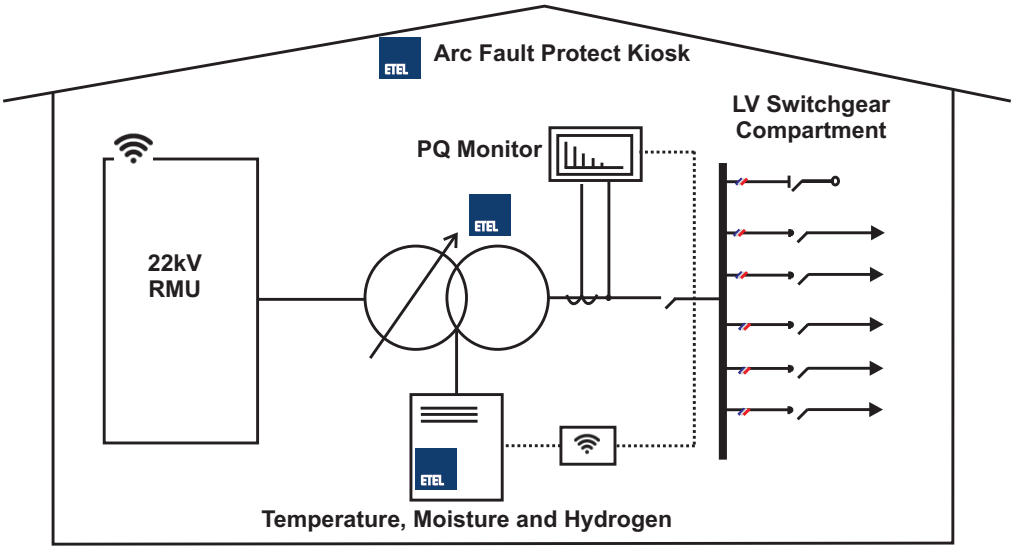

Figure 1.3: 2016 ETEL Smart Transformer Kiosk Concept Diagram [6]

was to support electric vehicle (EV) charging [6]. Although still in development, the features intended for this transformer were:

Insulation Bio-ester oil and thermally upgraded Kraft paper

Housing Arc fault protected transformer kiosk

Control Automated ring main unit (RMU) with remote communication

Thermal Monitor ETEL's patented fibre optic hot spot sensor

Moisture Monitor ETEL's patented fibre optic moisture sensor

Condition Monitor ETEL's patented fibre optic hydrogen sensor

Power Quality Commercially-available power quality meter – line currents and voltages

Voltage Regulation Commercially-available on-load tap changer (OLTC)

In 2017, ETEL released a commercial version of the Smart Transformer with the following features [7]:

Insulation Mineral oil and thermally upgraded Kraft paper

Housing Stainless Steel Arc fault protected transformer kiosk

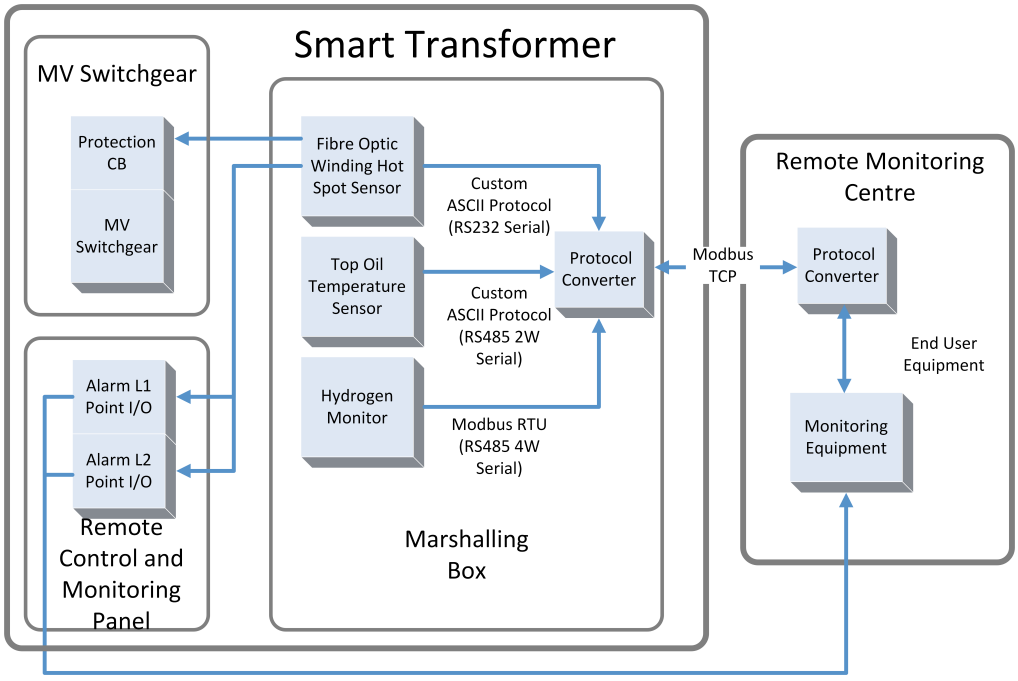

Figure 1.4: 2017 Commercial ETEL Smart Transformer Kiosk Concept Diagram [7]

Protection RMU with circuit breaker triggered by ETEL hot spot sensor

Hot Spot Monitor ETEL's patented fibre optic hot spot sensor

Top Oil Monitor Commercially-available temperature probe

Condition Monitor Commercially-available hydrogen sensor

Sensor Integration and Remote Monitor Commercially-available protocol converter

However, as this commercial release did not incorporate support for EV charging or network control, it had still not achieved ETEL's vision for a Smart Transformer. This research was commissioned in 2018 to fulfil this vision. However, in early 2019, personnel changes within ETEL resulted in a shift in focus of the research from realising the original Smart Transformer vision to the development of algorithms to support future Smart Transformer concepts. Thus, the research scope was to examine how the thermal inertia, inherent in liquid-filled transformers with external radiant cooling, could release additional capacity to support the larger and more dynamic loads associated with EV charging and develop algorithms capable of achieving this aim. In addition,

the algorithms should ensure that the loading levels comply with the manufacturer's specifications, IEC and IEEE standards and customer expectations around usable transformer lifetime. For this research, all the loads investigated are $3-\phi$ and balanced. The transformers are of the type: oil natural air natural (ONAN), which means they use the natural convection of the insulating oil and external radiator fins for cooling. As ONAN-type transformers do not use external pumps or fans, their inclusion is outside the scope of this research.

1.2 Contributions

There are two main contributions from this thesis, which are listed as follows:

The Empirical Design Method This thesis introduces a new "designing for maximum utilisation" approach to transformer design that allows new transformers retirement age and expected end-of-life to coincide. Within this approach is a method to determine the maximum loading for transformers already in service, utilising empirical thermal characteristics. This runs counter to existing approaches based on designing for peak loads, which often results in the over-specification of distribution transformers. A secondary contribution is a comprehensive methodology employed to ensure no aspect of utilisation maximisation compromises standards throughout a distribution transformer's lifetime, thereby realising the proposed approach practically.

Thermally-Based Dynamic Load Management Approach The thermally-based dynamic load management approach is an algorithmic assessment process for determining in real-time the maximum loading a transformer can accommodate throughout any given day. Because it combines knowledge of existing base loads that it must accommodate, it is particularly suited for scenarios where loading is more uncertain, such as supplying areas with high-penetration of electric vehicles.

In addition, placing each loading assessment into the context of a transformer's daily load cycle ensures that requirements, such as minimum lifetime, maximum pressure, voltage regulation and thermal limits, are maintained.

1.2.1 Publications

i. M. Bunn, B. Seet, C. Baguley and B. Das, "A Smart Supervisory System for Distribution Transformers", *2018 Australasian Universities Power Engineering Conference (AUPEC)*, Auckland, New Zealand, 2018, pp. 1-6, doi: 10.1109/AUPEC.2018.8757994.

ii. M. Bunn, B. P. Das, B. Seet and C. Baguley, "Empirical Design Method for Distribution Transformer Utilization Optimization", *IEEE Transactions on Power Delivery*, vol. 34, no. 4, pp. 1803-1813, Aug. 2019, doi: 10.1109/TPWRD.2019.2926328.

iii. M. Bunn, B. Seet and C. Baguley, D. Martin, "A Thermally-based Approach to the Dynamic Load Management of Distribution Transformers", *IEEE Transactions on Power Delivery*, 2022, doi: 10.1109/TPWRD.2022.3171204.

1.3 Thesis Structure

The thesis is structured as follows:

Chapter 2 presents background information of topics related to, but not directly addressed in the thesis. Topics include the historical significance of the distribution transformer to the realisation of the modern electrical distribution system, why transformer utilisation levels have traditionally been low, why lifetime is vital to realising increased utilisation and addresses some limitations with existing load management strategies. Also covered is an overview of the Smart Grid concept and its enabling

communication protocols and an introductory explanation of the fibre optic technology used in this research.

Chapter 3 is the literature review, which includes a description of the systematic process for collecting the body of research to examine. The topics include, the impact of EV charging on distribution networks, and particularly the impact on distribution transformers. How real-time monitoring has been used and the rationale for its use, such as perceived benefits. Dynamic thermal modelling is a large topic and is divided into related sub-sections, which examine the challenges and limitations of modelling the transformer's thermal behaviour, methods that have been adopted to improve the accuracy of dynamic thermal models, such as using empirical model parameters, computational numerical methods, artificial intelligence, equation-fitting and modelling methodologies. In the next section, dynamic rating is defined and descriptions of two implementation concepts are presented. The use simulations with modelled thermal characteristics, which can be either empirically-based, or probabilistic in nature. The second is also simulation-based, this time using measured thermal characteristics. Algorithmic approaches to condition monitoring are examined next, with the final topic examining design optimisation strategies. These strategies have been grouped into dimensioning the load to fit the transformer, minimising losses, using multiple designs, optimising transformer geometry, thermal behaviour, minimising material cost or total cost of ownership or a multi-objective optimisation strategy. Identified gaps are presented in the form of research questions that are addressed in this thesis.

Chapter 4 introduces the empirical design method which takes a novel "designing for maximum utilisation" approach to distribution transformer design. This algorithm provides a method for the customer to know what the transformer lifetime will be based on predicted loading increase.

Chapter 5 introduces a novel method for determining the maximum dynamic loading a transformer can accommodate each day that it is in use, the thermally-based

approach to dynamic load management. This is quite a separate concept from the design methodology of the empirical design which assumes that a load profile is known and predictable throughout the day and does not require active engagement.

Chapter 6 describes future work and additional capabilities possible for the empirical design method and thermally-based approach to dynamic load management of distribution transformers.

Chapter 7 provides concluding remarks, and summarises the contributions to knowledge and future work generated from the research presented in this thesis.

Chapter 2

Background

This section provides background information intended to contextualise and offer a broad overview of the technologies relevant to this research, including distribution transformers, smart grid, and fibre optic technology.

2.1 Distribution Transformers

In this research, the term “distribution transformers” is used to refer to transformers in a distribution network. However, according to IEC Standard 60076-7:2018, technically the description for the transformers investigated is “medium power transformers” [8], although the current standard in use in Australia and New Zealand, AS/NZS 60076.7:2013, still refers to them as “distribution transformers” [9]. Although this research pertains to transformers primarily used in Australasia, given that the research is forward-looking and the next AS/NZS standard is likely to be aligned to the current IEC descriptions, the IEC values have been adopted. The most significant being the reduction in short-term emergency overload from 2 p.u. to 1.8 p.u.

To better understand the background rationale for this research, rather than explaining “what” a distribution transformer is, the remainder of this section will explore the

"why" behind their existence.

2.1.1 History

The distribution transformer, and transformers in general, exist in somewhat of a paradox. They are simultaneously the most expensive individual components in an electrical distribution network and the reason the modern electrical system is economically viable. This is even more remarkable when tracing through the three epochs that defined the journey of discovery leading to the birth of the transformer. In the first epoch, the age of "electrostatic charge", there was no concept of constant current. Neither was it possible to generate alternating current in the second epoch, the era of "Galvanic current", and there was outright hostility towards it in the third epoch, the era of "electromagnetically generated direct current". A brief synopsis of this journey is discussed in the rest of this section.

The "Electrostatic Charge" Era

The age of "electrostatic charge" arguably began in 1600 with the publication of William Gilbert's "De Magnete" that had a chapter on his findings of materials capable of becoming electrostatically charged. Not only did his work and methods elicit the curiosity of future experimenters, but it also provided them with a template for how to conduct such experimentation [10]. However, the first advance in a practical sense occurred around sixty years later when Otto von Guericke invented the first electrical machine, an electrostatic charge generator [11], a derivation of this device generated the charge that resulted in the accidental discovery of the Leyden jar. As the first practical method for storage and portability of an electrical charge [12], the Leyden jar itself further expanded the scope of possibilities for electrical experimentation. For example, a Leyden jar enabled Benjamin Franklin's famous kite experiment to verify that the

"electric fire" of lightning and an electric spark were one in the same. His prolific experimentation with the Leyden jar also led Franklin to introduce the terms "positive" and "negative" as descriptors of an electrical charge [13]. Charles Augustin Coulomb also used Leyden jars to charge the spheres in his experimentation into the force two charges exert upon each other that he discovered to be inversely proportional to the square of the distance between them [14].

While von Guericke's machine was one of the main drivers for experimentation in the electrostatic era, it was also indirectly responsible for the end of the era and ushering in the new epoch, the era of "Galvanic current". Luigi Galvani's experiments into "animal electricity" began when a spark from a nearby Guericke machine operated by one of his assistants resulted in a twitch in the legs of a dissected frog he was examining. After conducting many experiments related to the phenomenon, Galvani published his findings. In particular, he described the metals used when eliciting twitches when the machine was not operating. Alessandro Volta, initially persuaded by Galvani's findings, began to question the origin of the electricity causing the reaction, deciding instead they were not producing the electricity, but instead sensitive detectors [15]. This line of thinking led him to wonder if the electrical phenomenon was due to a reaction between the dissimilar metals, resulting in the invention of the Voltaic pile announced in 1800.

The "Galvanic Current" Era

Volta had ushered in a new epoch, that of chemically generated direct current, or "Galvanic current" as it was known at the time. Already associated with the Royal Society in London, Volta did not hesitate in reporting his findings, sending them as two separate letters which were printed in the *Transactions of the Royal Society* later that year.

Within a year of Volta's discovery, electroplating became the first practical use of electricity [1, 16]. By the end of the 1840s, galvanic batteries had improved to the point

that powering electric arc lights was finally practical. Arc lights themselves had been practical since 1812 when Sir Humphrey Davy first presented them, having experienced a blinding arc from a high energy Voltaic Pile he and William H. Pepys had made in 1802 [17]. It is noteworthy that electroplating and arc lighting, two of the earliest applications and discoveries in direct current experimentation, also played a significant role in influencing the development of the alternating current distribution system [1]. However, no such system was feasible until Hans Christian Ørsted established the link between electricity and magnetism in 1820 [18]. However, although Ørsted's discovery did allow for alternating current to be generated, the third epoch was the era of electromagnetically generated direct current.

The "Electromagnetically Generated Direct Current" Era

Having noted the way magnetic compasses were affected in a thunderstorm, Ørsted surmised that electricity and magnetism were somehow related. However, his first experiment appeared to belie this assertion, where pointing a compass toward a conductor supplied by a voltaic pile yielded no observable effect. However, the thought to place the compass parallel with the conductor, resulted in the needle deflecting. [19] After further experimentation to validate that the flow of current was the cause, he published his findings in Latin [18]. Francois J.D. Arago, who was in Denmark at that time, presented Ørsted's findings to the Acadèmie des Sciences in Paris. Having heard Arago's presentation, André-Marie Ampère began experimentation in September of the same year [18]. His experimentation not only validated Ørsted's discovery but, as a mathematician, Ampère was able to describe his experiments in mathematical form [20]. Along with Ampère, another significant figure in this era was the protégé of Sir Humphrey Davy, whose pioneering experimentation did so much to advance applications powered by the electrical pile conceived by Volta. However, it was Hans Christian Ørsted's 1820 discovery that provided Sir Michael Faraday with his own

pioneering experimental path to follow.

Although Faraday's focus was electromagnetism, like Davy, he used a battery to power his induction experiments, creating the changing field by making and breaking the contact. He did note that when the current collapsed, the induced voltage reversed, as when passing a magnet forwards and backwards through a coil [1]. However, not seeing any practical use, Faraday simply ignored the finding [2]. Similarly, Ampère suggested implementing a mechanical commutator to rectify an alternator's output, so it functioned as a DC generator rather than use the alternating current directly [1, 21].

Throughout this era Ampère's more mathematical approach appears to have complemented the more practical experimental approach taken by Faraday, who by his own admission "lacked strength in mathematics" [22]. However, one significant point of contention between the two was their explanations for the force surrounding a conductor. Ampère subscribing to a force at a distance Newtonian concept, analogous to gravity, and Faraday's concept of "lines of force". These seemingly disparate concepts were harmonised by Faraday's Royal Institute colleague, James Clerk Maxwell, whose 1873 "Treatise on Electricity and Magnetism" was the culmination of his equation development, a work in progress since his first publication of them in 1865's, "Dynamical Theory of the Electrodynamic Field". Maxwell's equations showed that neither Faraday nor Ampère was incorrect. They were instead describing different phenomena, Faraday the magnetic field and Ampère the electric field. This was thought likely to be the case, as elucidated by Maxwell in 1862, "*The theory that electric currents are linear, and magnetic forces rotatory phenomena, agrees so far with that of Ampère and Weber; and the hypothesis that the magnetic rotations exist wherever magnetic force extends, that the centrifugal force of these rotations accounts for magnetic attractions, and that the inertia of the vortices accounts for induced currents, is supported by the opinion of Professor W. Thomson. The magnetic state, however, is characterized by a well-marked rotatory phenomenon discovered by Faraday*" [23].

Sir William Thomson, the future Lord Kelvin, first introduced Maxwell to the study of magnetism while Maxwell was an undergrad at Trinity College in Cambridge [24]. Thomson also collaborated with Faraday in developing his "lines of force" concept [25]. He shared Faraday and Ampère's ambivalence towards alternating current, as evidenced by a comment in 1883 to the technical advisors of the Niagara Falls electrical generation development, "Trust you avoid gigantic mistake of adoption of alternating current." [26].

Alternating current appeared to be a nonsense proposition, Edison's invention of the electric bulb in 1879 [27] and subsequent electrification of Manhattan [28], appeared to have cemented direct current as the dominant method for electrical generation and distribution. This dominance was supported by DC motors, which created a market for power consumption throughout the day in addition to the lightbulbs at night. Edison's system also included metering of the electricity usage [28]. However, the high cost of copper conductors and high line losses meant that the customers receiving electric service had to be within a radius of only a mile or two of the generating station [29].

In this DC-only era, alternating current still managed to carve a niche for itself supplying electroplating workshops, where it was discovered to be both cheaper and safer to operate the generator without the commutator. Flame-arc lamps, of the type invented by Sir Humphrey Davy, were also found to be suitable for alternating current transmission, with the "Jablochkoff candle" specifically requiring an alternating current supply [1].

The "Alternating Current" or "Transformer" Era

In 1882 Lucien Gaulard and John Dixon Gibbs patented what they described as a "secondary generator". Despite Maxwell having demonstrated in 1865 that the secondary voltages cannot be controlled independently when the primary is connected in series, Gaulard and Gibb's voltage step-down device had a series-connected primary winding,

a parallel-connected secondary, and an open core. While presenting the secondary generator at an 1884 exhibition in Turin, Italy, Gaulard was quizzed by a young Hungarian engineer, Otto Bláthy, why a closed iron core was not used? To which Gaulard replied it "would have been harmful and uneconomical" [30]. The following year Max Déri, Otto Bláthy, and Karl Zipernowsky, from the Ganz factory in Budapest, demonstrated to the world their "transzformátor", a parallel-connected primary, closed core device that successfully powered 1,067 Edison incandescent lamps at the Industrial Exhibition of Budapest in 1885 [1].

It was not just the transformer that Déri, Bláthy, and Zipernowsky demonstrated. It was the system. They had provided a prototype for the electrical system still in use today. Use high voltage and low current to minimise the ohmic losses that plagued DC distribution and drop to low voltage and higher current for usability by the customer. Further developments, such as a lower cost, better insulated, and higher voltage laminated core transformer construction method pioneered by William Stanley, Jr. in 1886 [31], induction motors and polyphase transmission further cemented alternating current as the preferred transmission method. Despite the odds stacked against it, alternating current prevailed thanks in no small part to the invention of the transformer. As electrical distribution systems continue to evolve and adapt, it is the contention in this thesis that the role that distribution transformers contribute to electricity distribution should also evolve and adapt to these changing circumstances.

2.1.2 Rationale For Historically Low Utilisation Levels

Managing the utilisation level of distribution transformers is a challenge for operators of low voltage distribution networks. How to balance fiscally inefficient underutilisation against overutilisation and the risks that overloading can result in damage within a transformer even catastrophic failure [8, 9], which compromises network security.

Consequently, and to assure performance in terms of System Average Interruption Duration and Frequency Indices (SAIDI and SAIFI) respectively, network operators may choose to underutilise distribution transformers. Historical evidence of such an approach is given in [32], with an example of its implementation is given in [33], which recommends procuring a larger rated distribution transformer than required. A more recent example is from a network operator who supplied load data for the Winter months of 2017 for their 200 kVA distribution transformer shown in Fig. 2.1 and for March 2018 in Fig. 2.2. Here the peak utilisation was only 0.35 p.u. and the highest average utilisation was only 0.16 p.u.

However, with the expected and significant increase in distribution transformer loading that will result from increased electric vehicle (EV) penetration into distribution networks, the continued underutilisation of distribution transformers is becoming economically unjustifiable [34]. This difficulty relates not only to the higher capital cost of larger transformers but also to higher operational losses. This possibility was allowed for in [35], where larger distribution transformers were replaced by smaller versions with lower no-load losses and high-temperature insulation systems, resulting in an average 22.7 % reduction in losses. Additional research has shown dynamically rating transformers through assessment, or measurement can improve utilisation without compromising network security, such as [36], where a definition for dynamic rating of power transformers was provided in terms of varying ambient temperature Θ_A, the oil's thermal time constant (τ_{oil}), and the cumulative ageing process of the insulation paper due to thermal effects.

To arrive at this definition, the study utilised Annex G. from the IEEE Loading Guide, which highlighted that the hot spot temperature Θ_{HS} was often higher than estimated, when modelling was based on measured or calculated top oil temperature Θ_O. The authors further presented an algorithm for dynamically rating power transformers, utilising a continually updated integral to determine the remaining life based on the

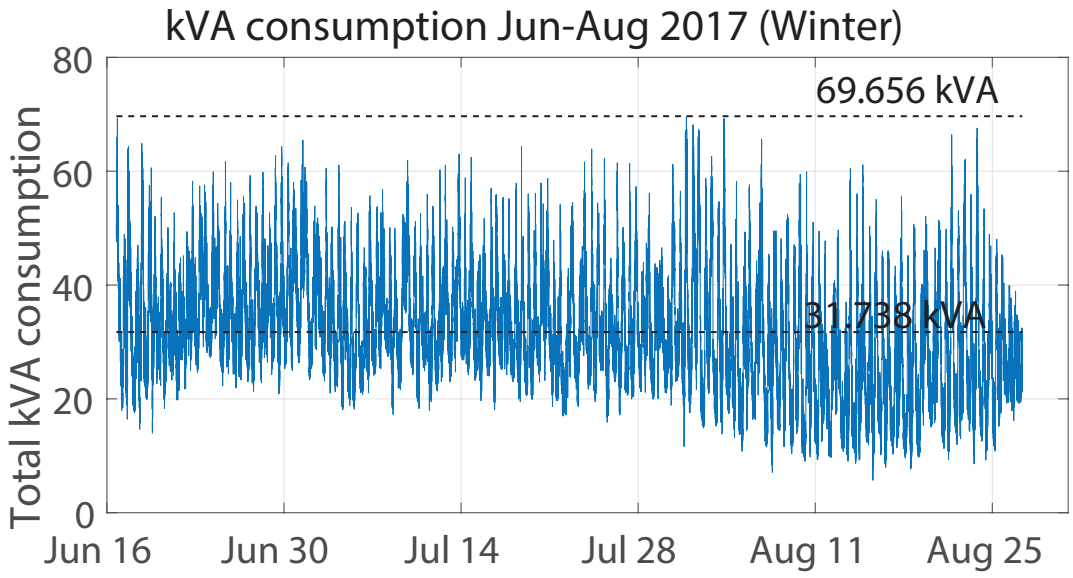

Figure 2.1: Winter 2017 Distribution Transformer kVA Consumption Pattern

thermal effects. In [37], a combination of dynamic rating with demand response allowed transformer utilisation to be increased significantly and in a manner that did not compromise network security, relative to the demand response capability of the load.

An alternative method described in [38], utilised a combination of dynamic rating with distribution network reconfiguration and load transfer. This method outperformed traditional methods of overrating transformers, even for worst-case conditions. In [39–42], Θ_{HS} was determined through modelling, and with air temperature and current measurements providing empirical data for the model.

While techniques based on changing the load connected to dynamically rated transformers can improve utilisation without reducing transformer lifetime, the results can be unsatisfactory if distribution transformer design and sizing are incorrect during planning stages. For instance, load transfers may interrupt electricity supply for short durations, and load scheduling may limit supply to undesired times. Therefore, improved design approaches are required. An example related to a planning stage, incorporating load, thermal, lifetime, and economic models for the sizing of distribution transformer in

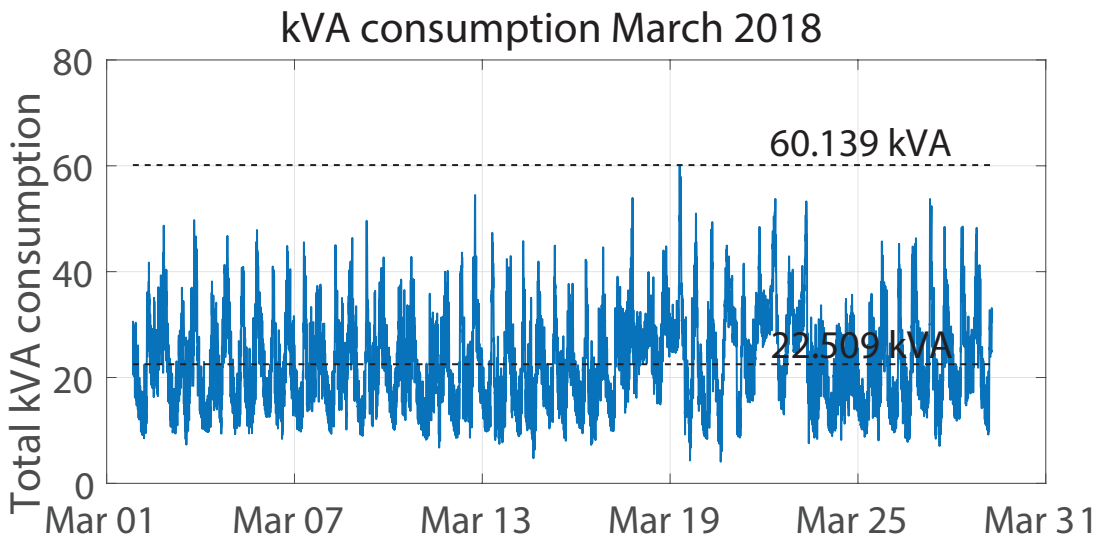

Figure 2.2: March 2018 Distribution Transformer kVA Consumption Pattern

suburban neighbourhoods was proposed in [43]. These models aligned with field experience, resulting in distribution transformer utilisation without the additional overhead usually required to compensate for uncertainties. However, the approach described does not accommodate other practical and significant factors affecting distribution transformer lifetime, other than Θ_{HS}. For example, oil leakage due to tank rusting [44]. Additionally, it does not account for the limit on distribution transformer utilisation imposed by voltage regulation specifications, such as AS/NZS 3000:2018 [45] and ANSI C84.1-2016 [46]. For example, utilisation resulting in a distribution transformer power level above nameplate ratings may be thermally tolerable for short periods but result in voltage levels lower than allowed by standards. An example is [47], where the concept of a distribution transformer critical power limit was proposed and utilised, to support their distribution transformer overloading algorithm for EV charging. However, as only distribution transformer temperature is considered, the potential for the low voltage (LV) regulation to be outside IEC and IEEE limits [45] is not addressed.

2.1.3 Relevance of Lifetime to Maximising Distribution Transformer Utilisation

Distribution transformer lifetime most commonly refers to the degree of polymerisation (DP) of the Kraft paper insulation used within the winding structure. Physically, DP relates to the unbroken length of cellulose chains which make up the fibres. The greater the chain length, the higher the mechanical strength of the fibre. A DP of 1000 is considered "not-aged", and a DP of 200, or approximately 35 % retained tensile strength, is considered end-of-life. The factors that most contribute to the breakdown of the cellulose chains are heat and moisture, with thermal considerations predominating. For example, operation of thermally upgraded Kraft paper at 110 °C, and no moisture or oxygen, would correspond to approximately 17.2 years of operational life according to AS/NZS 60076-7:2013 [9] and 15.3 years according to IEC 60076-7:2018 [8]. As previously described, this relates only to its mechanical strength, not its dielectric strength. Therefore, even with a DP of 200, the distribution transformer will likely still function for day-to-day operation. However, without the mechanical strength to withstand the shear stresses associated with a short-circuit event, should such an event occur, the distribution transformer will fail. Operation above 110 °C accelerates the ageing and below slows it. This rate of decay is modelled by the Arrhenius relationship [8]:

$$\frac{1}{DP_T} - \frac{1}{DP_0} = A \cdot e^{-\frac{E_A}{RT}} \cdot t \tag{2.1}$$

where DP_0 = initial DP value, DP_t = DP value at time t, R (Molar gas constant) = $8.314 m^2 kg s - 2 K^{-1} mol^{-1}$ and Θ_{HS} is hot spot temperature in degrees Kelvin. A (environmental factor) depends on the quantity of dissolved oxygen and moisture

content. When moisture is at 1.5 %, the distribution transformer is determined to be end-of-life, therefore $A = 3 \times 10^4$ [8]. At rated value with no oxygen and 0.5 % moisture (the maximum allowable when the distribution transformer leaves the factory), $A_r = 1.6 \times 10^4$. The activation energy (E_A) is the rated activation energy $(E_{A_r}) = 86kJmol^{-1}$. The initial distribution transformer ageing rate (V) is calculated as [8]:

$$V = \frac{A}{A_r} \cdot e^{\left(\frac{1}{R}\right)\left(\frac{E_{A_r}}{383} - \frac{E_A}{\Theta_{HS}+273}\right)} \tag{2.2}$$

Due to the varying nature of Θ_{HS}, a weighted LOL rate Θ_{HS_W} and weighted activation energy E_{A_W} are used and calculated as [48]:

$$\Theta_{HS_W} = \frac{1}{\frac{-R}{E_A \cdot ln\left(E_{A_W}\right)}} \tag{2.3}$$

$$E_{A_W} = \frac{\Sigma\left(\frac{-E_A}{e^{(\Theta_{HS}+273)}}\right)}{n} \tag{2.4}$$

where n is the number of interval steps for the LOL calculation. E_{A_W} is then used to calculate DT_{HS_W} which is then used to determine the time required for $DP_0 = 1000$ to fall to $DP_{final} = 200$. To accommodate the phase imbalance an extension to the IEC thermal model proposed in [49] is used. Equation (2.5) is a combination of the RMS for each of the individual phase load factors in p.u. Utilising this approach better reflects the heating effect each phase has within the distribution transformer than just using the single thermal as specified in [8].

$$K_{unb} = \sqrt{\frac{1}{3} \times \left({K_a}^2 + {K_b}^2 + {K_c}^2\right)} \tag{2.5}$$

K_{unb} then replaces K in the top oil to ambient temperature thermal model differential

equation, modifying it from:

$$\Delta\Theta_{O_R}\left[\frac{1+RK^2}{1+R}\right]^x = k_{11}\tau_O\frac{d\Theta_O}{dt} + (\Theta_O - \Theta_A) \tag{2.6}$$

to:

$$\Delta\Theta_{O_R}\left[\frac{1+RK_{unb}{}^2}{1+R}\right]^x = k_{11}\tau_O\frac{d\Theta_{O_{unb}}}{dt} + (\Theta_{O_{unb}} - \Theta_A) \tag{2.7}$$

Pressure is calculated using the following equation [50]:

$$P_f = 0.145 \cdot P_0\left(\frac{\Theta_{HS}}{\Theta_A}\right)\left(\frac{V_{l_0}}{V_l}\right)\left[\frac{K_{i_0} + \left(\frac{V_{g0}}{V_{l_0}}\right)}{K_i + \left(\frac{V_g}{V_l}\right)}\right] \tag{2.8}$$

where

P_f is calculated final pressure (psi)

P_0 is ambient pressure (psi)

V_g is the final gas volume at Θ_{HS} (l)

V_{g_0} is the initial volume (l)

V_l is the oil volume in the tank at Θ_{HS} (l)

V_{l_0} is initial oil volume (l)

K is the solubility factor

K_{i_0} is solubility at ambient temperature

K_i is the solubility at the final temperature

These are not the only factors that limit the distribution transformer lifetime in normal use. The material of the tank is also a factor. Stainless steel is essentially maintenance free as it is not subject to corrosion. However, due to its cost, its usage is not widespread, mild steel being more common. For mild steel, as paint acts as a barrier to corrosion, the time to the first service of the paint is a factor. AS/NZS 2312.1:2014 [51], specifies these periods according to paint thickness, as shown in Table 2.1 for limits. Once the

Table 2.1: Maintenance-Free Period for Mild Steel

Paint Thickness	Years to Maintenance (C4 Environment)
$325\mu m$	25 Years
$250\mu m$	10-15 Years

paint begins to fail, the steel is exposed to the elements, leading to rust in the tank wall. The distribution transformer is severely compromised at this point, with the possibility of oil leaks in the worst case or moisture ingress in the least worse case. Correct distribution transformer design and sizing should consider which factor imposes the most significant limit on distribution transformer lifetime. This may, or may not, be ageing of the winding insulation paper. Many factors can necessitate distribution transformer refurbishment. Should the associated costs be excessive, a distribution transformer may be retired prior to the DP falling to 200. For example, tank rust, or oil leaks through the bushings, due to cable stress and external short circuits. Therefore, additional fittings, such as bushings, on-load tap changers (OLTC) and switchgear should also be assessed prior to the overloading of a distribution transformer, to ensure their lifetime will not be compromised.

Thus, beyond the lifetime required by the network operator, optimal distribution transformer design should ensure that insulation lifetime is coincident with other such factors. For the purposes of the research in this thesis, it is assumed that the sizing of such components will be determined as a result of the degree to which overloading of the distribution transformer is permissible, or have been verified as able to cope with the additional loading. Consequently, they are not considered as initial limiting factors in the algorithm. The factors which do directly limit the distribution transformer have been addressed in the algorithm outlined in Chapter 4, Section 4.2 and detailed in Section 4.3.

2.1.4 Recent Load Management Strategies

In [52], two dynamic online approaches to manage loading were presented. However, as even the uncoordinated charging load did not exceed 1 p.u., it can be assumed that this approach is not intended to allow for operation of distribution transformers beyond their nameplate rating. However, the rising demand for EV charging is creating load planning challenges for network operators, particularly with regard to the sizing of transformers in distribution networks, buildings, industrial complexes and campuses. For example, studies have shown that the EV penetration levels needed before existing transformer nameplate ratings are exceeded may be as low as 40 % [53], or 50 % [54] of consumers on a network. Under such scenarios, and in the absence of alternative approaches, large scale transformer replacement may be undertaken at considerable expense [55]. Therefore, solutions to lessen this expense by delaying the need for transformer upgrades have been investigated. One solution is EV charge scheduling, which may be applied on the basis of the transformer nameplate rating [56–59]. Another solution is the use of network aware algorithms [60]. These incorporate LV network parameters into constraints related to loading levels to limit the EV charging power allowed through curve-flattening [61], utilizing low-demand windows (valley-filling) [62–64], or using a combination of curve-flattening and valley-filling [65]. Common to [56–59] and [61–65], is to limit the available capacity to the transformer nameplate rating, which allows the lifetime of a transformer to be regulated. However, this approach does not explicitly consider temperatures within a transformer. An improved approach in this respect is to base transformer loading on a hot-spot temperature, Θ_{HS}, and not a kVA rating, as this impacts directly on the integrity of the winding insulation and, therefore, lifetime. Both the IEEE [66] and IEC [8] hot spot temperature equations calculate Θ_{HS} as a rise over the top oil temperature Θ_O as given by.

$$\Theta_{HS} = \Theta_A + \Delta\Theta_O + \Delta\Theta_{HS} \tag{2.9}$$

This improved approach has been adopted in recent work. For example, the decentralized strategy in [67] considers Θ_{HS} with the goal of minimizing transformer ageing. However, while a recommendation for the maximum EV penetration level is given, the method is limited as it does not support loading the transformer beyond its nameplate rating. Load management is considered as an outcome of the day-ahead operational planning task for EV charge scheduling in [68]. The cost implications of a rising Θ_{HS} on transformer insulation lifetime due to the addition of EV charging loads is also considered. However, a limitation with this approach is the lack of consideration given to the maximum Θ_{HS} specified for operating transformers in IEEE [66] and IEC standards [8].

Load management is also implemented in [69] using a fuzzy logic-based system that allows additional loading based on the predicted loading for the next hour. However, as transformers usually operate on a 24-hour repeating cycle [8, 66], a better approach would be to predict loading based on its daily load cycle. Each of [67–69] rely upon flattening the load profile, including through load shifting. This may not always be feasible. For example, load shifting is undesirable for an EV in need of fast charging within a limited time frame to enable the next journey. Further, and significantly, [67–69] do not realize the benefits that can arise from utilizing transformer thermal inertia. Incorporating thermal inertia into calculations provides greater accuracy in determining the duration a transformer can be overloaded without exceeding any temperature limits. Therefore, having an accurate knowledge of relevant transformer thermal time inertias is essential to determine the allowable level and duration of transformer overloading. This approach is seen in the case studies in [70], which demonstrated a design approach based on an assessment of the impact of periodically exceeding nameplate ratings for

an historical load profile. Similarly, in [71], it is shown a Θ_{HS} of 140 °C would not be reached within a two-hour window given a 1 p.u. base load and an overload to 1.3 p.u. However, a shortcoming of both of these approaches is the lack of relevance to EV charging loads through the reliance on a fixed load profile. This does not suit the dynamic loading scenarios likely to occur with EV charging and taking into account the ability of transformers to be overloaded for short time periods. Specifically, these approaches do not allow for the dynamic determination of when, to what level, and for how long the overloading of transformers can be tolerated.

2.2 Smart Grid

There does not appear to be a consensus opinion as to exactly what constitutes a Smart Grid. However, in an attempt to garner a broad perspective, overviews from key stakeholders driving the development of the Smart Grid are presented. The stakeholder perspectives are from the US Department of Energy (USDoE), the IEC and IEEE. The following provides the Smart Grid perspectives and perceived benefits:

USDoE It is the digital technology that allows for two-way communication between the utility and its customers, and the sensing along the transmission lines that makes the grid smart. The benefits associated with the Smart Grid include [72]:

- More efficient transmission of electricity
- Quicker restoration of electricity after power disturbances
- Reduced operations and management costs for utilities, and ultimately lower power costs for consumers
- Reduced peak demand, which will also help lower electricity rates
- Increased integration of large-scale renewable energy systems
- Better integration of customer-owner power generation systems, including

renewable energy systems

- Improved security

IEC There is no well-defined and commonly accepted scope of what "smart" is and what it is not. It is generally understood that the smart grid encompasses the modernisation of the electric grid. This comprises everything related to the electric system between any point of generation and any point of consumption. Smart grid technologies allow the grid to become more flexible, interactive and enable it to provide real-time feedback. It incorporates technologies and services that facilitate intelligent monitoring, control, communication and self-healing technologies. A smart grid helps intelligently integrate different needs and activities in order to efficiently deliver a sustainable, affordable and secure electricity supply [73].

IEEE The smart grid is a revolutionary undertaking—entailing new communications-and-control capabilities, energy sources, generation models and adherence to cross-jurisdictional regulatory structures. Successful rollout will demand objective collaboration, integration, and interoperability among a phenomenal array of disciplines, including computational and communications control systems for generation, transmission, distribution, customer, operations, markets and service provider.

The IEEE sees its role as unifying the smart-grid movement, providing expertise and guidance for individuals and organisations involved in the modernisation and optimisation of the power grid, anticipating and determining the direction of existing, new, and emerging technologies and related issues, and spearheading their investigation and development [74].

2.2.1 Communications and Control Protocols

IEC 61850

The IEC 61850 standard was developed for device communication in the Smart Grid and substations [75]. However, it is not just a communications protocol, but also describes the devices connected to it [76]. Communication using IEC 61850 uses abstract communication service interface (ACSI) models [77], which provides utility information and information exchange services.

IEC 61850 covers multiple aspects of a Supervisory Control and Data Acquisition (SCADA) system [78]:

i. The definition of data structures. These data structures contain the information about the current state of the system (e.g. status information, measurements), the information required to operate the system, as well as parameters that can change the behaviour of the system. These data structures are implemented in the devices.

ii. The definition of communication services to access the data including the protocols to realize these communication services.

iii. The definition of a model that describes the configuration of the system. That model is used during the system design to exchange information between different engineering tools.

Data objects are the lowest level in ACSI model which are identified with a name that also provides information about the semantic (meaning and usage) of the data. The next level up from the data object is the logical node (LN), which performs a single function – switch control for example. The next level up in the ACSI model is the logical device (LD), which is essentially multiple LNs. The highest level in the ACSI models is the server, which is the interface with the real world. It is important to be

aware of this information as no device designed to be compatible with IEC 61850 can be implemented without adhering to the ACSI model.

The following are examples of devices defined by IEC 61850:

Merging Unit (MU) A device that collects and samples analogue information from multiple sources [79]. Data transfer is facilitated utilising manufacturing message specification (MMS) or sampled value (SV) data [80].

Intelligent Electronic Device (IED) A device incorporating one or more processors with the capability to execute application functions, store data locally in memory and exchange data with other IEDs over a digital link.

Finally IEC 61850 defines three traffic classes [80]:

MMS traffic Manufacturing Messaging Specification (MMS) or ISO 9506 is defined in IEC 61850-8-1, and allows an MMS client such as the Supervisory Control and Data Acquisition (SCADA), the utility's control and monitoring system, a server or gateway to access the IED control or internal reporting locations referred to as objects.

GOOSE traffic Generic Object Oriented Substation Event (GOOSE) is defined in IEC 61850-8-1, and allows IEDs to exchange data, especially status and tripping signals, and often for interlocking.

SV traffic Sampled Value (SV) is defined in IEC 61850-9-2, and carries voltage and current samples. This traffic is also used for busbar protection and phasor measurement.

Distributed Network Protocol 3

Distributed Network Protocol 3 (DNP3), also known as IEEE Std 1815 can be considered a precursor to IEC 61850, as a number of features were adapted for use in the new protocol. Although DNP3 is still used, its functionality can be considered a subset

of IEC 61850. For example, it uses a model that describes the configuration of the system, but is not as detailed as IEC 61850 with regard to the data structures. It also uses numbers rather than names to identify the objects and because it does not define the semantic behind the objects, identification is a more involved process.

Modbus RTU and TCP

Unlike IEC 61850 and DNP3, Modbus is not intended for control functionality rather it is a request/reply protocol for industrial client/server communication between devices connected on different types of buses or networks. The Modbus Organisation *modbus.org* describes MODBUS as the de facto standard for industrial serial communications since 1979. Services are specified by function codes which are elements of MODBUS request/reply protocol data units, and is currently implemented using:

i. TCP/IP over Ethernet (MODBUS TCP, with port 502 reserved for MODBUS on the TCP/IP stack)

ii. Asynchronous serial transmission over a variety of media (wire : EIA/TIA-232-E, EIA-422, EIA/TIA-485-A; fibre, radio, etc.) (MODBUS RTU)

iii. MODBUS PLUS, a high speed token passing network

2.3 Fibre Optic Technology

Optical fibres work by light propagating throughout the fibre according to the principle of total internal reflection. The core, which is the centre of the fibre cable has a higher refractive index than its cladding. The difference between the refractive index of the core and cladding creates a mirror-like surface, guiding the light along the core. It is this principle that causes the light to bounce through the core from one end to the other [81]. Total internal reflection occurs between the different media when the incident angle for

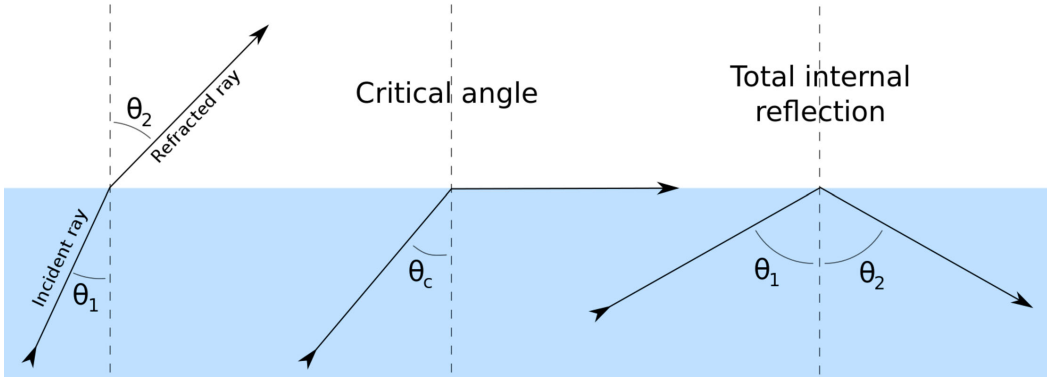

Figure 2.3: Effect of Incident Angle, Critical Angle and Total Internal Reflection from [82]

the light is greater than the critical angle, preventing any light escaping from the media, (see Fig. 2.3).

Fibre optic cores are typically one of three types [81]:

Single-Mode Step Index These fibres have extremely small core diameters, ranging from 5 to 9.5 μm, surrounded by a cladding of 125 μm, with an external jacket providing mechanical protection and are always made of glass. Capable of carrying signals for long distances with low loss, they are mainly used in communication systems. Single-mode operation only occurs when the wavelength approximately equals the core diameter, 1310 nm, for example. Consequently, the fibre cable permits only one mode.

Multi-Mode Step Index These fibres have diameters ranging from 100 to 970 μm, and are available as glass core and cladding, glass core with plastic cladding and plastic core and cladding. They are also the widest ranging, although not the most efficient in long distances, and they experience higher losses than the single-mode fibre cables. As the name suggests light rays for different ray paths reflect at different angles, resulting in different path lengths too. A ray that goes straight down the centre of the core without reflecting arrives at the other end faster, other rays bouncing off the walls take slightly longer and arrive later. When light

rays enter a fibre at the same time, but exit at the other end at different times, a spreading of the light results, referred to as modal dispersion, effectively limiting their use to short range applications.

Multi-Mode Graded Index These fibres have core diameters of 50, 62.5 or 85 μm, with a cladding diameter of 125 μm. The core consists of numerous concentric layers of glass, analogous to tree or onion rings. Each successive layer expanding outward from the central axis of the core until the inner diameter of the cladding has a lower index of refraction. Light travels faster in an optical material that has a lower index of refraction. Thus, the further the light is from the centre axis, the greater its speed. Each layer of the core refracts the light according to Snell's law. Instead of being sharply reflected as it is in a step-index fibre, the light is now bent or continually refracted in an almost sinusoidal pattern. Those light rays that follow the longest path by travelling near the outside of the core have a faster average velocity. The light ray travelling near the centre of the core has the slowest average velocity. As a result, all rays tend to reach the end of the fibre at the same time. Thus, one way to reduce modal dispersion is to use GRIN fibres. This type of fibre-optic cable is popular in applications that require a wide range of wavelengths, in particular telecommunication, scanning, imaging and data-processing systems. Fibre cables are designed for a specific wavelength, called the cut-off wavelength, above which the fibre carries only one mode. A fibre designed for single-mode operation at 1310 nm has a cutoff wavelength of around 1200 nm. Although optical power is confined to the core in a multi-mode fibre, it is not so confined in a single-mode fibre. This diameter of optical power is called the mode field diameter. It is usually more important to know the mode field diameter than the core diameter.

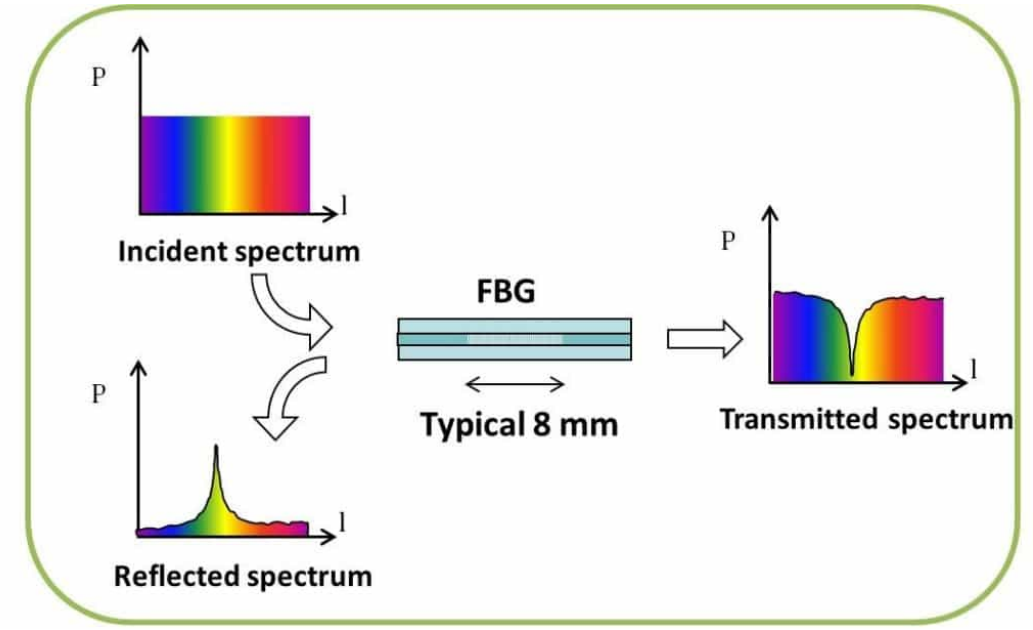

Figure 2.4: Effect of Bragg Grating on Incident Light from [83].

2.3.1 Fibre Bragg Grating

The type of fibres our research and development partner, ETEL Limited, uses for their fibre-based temperature measurement system are of the type "Draw Tower Gratings" (DTG). The term DTG refers to the manufacturing process, the underlying process by which DTG fibres operate is using a Bragg grating [83].

Operating Principle

Fibre Bragg Gratings (FBG) are made by exposing a single-mode fibre to a pattern of intense laser light, which permanently increases its refractive index, creating an exposure pattern, called a grating.

The light signals produce one large reflection when the grating period is equal to approximately half the input light's wavelength ($\lambda/2$), referred to as the Bragg condition, and the reflection wavelength is the Bragg wavelength. The grating is essentially transparent to other wavelengths, Fig. 2.4.

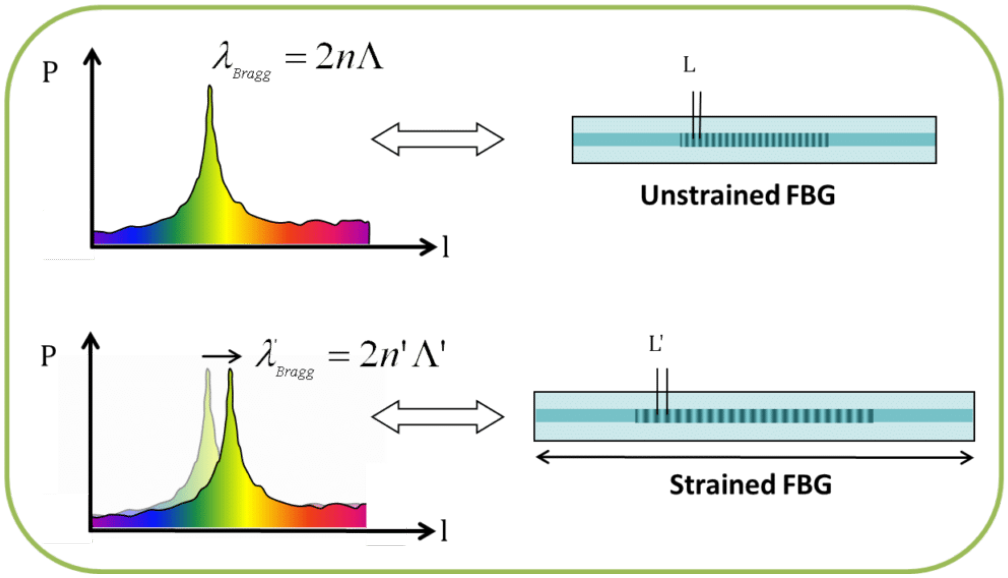

Figure 2.5: Effect of Strain on Bragg Grating on Wavelength of Reflected Light from [83].

Therefore, light propagates through the grating with negligible attenuation or signal variation. Only those wavelengths that satisfy the Bragg condition are affected and strongly back-reflected. The ability to accurately set and maintain the grating wavelength is a fundamental feature and advantage of fibre Bragg gratings.

The central wavelength of the reflected component satisfies the Bragg relation: λBragg = $2n\Lambda$, with n the index of refraction and Λ the period of the index of refraction variation of the FBG. Due to the temperature and strain dependence of the parameters n and Λ, the wavelength of the reflected component will also change as function of temperature and/or strain, see Fig. 2.5. This dependency is well known what allows determining the temperature or strain from the reflected FBG wavelength [83].

2.4 Chapter Summary

In this chapter, topics related to the research conducted in this thesis were presented. First, the significant contribution that distribution transformers make in the delivery of

electricity to the consumer was discussed, along with the developments leading to their invention. Reasons that they have historically been a limitation on supply and operated at much lower utilisation levels than they are capable of delivering were highlighted. In discussing the challenging relationship between transformer lifetime and utilisation, it was shown that low utilisation results in unnecessary transformer retirement, but higher utilisation can lead to failures if not properly managed.

The Smart Grid concept to which distribution transformers have the potential to contribute intelligence was overviewed, along with communications protocols used within it. Fibre optic technology and its application for use in distribution transformers was the final topic discussed. Special mention was made of fibre Bragg grating technology and its potential to provide a low-cost, high-accuracy temperature sensing solution.

Chapter 3

Literature Review

3.1 Introduction

Transformer loading is expected to increase as the number of EVs increase as a proportion of vehicles sold. Therefore, this research seeks to extend the understanding of design optimisation strategies and transformer operation in the presence of volatile loading. This introductory section outlines the methodology used in the systematic literature process, the exclusions, and initial inferences. This will be followed by a review of existing works relevant to the design and performance of distribution transformers, including EV charging impact, real-time monitoring, dynamic thermal modelling, dynamic rating, condition monitoring, and design optimisation strategies.

3.1.1 Systematic Literature Process Overview

A systematic literature review using multiple search strings in Clarivate's Web of Science^{TM} search engine established the current understanding of the dynamic operation in distribution transformers. Search one used the search string *((ALL=(Transformer AND "Dynamic Rating")) OR ALL=(transformer AND thermal)) OR ALL=(Transformer AND temperature)* between the years 2016-2021, search two used the search term

ALL=(Transformer AND Dynamic AND Rating) between the years of 1996 and 2021, search three used *ALL=(Transformer AND Dynamic AND Thermal)* between the years of 1996 and 2021, search four *ALL=(Transformer AND Design)* between the years of 2016 and 2021, and search five *TI=(transformer) AND TI=(design)* between the years of 1996 and 2021.

3.1.2 Exclusions

The following details the types of papers excluded and the reason for their exclusion

Conference Papers Either the concepts are brand new and therefore not developed enough to be worthy of submission as a journal article or were not significant enough to develop to the point where the concept was worthy of journal publication.

Dry Type Transformers The transformers tested in this thesis are all of the liquid-filled type. So while dry-type transformers may exhibit suitable characteristics for dynamic loading, no such behaviour was examined in this research. Therefore Dry-type transformers are considered OOS.

Small Power Transformers This research did not examine the thermal behaviour of transformers without external cooling, so such transformers are considered OOS.

Large Power Transformers The largest transformer ETEL has presently manufactured is 4500 kVA. All high power testing was carried out at ETEL Limited. As the physical size of the HV lab prevented experimentation on transformers larger than this, any papers not including Medium Power Transformers in their results are considered OOS.

Liquid-Filled Transformers Not Using Mineral Oil Transformers filled with bio-ester, mixtures or nano-particles were not investigated, only those filled exclusively with mineral oil.

Thermal Models Not Investigating Dynamic Loading Behaviour This research explores distribution transformer behaviour in the presence of dynamic loading. Steady-state behaviour is OOS.

Free-Breathing Transformers OOS. Free-breathing transformers typically have moisture levels higher than hermetically sealed transformers. Additionally, internal pressure is not a consideration in free-breathing transformers. ETEL presently only manufacture hermetically sealed transformers, so for these reasons, research that does not include hermetically sealed transformers is considered OOS.

Transformers Without Thermally Upgraded Kraft Paper ETEL's default position is to supply transformers with thermally upgraded Kraft paper (TUKP). As all experimentation was on transformers using TUKP, papers investigating transformers with a normal lifetime based on 98 °C are considered OOS.

Traction Transformers Only static transformers for electrical distribution were investigated, so traction transformers are considered OOS.

Wind Farm Transformers Wind farm transformer loading tends to be high-harmonic low current, leading to high partial discharge and low thermal loading. This research focuses on thermal behaviour. Partial discharge was not examined, so is considered OOS.

Voltage Rise Management In the presence of distributed generation, particularly with high photovoltaic (PV) penetration, voltage rise into the grid tends to be a concern. However, in the presence of high loading, as $V = IR$ and R is essentially constant, I has the effect of constraining any increase in ΔV. Additionally, transformer heating is predominately due to I^2R. Therefore, papers that examine voltage rise with light loading are considered OOS.

3.1.3 Initial Findings

This literature review can be considered comprehensive as there are no journal publications addressing dynamic rating prior to 1996. Thus the following inferences may already be drawn:

1. Dynamically rating transformers is a relatively recent concept for academic study
2. It is unlikely that the use of dynamically rated equipment is widespread within industry
3. Historically there has been little to no requirement for dynamically rated transformers
4. Unless there is a significant motivation for change in the delivery or usage within electrical distribution networks, there is unlikely to be any requirement for dynamically rated transformers in the future

The remainder of this chapter begins with an examination into the expected impact of EV charging on distribution transformers.

3.2 EV Charging Impact

A study examining the impact of EV charging and the potential for overloading of two transformers supplying a Toronto neighbourhood was presented in [84]. This study was entirely simulated, with no empirical temperature measurements of the transformer taken at any time, and results were only presented in terms of the load value. However, the following recommendations for utilities based on the results were presented:

i. Small chargers are unlikely to affect system loading. However, they may affect transformer cooling cycles.

ii. Medium-sized chargers are unlikely to overload the system components. But

may impact the spare capacity of transformers, impacting their ability to absorb loading in an outage.

iii. Large chargers significantly impact system equipment capacity and safety margins. Therefore, system upgrades are required to accommodate EVs.

iv. Overloading capacity of system components is limited in the summertime due to higher ambient temperatures.

v. Additional studies are required for commercial and industrial loading.

vi. Simulation studies are required.

Another simulation study was presented in [85], which modelled the impact of 6 houses with a maximum of 6 plug-in EVs (3 plug-in hybrid EVs and 3 battery-only EVs), demonstrating a significant impact on the transformer's lifetime. However, the modelled 25 kVA transformer was assumed to have the same parameters as a 25 MVA transformer from work done by Susa et al.in [86]. Furthermore, the modelled hot-spot temperature rose instantly with the rise in load in [85], resulting in hot-spot temperatures in excess of 160 °C, Fig. 3.1.

If this modelling is correct, then any overloading, even for the 30 minutes at 1.8 p.u. specified in IEEE and IEC loading guides [8, 66] would not be possible. Furthermore, it is worth investigating whether temperature differentials in excess of 60 °C between the hot-spot and top-oil are physically possible.

A contrast was presented in [87] which considered the impact of the additional load on the grid against the over-supply of voltage due to distributed PV generation. The authors acknowledge that the scenario they investigated was not ideal, as the periods of peak generation and charging were not coincident. However, they demonstrated that, even with a slight overlap, increased PV reduced the transformer's load. This result

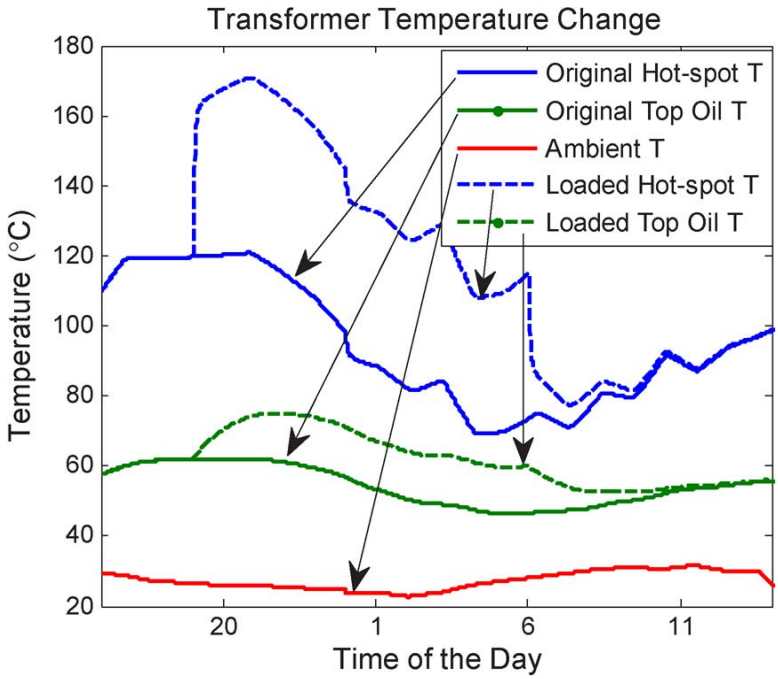

Figure 3.1: Calculated hot-spot temperature based on loading from [85].

indicates that this approach is best applied for business or industrial parking or when a second EV is parked at home.

3.3 Real-Time Monitoring

Real-time monitoring of soil temperature and load was used to effect a "Dynamic Rating" of sorts for two sub-station transformers in [88]. However, this reference is only tangential to the paper's primary focus, which is the dynamic rating of conductors. Although intended for power cables, this paper does provide a helpful description for why dynamic rating is possible: *"Because of the conservative heat transfer assumptions used in static thermal rating calculations, under normal conditions, actual critical temperatures are less than the temperature limits even when the electrical load equals the thermal rating. In addition, electrical loads are usually much less than the high pre-loadings typically assumed in static emergency rating calculations, and real-time*

emergency loadings usually exceed static emergency ratings. Finally, circuit loads are not constant, and consideration of load "shape" can yield an effective increase in emergency ratings."

In other words, because transformers typically operate at loads lower than what the transformer is rated for, its internal operating temperature is lower. However, the published overload recommendations assume the transformer is operating at rated load, and it takes longer for a transformer operating at a lower load to heat up to the temperature assumed in the overload recommendation. Two equations were used (3.1) for determining the new current limit and (3.2) for the temperature rise.

$$I = I_{NP} \cdot \left(\frac{T_{MAX} - T_A}{T_{MAX_{NP}} - T_{A_{NP}}} \right)^{\frac{1}{n}} \tag{3.1}$$

$$T_{(t_{(i+1)})} = T_{t_i} + \left[T_{ULT_{(i+1)}} - T_{t_i} \right] \cdot \left[1 - e^{-\left(\frac{t_{i_{t_1}} - t_1}{\tau} \right)} \right] \tag{3.2}$$

where

$$T_{ULT_{(i+1)}} = \left(\frac{I_{i+1}}{I_{NP}} \right)^n \cdot \left[T_{MAX_{NP}} - T_{A_{NP}} \right] + T_{A_{i+1}}$$

where I is the dynamic current rating (A), I_{NR} is the nameplate current rating (A), T_A is the measured ambient temperature (°C), T_{MAX} is the maximum measured equipment temperature (°C), $T_{A_{NP}}$ is the maximum ambient temperature for nameplate rating (°C), $T_{MAX_{NP}}$ is the maximum allowed equipment temperature (°C), n is 2 i is the current time index, t is the time of day and T_{ULT} is the temperature rise achieved if the load and ambient temperature remain constant. Increased load and current handling is possible whenever the ambient temperature is lowered without damage to the transformer.

In [89] a lack of knowledge as to the actual performance and simplified calculating

procedures are two reasons provided as to why transformer ratings have historically been conservative. The use of an UPRATE ^{TM} system, which measures power, wind speed and ambient temperature, is recommended to achieve higher maximum and average loading levels within the system. In effect, this is a method to implement dynamic rating. The authors determined that transformer nameplate ratings limited additional capacity unless cooling systems were improved. They also asserted that short thermal time constants meant transient ratings also provided minimal benefit and cooling system performance could put the transformer at risk when loading well below nameplate rating, and their system was ideal for condition monitoring. However, while lauding their temperature system, no information was provided to the reader to independently validate their assertions as to its accuracy.

The measurements taken over a 24-hour period by a remote monitoring system for transformer power and temperature was presented in [90]. No information was supplied as to the nameplate rating or cooling method of the transformer. However, as the maximum temperature was only 34 °C, it indicates that loading was light and as the impact on transformer lifetime would be negligible. Therefore, the cost of maintaining the regular monitoring is unlikely to provide a return to justify its continuation.

3.4 Dynamic Thermal Modelling

The monitoring systems described in Section 3.3 demonstrate that direct temperature measurement, particularly of hot-spot temperature is uncommon. Therefore, it is appropriate to determine the current state of thermal modelling and their suitability for assessing temperature in dynamic loading situations.

3.4.1 Challenges and Limitations

The current state of dynamic thermal modelling was examined in [91], with the following factors highlighted as potentially impacting on internal temperature rise but whose behaviour was not addressed in existing thermal models

i. The dynamics between DC resistance of the windings increasing due to temperature against the oil's capacity to remove this heat due to its increased viscosity.

ii. The ability of low-temperature high viscosity oil to reduce winding hot spot temperature.

iii. The impact of harmonic content.

iv. Impact of environmental conditions such as wind velocity and solar irradiation, as favourable wind conditions could improve the effectiveness of the radiant cooling. Conversely, solar irradiation may increase heating, with factors such as the emissivity of the tank due to its colour requiring consideration.

v. The impact of changing tap position.

vi. Whether geomagnetically induced current is causing the transformer to stop operating in linear range and move into saturation, as its behaviour would become less deterministic.

vii. The degree to which moisture ingresses into the oil.

This paper also highlights a range of factors contributing to very little empirical data on winding hot spots having been gathered. These are factors such as the high cost of removing a transformer from service to install sensors, that hot spot measurement does not provide any predictive insight into the transformer's loading capability, and the impossibility of hot-spot investigation via measurement due to factor interdependency.

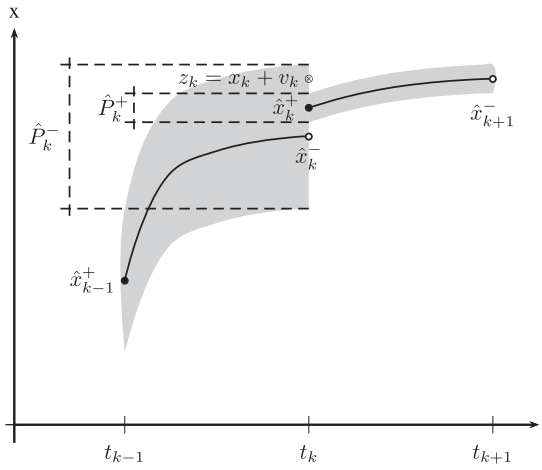

Figure 3.2: Extended Kalman filter graphical representation from [92]

A method for gaining predictive insight to transformer loading was presented in [92] which used a Kalman filter as its prediction mechanism.

Fig. 3.2 provides a graphical representation of the extended Kalman filter algorithm which is described below:

i. $\hat{\mathbf{x}}_{k-1}^+$, is an estimation with a covariance of the error, $\hat{\mathbf{P}}_{k-1}^+$, at time, t_{k-1}.

ii. The initial values above are then used to make a future state prediction, $\hat{\mathbf{x}}_k^-$, at time, t_k.

iii. The error propagated by the uncertainty of the initial values is modelled by the covariance matrix, $\hat{\mathbf{P}}_k^-$.

iv. At time, t_k, a set of measurements, $\mathbf{z}_k$, with unknown errors, $\mathbf{v}_k$, is assumed to be available.

v. These values are used by the extended Kalman filter to provide future state updates to $\hat{\mathbf{x}}_{k-1}^+$ and covariance matrix, $\hat{\mathbf{P}}_k^+$.

vi. This process is repeated each time new load and ambient temperature measurements are received.

Although the approach in [92] was to determine the top-oil temperature, the authors did express an expectation that this approach could be extended to hot-spot temperature determination in the future.

Furthermore, the assertion that investigation into the hot-spot is an impossibility appears to be contradicted by the empirical measurements taken by the authors in [93]. In this paper, a distributed fibre sensor was installed throughout a distribution transformer, with temperatures measured at various intervals throughout the heat-run test. The results presented show the hot-spot was always measured at the same spot for each winding. This finding corresponds with research undertaken by ETEL Limited and reported in [7], which also found the hot-spot to be present in the same location.

The following five errors were presented as causes of error in determining top oil temperature of dynamically loaded transformers in [94]

- inadequate data gathering
- inadequate fundamental model
- improper discretisation
- erroneous data
- selection of training and validation data sets

Section 3.4.2 examines literature describing improvements to dynamic thermal modelling, providing insights as to whether these issues have been addressed, or to what degree there is an agreement with the assessment of the authors in [94] as to how significant these factors are as causes for errors.

3.4.2 Accuracy Improvement Methods

A variety of different approaches have been taken as methods to improve the accuracy of thermal modelling. For example, some approaches have been to improve the parameters in existing IEEE and IEC empirical models. Other approaches use artificial intelligence

(AI) or equation-fitting. The papers presenting these different approaches have been grouped under the various approach methodologies.

Empirical Model Parameters

In [95,96] a focus was placed on refining the definition of non-linear thermal resistances, having considered the way winding design differences impact the fluid flow around them. The equivalent thermal capacitances of the transformer oil for different transformer designs and winding-oil circulations resulted in an observation that the transformer's top-oil temperature time constant is shorter than the time constant suggested by the present IEC loading guide. Therefore, winding hot-spot temperatures would be higher than those predicted by the loading guides during transient states after the load current increases, before the corresponding steady-states have been reached. This assertion does appear contrary to Fig. 3.3 from [95]. The IEEE model overestimated the initial rise. However, the 2 p.u. rise is underestimated. This trend is further observed in Figs. 15 and 16 in [96], which introduces a model based on the non-linear thermal resistance between the top level winding insulation surface and the bottom oil temperature. However, from Fig. 3.4, both the proposed and IEEE models slightly overestimate the top-oil temperature rise. Other results presented in the papers also show measured hot-spot temperatures higher than determined by the model.

A dynamic thermal model of an oil-immersed power transformer housed in a kiosk enclosure that modelled heat transfer due to natural ventilation based on pressure due to thermal buoyancy and associated pressure drop on the air path was presented in [97]. Fig. 3.5 shows the airflow used in the modelling. However, the authors did note that if a sidewall is exposed to strong solar irradiation, the airflow can be reversed. It is of note that just as the internal cooling relies on natural convection of the oil, a similar phenomenon exists externally with the airflow, even in an indoor environment.

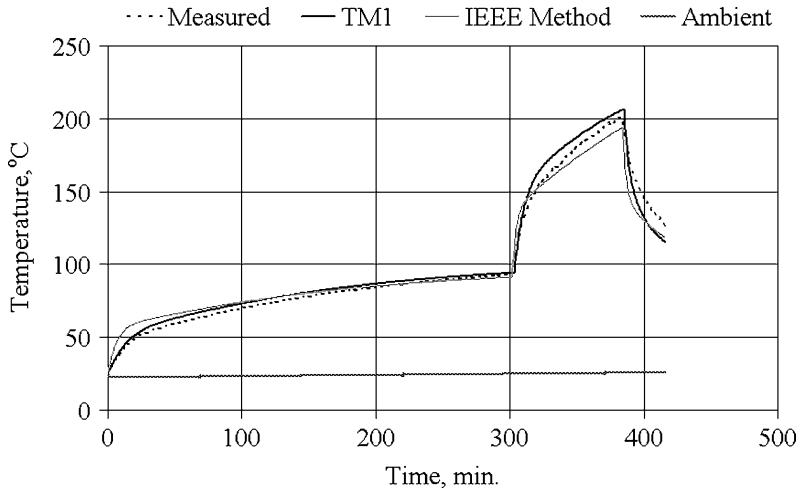

Figure 3.3: Hot-spot temperature measurement (0-299 mins at 1 p.u., 300-397 mins at 2 p.u. 398 mins+ at 0 p.u.) from [95].

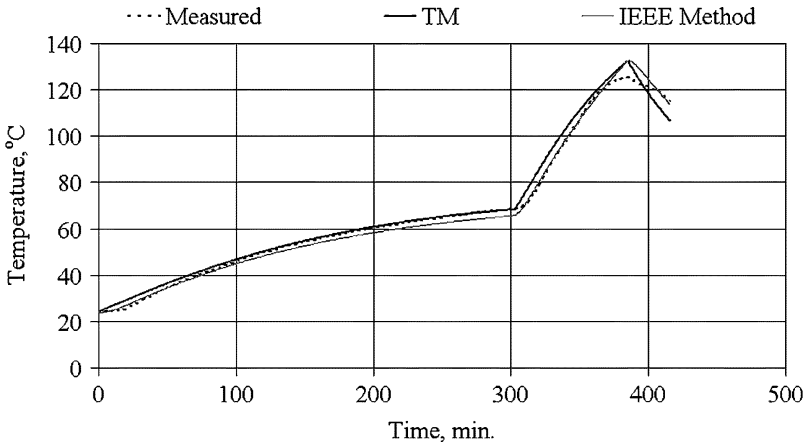

Figure 3.4: Top-oil temperature measurement (0-299 mins at 1 p.u., 300-397 mins at 2 p.u. 398 mins+ at 0 p.u.) from [95].

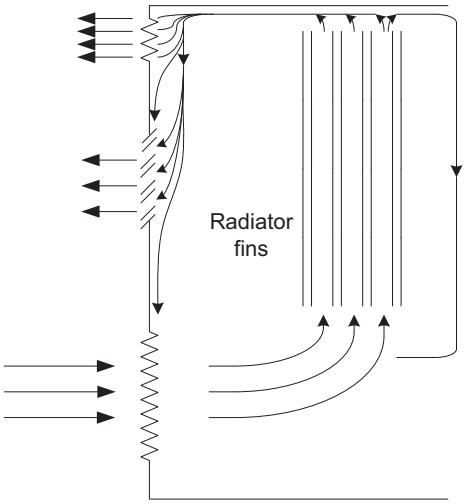

Figure 3.5: Arrows demonstrating convection airflow around transformer cooling radiators when housed inside a kiosk enclosure, from [97].

The influence that solar irradiation plays on heating the transformer was also examined in [98]. A new modelling component was introduced, the thermal radiation model with solar radiation ($TRM\omega SR$). Experimental results presented in the paper comparing the measured oil temperature of the transformer shielded from and exposed to the sun revealed an approximately 5 K increase in recorded temperatures when exposed to the sun. However, the modelled results using $TRM\omega SR$ showed sun exposure resulting in around 3 K increase. The authors provide a solution for how the solution can be adapted for real-time monitoring, requiring measured power and ambient temperature and computation carried out on a programmable logic controller. From this paper, solar irradiation does appear to raise internal oil temperature. However, limitations with this approach are that its effectiveness for painted transformers and those housed in kiosks is not addressed. The authors also proposed another improvement in [99], which has a high correlation with thermal rise, as well as steady-state referred to as the electro-thermal resistance model (E-TRM). The thermal time constant of the oil, τ_O is equal to $C_0 \cdot R_o$ applying the CR time constant electrical analogy, where C_0 is the thermal capacity of the oil and R_o is the oil to environment thermal resistance and ranging between 180-240

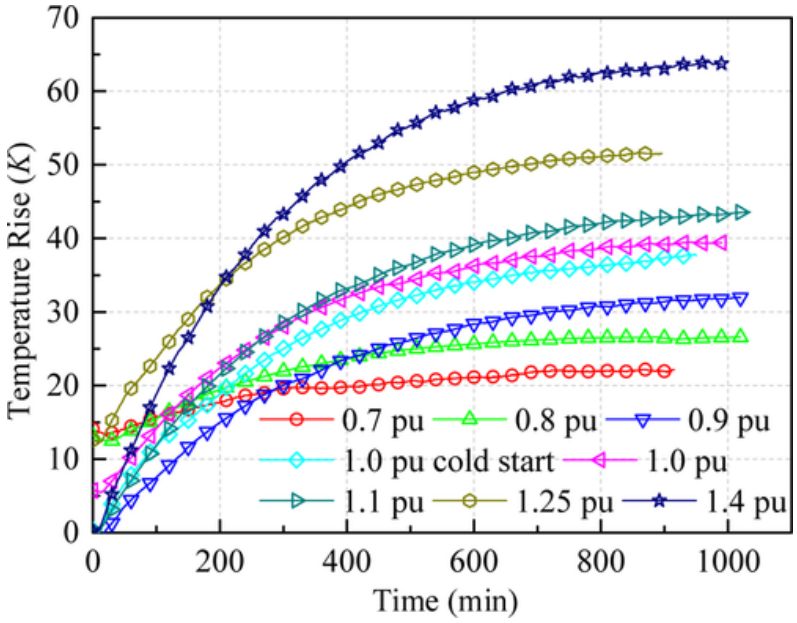

Figure 3.6: Measured oil rises at various loading and starting temperatures, from [100].

minutes. This result is of note as the IEC loading guide provides 180 minutes [8], but the authors determined these results provide time constants up to an hour longer. The 45 °C ambient temperature used for testing is higher than the 40 °C maximum specified in the standards, so it is aberrant for a significant portion of the world. The accuracy of the approach was shown using steady-state analysis. However, if the transformer is designed correctly, the steady-state value should always be around 55-70 K, which was reflected in the results.

This issue of an inconsistent time constant was explored in [100] where the authors proposed the concept of the relative thermal time constant (RTTC). The RTTC covers both oil and winding time constants and is intended to address the cold-start scenario, where oil has a higher viscosity. To validate this approach, a 200 kVA 3-phase ONAN transformer was used for the experimentation. A difference does exist between the measured rises at 1 p.u. from a cold start and when pre-loaded, Fig 3.6.

A question that arises from this paper is whether a calculated time constant can be determined without an empirical understanding of the influence of external cooling on

the oil's behaviour? A study of the results confirms that the specified time constant of 294 minutes appears accurate for this transformer. However, this is 1.6 times the 180 minute time constant recommended in IEC 60076-7.

Computational Numerical Methods

A numerical computation method was used to calculate the winding hot-spot temperature in a 100 kVA transformer in [101]. Finite-element or finite-volume methods were used to provide the assessment for each component that was then used as inputs for a sequential analysis method called indirect coupling. This approach solves each new factor only considering the impact the previously assessed factors have on the newly added one. The results in this approach correspond with those reported in [102], using the same external measurement locations, which are shown and discussed in Section 3.4.2. All measurements were taken at static loading levels, and without any reference to the computational duration. Therefore, this approach does not appear to be intended for dynamic loading scenarios.

Artificial Intelligence

An improved hot-spot determination technique using evolving fuzzy system models was proposed in [103, 104]. The authors benchmarked their models against hot-spot temperatures measured using a fibre-infused 25 kVA distribution transformer and those calculated using the IEEE model. In both papers, two datasets were presented, dataset one that did not include overloading and dataset two that did. Dataset one demonstrated a significant accuracy improvement compared with the IEEE model. However, in dataset two, the results were harder to differentiate, although the IEEE model did underestimate the rate of cooling towards the end of the dataset. The authors demonstrate that using root mean squared error, non-dimensional index error, and mean absolute error is the most highly correlated with the measured values. However, the challenge for the reader

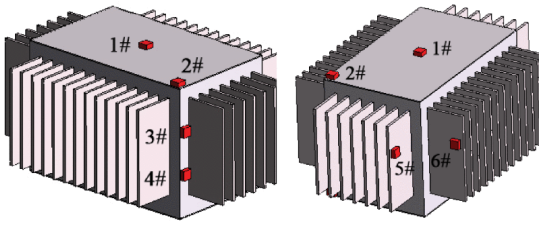

Figure 3.7: External temperature measurement locations for SVR approach in [102].

is that as all the values are normalised and without relating the error to a ±temperature differential, it is not apparent how beneficial this approach is relative to the IEEE model.

Another similar approach was taken in [102] which used support vector regression (SVR) as a hot-spot prediction method. This produced an accuracy within $\pm 3K$. The reason for the accuracy of this approach was that it did not solely model the output using the load but also incorporated multiple temperature measurement points on the outside of the transformer, Fig. 3.7.

Another learning approach to determine hot-spot values is an "Artificial Bee" algorithm [105]. This approach took in measured power and top-oil temperature data and used the artificial bee algorithm running on a computer to estimate the hot-spot temperature. However, as no hot-spot measurements were presented, it is unclear how its accuracy compares with alternative approaches.

Equation-fitting

Polynomial fitting was used to fit an equation to the measured hot-spot data in [106]. The data was measured using multiple fibre optic sensors placed throughout the windings. The polynomial fitting approach was also used to determine the loss of life rate. However, as the loss of life is not instantaneous, a more accurate approach is to take a weighted average temperature across the day, as presented in [48]. Another challenge with polynomial fitting is that there is no guarantee that your fitted equation works for loading situations apart from the scenario in which the data was measured.

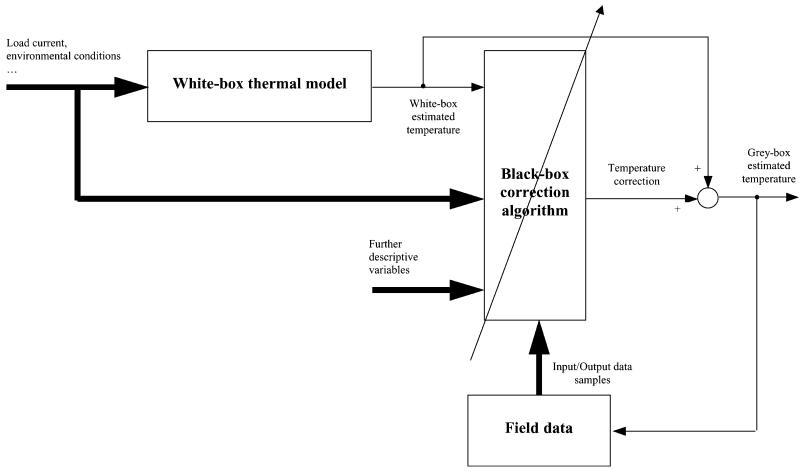

Figure 3.8: Grey-box modelling architecture from [107].

Modelling Methodologies

In [107] three modelling methodologies are presented:

i. White-Box Models – First-principle models that condense the physical insight of the expert. They might contain both physical constants and unknown parameters.

ii. Black-Box Models – A family of linear or non-linear models whose parameters do not have any physical significance. The goal of black-box modelling is to fit the data rather than gaining insight into the phenomena at hand, and thanks to their data-driven nature, these models can be used in an adaptive way to cope with time-varying problems.

iii. Grey-Box Models – An intermediate approach that aims to preserve the best from the previous approaches by integrating knowledge coming from the expert with empirical evidence provided by observations; in particular, the adaptive feature of black-box models is preserved Fig. 3.8.

The Grey-Box model is the closest analogy to the experimental approach taken in this research and leads to RQ2.

3.5 Dynamic Rating

In this section, the review of the existing implementations for dynamic rating in literature, both practical and simulated, are presented.

3.5.1 Definition and Concepts from a Practical Implementation

Formally defined in [36], dynamic rating is *"the maximum loading which the transformer may acceptably sustain under time-varying load and/or environmental conditions."* Several concepts are presented in this paper, providing guidelines for research and implementation of a dynamically rated transformer. These concepts are outlined below:

i. 24-Hour Investigation Period – To establish the thermal behaviour and impact on transformer lifetime, it is appropriate to base any analysis as closely as possible on its operating cycle

ii. Use of a Weighted Temperature – While it is important to assess the instant temperature value to ensure that the maximum limits of 115 °C is not exceeded for Θ_O and 140 °C for Θ_{HS}, it is the averaged weighted temperature that provides a suitable metric for determining loss-of-life due to the fall in DP.

iii. Use of Empirical Data – There is always a compromise with models. Assumptions reduce the complexity but are almost certainly a source of error. Increasing the number of parameters can improve accuracy but increases the model's complexity. Empirical data, when available, allows for the number of assumptions to be reduced, without increasing model complexity, thereby improving accuracy.

iv. Use of an Iterative Algorithm – Temperature is constantly updated based on the current level of loading

3.5.2 Simulation using Modelled Thermal Characteristics

Empirically-Based

A study into the feasibility of applying dynamic rating to distribution assets was presented in [108]. In this work, peak loading was limited to ensure the transformer hot-spot temperature did not exceed the thermally upgraded Kraft paper normal of 110 °C. However, the maximum overload they were able to achieve with sub-zero ambient temperatures was approximately 1.275 p.u. which raises the question: Would improved information about the internal thermal behaviour of the transformer allow for additional capacity? The authors acknowledge that their distribution transformer model would be more accurate if they had additional information, such as the mass of oil and no-load losses. Therefore, typical industrial values have been used, which adds uncertainty to the calculation. They also concluded that two distribution transformers were the most significant constraints on the network.

In [109] an optimal dispatch strategy for inclusion of PV in a network which utilised a DTR approach for the transformer was presented. This paper showed that relying just on DTR for the transformer would provide zero net benefit in this instance, as it did not account for voltage rise due to the PV installations. However, it did demonstrate that when coupled with active methods, it did provide the greatest increase in the available capacity of the circuit. This approach relied on the accuracy of the IEEE model [66] but did include thermal time constants for the oil and windings, indicating that they were empirically derived. No data was included to show whether increased numbers of EVs would offset the voltage rise enough so that DTR could be used as a solution in isolation of the active methods proposed.

K-Means clustering was presented as an overloading risk assessment tool in [110]. This unsupervised machine learning method was used to determine the transformer

loading thresholds throughout a year, rank the clusters based on their impact on transformers, calculate the transformer temperatures and life loss for each cluster relative to the number of services, and estimate temperatures and the loss of insulation life for a new transformer. The per unit loading levels determined using this approach exceeded the maximum p.u. loading specified by the IEC [8], so would need to be adapted for use outside of North America. A challenge with this approach is, while accounting for seasonal variation, it does not account for unexpected additional loading, such as households purchasing EVs.

In [111], a strategy combining a demand response compute program with DTR to ensure a transformer could accommodate the expected demand was proposed. Two 500 kVA transformers with ONAN cooling were used for the case study, along with measured load data and a calculated Θ_{HS} using Kraft paper with a normalised lifetime of 98 °C. Using constant loading and assuming a base load of 0.86 p.u. the authors proposed that an additional 0.49 p.u. could be added to the transformer while ensuring the acceleration factor remained below 1. The case study results showed that using such an approach did provide a modest improvement in the available capacity. The temperature rise was such that the transformer's lifetime and thermal limits would be compromised after only a brief period of operation beyond nameplate rating. If the empirical thermal rises were not as fast as those used in the prediction, it is likely that there may have been more available capacity than presented. However, another challenge with this approach is its reliance on a normalised lifetime, which is 17.2 years according to the IEC [8] or 20.5 years if referencing the IEEE [66]. Assuming the utility requires a lifetime of 35 years, the factor would have to be reduced to 0.491 or 0.585 respectively, to ensure the required lifetime is not violated. This same challenge exists in [112], which presents a solution that combines both dynamic line rating (DLR) with DTR, setting a maximum Θ_{HS} of 110 °C. Assuming that thermally upgraded kraft paper is used, this approach effectively keeps the acceleration factor ≤ 1. Therefore

the challenge with this approach is that unless the daily loss-of-life is determined, the transformer may be retired at a less than optimal time, as this may not coincide with the utility's capital expenditure plan or there is an unknown amount of useful life remaining.

Probabilistic

Probabilistic approaches for determining the appropriate loading levels for Dynamic Rating were proposed by the authors in [39, 113, 114]. The concept of the Hourly Expected Per unit Rating (HEPR) is adapted for transformer use in [39], and is calculated according to (3.3).

$$HEPR(I_h) = 100 - 100 \cdot \frac{I_{wmlc_h} \cdot I_h}{I_h} \tag{3.3}$$

where

I_{wmlc_h} is the weighted mean load curtailment, where 0 equals 100 % delivery of expected demand and I_h is the transformer load current expected for the hour. Recommended limits based on probabilistic analysis were presented in [113] and a probabilistic predictive tool, "SmarTrafo", was introduced in [114] as a means to implement dynamic thermal rating. This approach uses the probabilistic stress-strength framework, in which transformer load is the stress and the dynamic thermal rating (DTR) is the strength. The "probability of success" is the probability of the load not exceeding the DTR. It applies a predictive "Stress-Strength Evaluation Procedure" (SSEP) to determine the probability of success. This is followed by a second stage, the "Multi-Objective Alarm-Setting Strategy" (MOASS) on the predicted probability of success, to decide whether setting or not an alarm for the considered transformer. However, none of the probability methods described in [39, 113, 114] have assessed the probability that the predicted Θ_{HS} is itself accurate. This is acknowledged in [114] which includes addressing the validation of the proposal with experimental Θ_{HS} data as future work.

3.5.3 Simulation using Measured Thermal Characteristics

Similar to [103, 104] the solution proposed in [40] utilises temperatures measured on the external tank wall to aid with determining the internal temperature. The authors proposed (3.4) as a method for determining the loading capacity of a transformer.

$$LC = a + b \cdot \Theta_A + c \cdot \Theta_S \tag{3.4}$$

where

LC is the maximum loading capacity of the transformer, a,b and c are empirical factors derived from (3.5) and Θ_A and Θ_S are the respective measured ambient and station (transformer housing) temperatures (°C).

$$\Theta_{HS} = \Theta_O + HST_F \cdot G \cdot K^y \tag{3.5}$$

where

HST_F is the hot spot factor (1.1), G is is the temperature gradient between the winding and the oil at rated load, K is the current load in p.u. and y is the winding exponent (0.8).

In effect, this approach scales the measured temperature on the outside of the tank to the oil temperature inside. The authors indicated the only thermal model verification was measuring the top-oil temperature (TOT) and relying on an accurate value of G to calculate Θ_{HS}. The authors also noted that the use of the IEEE and IEC empirical models underestimated the TOT, potentially shortening the transformer's life.

Relying on measured data for increased accuracy was the methodology also used in [115]. However, unlike [40] which focused on TOT, [115] examined Θ_{HS}. Three comparative scenarios for Θ_{HS} determination were presented:

Scenario One Relies solely on IEC recommended parameters and thermal model

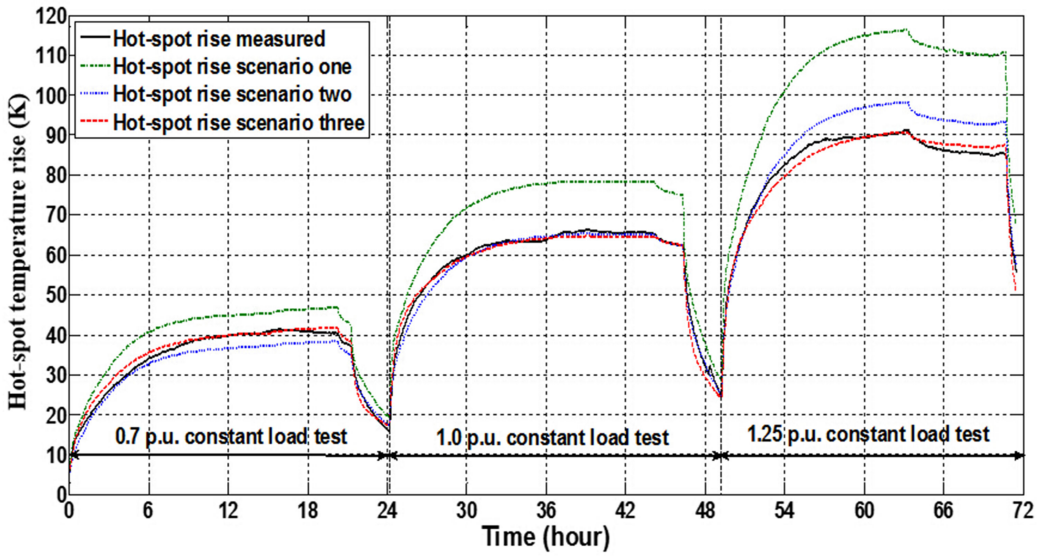

Figure 3.9: Measured and calculated hot-spot temperatures for scenarios one-three from [115].

Scenario Two Relies on empirical heat-run test to determine parameters for use with IEC thermal model

Scenario Three Measured Θ_{HS} values are available and equations are generated using curve-fitting

The results in Fig. 3.9 demonstrate that the more empirical information available, the more accurate the modelling. No explanation is provided for the minor dips, before the large one, where the load appears to be disconnected. However, it is reasonable to assume that it is dropped to a known load value as all the modelled parameters follow the same profile.

3.6 Condition Monitoring

A neural model proposed in [116] used measured Θ_{HS} data for training the model and load, top-oil and ambient temperatures plus weather station as inputs for the model, shown in Fig. 3.10. This approach demonstrates a very high degree of correlation with

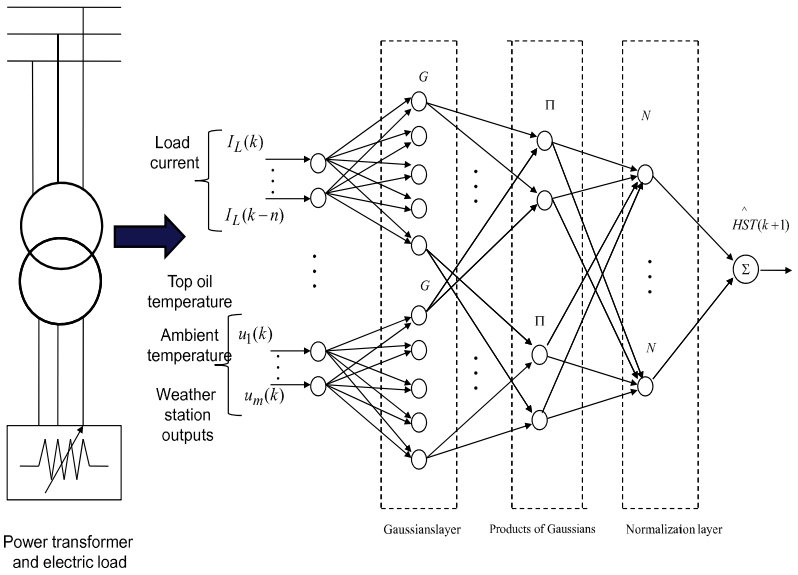

Figure 3.10: Neural model for thermal hot-spot determination in [116].

the measured Θ_{HS}. The authors advise that thermocouples were placed in the windings for Θ_{HS} and in the oil for Θ_O, with hall-effect current transducers measuring the load. Assuming this high degree of correlation is an expected normal, this approach allows the residuals to be used as an early detection metric for faults. When no faults are present, the measured and neural network output should differ only by any measurement noise affecting the sensors. Any difference outside of this range would indicate a potential issue.

Machine learning was also a factor in [117] which used a generic algorithm for indicating an issue with the monitored transformer. It uses four parameters, voltage, current, oil level and top-oil temperature. According to the authors, if the output of the generic algorithm produces a result 70 % or better parameters are bound together, and the health index registers behaviour is normal. Below 70 % the parameters are no longer bound, and an abnormal result is provided. The results presented did not appear to offer definitive evidence that the system worked as described.

3.7 Design Optimisation Strategies

3.7.1 Dimension The Load To Fit The Transformer

In most cases presented in this section, transformer design optimisation is intended to provide a best fit of the transformer to the load. However, in [118], the transformer size was fixed and a computer algorithm assessed if the transformer would be overloaded. If so, up to 1.3 times the standard distance away, the closest customer would be connected to another less-loaded transformer. This solution was appropriate for the South African demographic being served as their typical loading demand was light. However, such an approach is likely to be unsuitable for less densely populated areas or where there is higher average demand.

3.7.2 Minimise Losses

Reducing load and no-load losses to improve transformer efficiency is the stated goal of a three-dimensional finite element model (FEM) presented in [119]. According to the authors, using this approach results in an accurate estimate the transformer losses and short-circuit impedance which provides the following benefits:

i. Increased reliability and manufacturer credibility.

ii. Desired efficiency is achieved.

iii. Reduced material cost due to smaller design margin.

iv. Improved delivery time, as no transformer prototype is required to confirm the accuracy of transformer design. Neither are short-circuit tests under nominal voltage required.

A multi-objective design optimisation was presented in [120], also sought to better align the designed short-circuit impedance values with those prescribed. The FEM

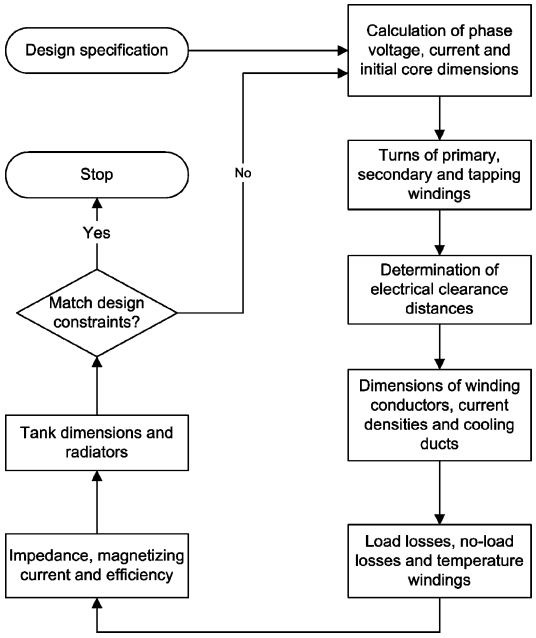

Figure 3.11: Object-oriented knowledge-based design process from [121].

techniques used in [119, 120] appear to provide a high accuracy approach for simulating the transformer magnetic field. However, other than the inclusion of cooling ducts to better assess the magnetic field, no consideration is given to the thermal behaviour of the transformer, limiting this approach for use in dynamic loading situations.

3.7.3 Multiple Designs

An "object-oriented knowledge-based" system for distribution transformer design was presented in [121]. The intention is to use the program to generate multiple outputs for a transformer design to determine which one best meets the customer's design specification in terms of impedance, efficiency, and magnetising current. The process is shown in Fig 3.11. A very similar solution was presented in [122], which also iterated the design process with considered factors very similar to [121] in its design algorithm. However, as neither of these processes considers thermal characteristics or the required lifetime, it is unlikely to be suitable for dynamic loading scenarios.

3.7.4 Optimise Geometry

FEM approaches typically incorporate a degree of geometric optimisation within the process. However, this was touted as a feature of a program presented in [123], which was used to optimise the geometry of the magnetic shielding in a distribution transformer design. However, like other FEM examples presented, the only consideration given to thermal behaviour was the inclusion of cooling ducts in the windings. This inclusion was as an examination of the magnetic characteristics, not the effectiveness of the ducts to contribute to controlling the wire temperature.

3.7.5 Thermal Behaviour

In [124] the thermal behaviour of the windings and oil-flow was extensively modelled. However, the authors assert that the only way to get Θ_{HS} is to calculate each conductor's detailed winding temperature distribution. The challenge with this approach is that it assumes your thermal model is correct. However, the heating due to the transformer's loading may not be enough to overcome the cooling effect of the oil. Such an effect is seen in Fig. 5.5 in Chapter 5, where $\Delta\Theta_{HS}$ at 0.5 p.u. is effectively zero. Therefore, despite the assertions that this approach delivers an exact value and position of the hot-spot temperature, no validation with empirical Θ_{HS} measurements was presented in the paper. Maximising transformer cooling was the objective in [125] using a response surface method, which is an experimental, or simulated, data-fitting approximation model. While improved cooling is advantageous to a dynamically loaded transformer, the value of this approach does not appear to be highlighted in the paper.

3.7.6 Minimise Material Cost

The optimisation methodology in [126] combines FEM techniques with a heuristic algorithm to minimise material costs according to

$$MC = min \sum_{i=1}^{4} c_i f_i(x) \tag{3.6}$$

where

MC is the material cost, c_i and f_i are the unit costs and weight of the i^{th} winding, core, oil, and structure materials. Unlike the FEM solutions in [119, 120], this approach considers the thermal rise of the transformer. While the algorithm output suggested the top-oil rise would be 48 K, the measured rise of 51 K is still within the ranges recommended by IEC [8] and IEEE [66]. Cost minimisation was also the optimisation objective in the simulation carried out in [127]. This approach used a "cuckoo search algorithm" which is a swarm intelligence-based optimisation algorithm. The reference to cuckoo is that its behaviour is similar to that of a cuckoo. If the solution is good, the "cuckoo" assumes it is one of its "eggs" and the solution is allowed to persist. If the solution is poor then the "cuckoo" recognises it is an "alien egg" and "tips it out of the nest", eventually resulting in an overall global optimisation.

Another approach using a tree-pruning algorithm was presented in [128]. This approach is similar to the cuckoo search algorithm. However, rather than being "kicked out the nest", the less ideal solutions are "pruned" from the optimisation "tree". This method was validated using a distribution transformer conforming to the algorithm output, with all factors found to be within specifications.

3.7.7 Minimise Total Cost of Ownership

Total cost of ownership (TCO) for distribution transformers is recognised as the purchase cost plus operational cost for the lifetime of the asset [129], and this is recognised in the TCO calculation in [130]

$$TCO = BP + A \cdot p_{core} + B \cdot p_{wdg} \tag{3.7}$$

where TCO is the total cost of ownership, BP is the bid or buy price, A is the unit cost of the no-load losses, p_{core} are the no-load losses, B is the unit cost of the load losses and p_{wdg} is the load losses. However, low utilisation affects the transformer's operating efficiency. Mid-to-high utilisation is the point of highest efficiency, and operation at this level contributes to minimising the transformer load losses.

3.7.8 Multi-Objective Optimisation

Minimising purchase cost, total lifetime cost, mass, and transformer losses using a proposed modified design variable approach was presented in [131]. However, as such an optimisation approach does not consider actual use and expected lifetime. If the transformer experiences low utilisation over its lifetime, then none of these optimisations will be realised due to higher capital cost and lowered efficiency.

Four sets of competing objectives were used in a multi-objective evolutionary algorithm approaches in [132–134]. This approach set

i. Purchase Cost against Total Loss

ii. Purchase Cost against TCO

iii. Total Mass against Total Loss

iv. Total Mass against TCO

subject to practical constraints. These approaches, while comprehensive, assume transformer losses alone dictate TCO. However, utilisation, reliability and a coincident retirement age and expected transformer lifetime, are also factors that contribute to the TCO equation.

A particle swarm optimisation approach was presented in [135] to minimise material costs while minimising losses to reduce the customer costs over the transformer's lifetime. The modelled saving when considering losses was in the region of $10k over 15 years. However, the copper loss amounts for both scenarios are speculative without insight into the realistic utilisation levels experienced by the transformer over its lifetime.

3.8 Research Questions

In this section, the research questions that arise from gaps in knowledge are presented along with where they are addressed in the thesis.

RQ1 Increasing the utilisation of transformers can reduce losses and allow for deferred capital expenditure. However, as no method has yet been presented in the literature that addresses the issue of how to design a transformer whose retirement age coincides with its end of life, what is required to design a transformer to last a specific lifetime when the IEC and IEEE recommended normal lifetimes do not agree?

RQ1 (a) What transformer parameters need to be assessed in such a process?

RQ1 (b) Can the fall in the degree of polymerisation provide a standards' agnostic lifetime determination methodology?

RQ2 Is there latent capacity beyond a transformer's nameplate rating that can allow for distribution transformers to be less of a constraint on the distribution network?

RQ2 (a) How can such capacity be assessed and utilised without risking transformer health or lifetime?

RQ3 The winding hot-spot temperature, Θ_{HS}, is assumed to be a rise over the Top-Oil temperature Θ_O. However, no comparison in literature examines whether there is any interdependence between the rate $\Delta\Theta_{HS}$ rises and $\Delta\Theta_O$. The empirical models imply that $\Delta\Theta_{HS}$ is solely due to τ_W and its rise is independent of τ_O. Therefore, how accurately do the thermal models presented in literature reflect measured $\Delta\Theta_{HS}$?

RQ3 (a) If any interdependence is observable, does it provide any insights that could contribute to better understanding to operation of a transformer in the presence of dynamic loading?

RQ3 (b) Can such an insight contribute to better accuracy in modelling $\Delta\Theta_{HS}$ and $\Delta\Theta_O$ in a transformer where empirical data exists?

RQ4 Can load forecasting be incorporated to provide an improved dynamic rating algorithm?

RQ4 (a) Is there a method to determine maximum instantaneous loading allowable in the presence of unknown future load if it is higher nameplate rating?

RQ4 (b) Which parameters and time constants, τ_O and τ_W, are relevant and required to support forecasting?

The research questions RQ1 and RQ2 and associated sub-questions are addressed in Chapter 4, while RQ3 and RQ4, along with their sub-questions, are addressed in Chapter 5.

3.9 Chapter Summary

The body of existing literature related to this work was examined in this chapter, particularly the current understanding of dynamically rating transformers with models and monitoring and dynamic thermal modelling. Four research questions that arose from the gaps in knowledge and addressed in this thesis were presented along with the original research chapters that address these questions.

Chapter 4

The Empirical Design Method

4.1 Introduction

This chapter contributes the introduction of a new paradigm: "designing for maximum utilisation" for the future design of distribution transformers. This paradigm runs contrary to the prevailing distribution transformer design methodology, where the customer requests a specific rating and the manufacturer supplies the transformer. If the customer made the nameplate rating determination to accommodate peak loads or a multiple of the existing load, to keep utilisation low leads to an over-specification for the nameplate rating of the transformer, with an expected lifetime many times the expected in-service lifetime of the transformer.

The "designing for maximum utilisation" paradigm is instead a collaborative approach between manufacturer and customer to design a transformer that lasts a specified lifetime allowing the transformer to be used to its capacity, and providing a mechanism for retirement date and end of life to coincide. A comprehensive methodology to achieve this goal is presented, which ensures no aspect of utilisation maximisation compromises standards throughout a distribution transformer's lifetime, thereby realising the "designing for maximum utilisation" approach practically. The distribution transformer design

algorithm proposed in this chapter also addresses the limit distribution transformer voltage regulation imposes on utilisation levels, while also allowing for the influence on distribution transformer lifetime of temperature, internal distribution transformer tank pressure and oil leakage through tank corrosion. In addition, the proposed algorithm permits accurate design for a particular distribution transformer age. Therefore, it can be easily integrated into asset management policies based on planned replacement, and before distribution transformer failure, to minimise the system average interruption duration index (SAIDI) and system average interruption frequency index (SAIFI) numbers. Asset management policies of this type may be necessary for future distribution networks heavily loaded by electric vehicle charging that operate high utilisation levels to avoid high outage levels.

The final contribution in this chapter is an extension to the "designing for maximum utilisation" approach, which we refer to as the dynamic degree of polymerisation (DDP) process. DDP allows lifetime determination to be assessed across the years of expected load increase, along with the number of years the percentage base load increase can be accommodated before the required lifetime of the transformer is no longer satisfied.

The remainder of the chapter is structured as follows. In Section 4.2, an overview of the design algorithm and motivations for its implementation are provided. Section 4.3 provides a detailed breakdown of the algorithm, explaining its component parts. Section 4.4 describes how it has been used and validates the approach, using design and in-service transformer case studies.

4.2 Overview of Design Algorithm and Implementation

The algorithm proposed in this chapter enables "designing for maximum utilisation", a unique approach to distribution transformer design. Finalised distribution transformer

designs using this approach are the result of a collaborative effort between the distribution transformer manufacturer and distribution network operator (DNO). Traditionally the DNO will specify a VA rating and the transformer manufacturer will supply the transformer in accordance with the specification. However, this does not assess the suitability of the distribution transformer to accommodate increasing loads or establish whether retirement age and distribution transformer end-of-life correlate.

In [136], 65 % of the transformer withdrawals were found to be due to retirements, not failure. The authors, while determining a typical useful life for distribution transformer of 20 years, also calculated a Kaplan-Meier mean life of 74 years and noted the mean life of an Australian DNO's 33 kV units was 58 years. While demonstrating the reliability of distribution transformers, this also highlights that short of a catastrophic failure, establishing the "when to retire" for a distribution transformer has not been an exact science.

The DNO referred to in this chapter, sought to reduce this uncertainty. Having already established the required lifetime for their assets, and predicted the likely loading increase over the distribution transformer's lifetime, the DNO sought a distribution transformer manufacturer who could provide a level of assurance that their specified retirement age and the expected life of the distribution transformer would coincide. To this end, they supplied the retirement age, current load and ambient temperature profiles and expected annual percentage load increases, prior to distribution transformer manufacture. This data was incorporated into the proposed design algorithm, which considers a wider range of factors impacting a distribution transformer's lifetime relative to other algorithmic examples in literature, such as [47]. This approach improves upon other algorithms in literature such as [39], which does not ask the question "when the distribution transformer should be retired?", and instead seeks to not exceed the nominal lifetime temperature of 110 °C. Another approach, utilising maximum limits specified

in IEEE Standard C57.91-2011, was used in [110]. However, once the transformer hot-spot temperature (Θ_{HS}) exceeds 140 °C, the oil starts to bubble, and with the increased moisture release, the lifetime accuracy is no longer as predictable. These approaches will ensure the safe operation of the distribution transformer and utilisation improvements, as mentioned in [37]. However, they do not validate compliance with all aspects of relevant standards at all times. For example, overloading the distribution transformer may comply with thermal constraints, but output voltage may drop below the specified regulated minimum, for instance, 216.2 V_{RMS}, in a New Zealand context [45].

Another novel aspect of the proposed concept is that the calculations assume a proportional, not linear, increase in loading. Proportional loading increases were also assumed by [137] in developing their risk-based transformer loading method. Proportionality is the most "true-to-life" representation of increased loading. For example, assuming 100 new dwellings are connected to an LV network, it can be reasonably expected that these new additions to the neighbourhood will still be at work and home in largely the same daily periods as their existing neighbours. Therefore, the impact to off-peak loading will be minimal compared with peak time. If a linear approach was taken, the increase in off-peak load would be the same as that for peak load. This increased base load would produce a higher Θ_{HS} throughout the day, reducing the ability of the distribution transformer to handle the increased peak loading and result in a reduced expected lifetime.

Algorithm 4.1 provides a logical flow for the algorithmic process to determine an optimum utilisation for a given distribution transformer lifetime. The algorithm is an iterative process that begins with the current load profile and increments the entire profile until it violates a parameter, as specified in Table 4.1. At each profile increment, each of the parameters is tested to validate they are still within the specified limits. The process optimisation is completed when a limit is violated, or the desired retirement age can no longer be attained. Whichever factor is exceeded first becomes the reference

Table 4.1: Limiting Factors for Optimal Distribution Transformer Design

Limiting Factor Description	Symbol	Maximum Specified
Maximum loading allowed by standards in p.u.	$EL_{(max)}$	1.8 or 2.0[1]
Highest winding hot-spot temperature before oil bubbling occurs	$\Theta_{HS_{(max)}}$	140 °C
Maximum top oil temperature allowed by standards	$\Theta_{TOT_{(max)}}$	115 °C
Maximum tank pressure specified by manufacturer	$P_{(max)}$	115 kPa or 150 kPa[2]
Local voltage regulation limits	$Reg_{(max)}$	±6 % V_{RMS}

[1]Maximum short-term overloading for medium and small power transformers

[2]Dependent on tank design

for the levels of all the other factors.

The algorithm can be utilised in different ways. For example, the DNO may wish to determine the maximum load that could be handled by the distribution transformer without violating any parameters and consequently, how long its lifetime would be based on that loading. Another application is for DNOs who know how long they would like to operate their distribution transformer for and therefore maximise its utilisation over that period. In section 4.4, examples are presented of how the algorithm has been applied to improve distribution transformer utilisation by DNOs.

4.3 Detailed Description of Design Algorithm

This section breaks the proposed algorithm down into its component parts and discusses each in detail. The algorithm has to achieve three main functions:

1. Establish initial conditions
2. Determine distribution transformer maximum loading based on initial conditions
3. Validate distribution transformer maximum loading

With these high-level goals as a backdrop, each functional block of the algorithm, as

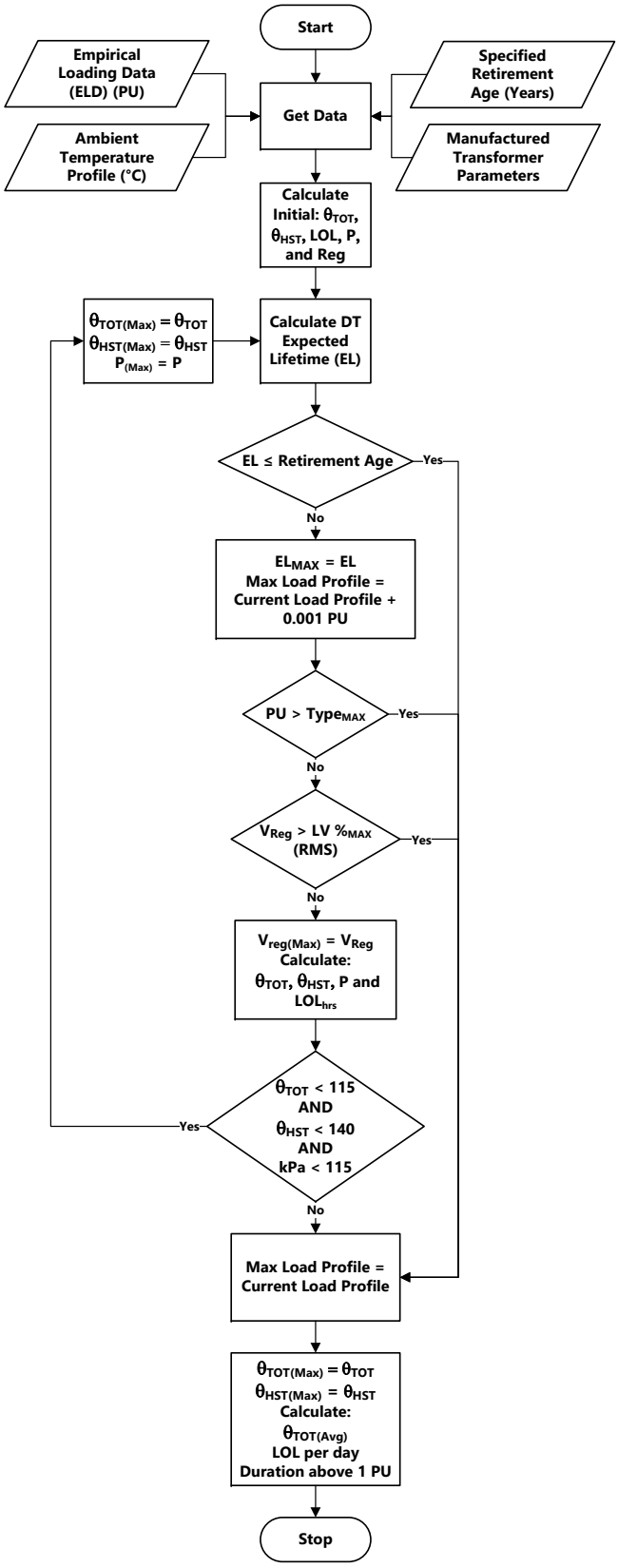

Algorithm 4.1: Logical flow of the optimal distribution transformer design algorithm

shown in Algorithm 4.1 will be covered.

Get Data The algorithm is designed to utilise empirical data for model accuracy, and while preferred, ideal or exceptional scenarios can be investigated as well. The required inputs are:

1. Loading Data
2. Ambient Temperature
3. Retirement Age
4. Manufacturer-Supplied Transformer Parameters

Loading Data Constant load and step load are the two scenario-based options for loading data that the algorithm presently supports, and can be set at modelling time. Empirically-based load profiles are taken from a representative sample of a minimum of 1 month's power consumption. The month was then separated into 24 hour periods, with each being overlaid on top of each other. The average of these profiles, in turn, provide the representative profile utilised by the algorithm for the empirical loading data (ELD) component. The non-linear step increase is set by the maximum loading permissible by the type of distribution transformer. This is significant as the distribution transformers referenced herein were all built according to AS/NZS 60076.7:2013, for which they meet the definition of "*Distribution Transformers*", with an associated short-term overload limit of 2 p.u. [9]. However, according to the recent update, IEC 60076.7:2018, they would be classified as "*Medium Power Transformers*", due to having external cooling fins, and be subject to a 1.8 p.u. limit [8].

Ambient Temperature The degree to which a distribution transformer can be overloaded is usually determined utilising an assumed Θ_A of 20 °C [8]. However, the algorithm also supports the use of a representative daily profile. This is particularly relevant where the Θ_A at peak utilisation is significantly higher than

the specified 20 °C, as this will likely hit the thermal limit before the maximum p.u. is reached. Conversely, a lower ambient can also raise this limit. The delta for each loading sample is taken relative to its corresponding Θ_A.

Retirement Age The operational life of the distribution transformer in years.

Manufacturer-Supplied Transformer Parameters These are the parameters such as tank and core-coil size and weight and heat-run test data, which improve the accuracy of the lifetime calculation.

Calculate Initial $\mathbf{\Theta_{TOT}}$, $\mathbf{\Theta_{HS_W}}$, $\mathbf{LOL_{org}}$, P and Reg The differential equation method is used for calculating the top oil temperature (Θ_{TOT}) and the transformer's hot-test spot temperature (Θ_{HS}), which is fed into equation (4.1) to calculate the winding hot-spot temperature (Θ_{HS_W}), used when determining the DP fall, from which the original loss of life rate ($\mathbf{LOL_{org}}$) is also determined. The internal pressure (P) is calculated using equation (4.2) which provides P in psi, and converted to kPA ($6.895 \cdot P_f$). The percentage deviation in voltage regulation (Reg) is determined using (4.3) from [138]:

$$\Theta_{HS_W} = \frac{1}{\frac{-R}{E_A \cdot ln\left(E_{A_W}\right)}} \tag{4.1}$$

$$P_f = 0.145 \cdot P_0 \left(\frac{\Theta_{HS}}{\Theta_A}\right)\left(\frac{V_{l_0}}{V_l}\right)\left[\frac{K_{i_0} + \left(\frac{V_{g0}}{V_{l_0}}\right)}{K_i + \left(\frac{V_g}{V_l}\right)}\right] \tag{4.2}$$

where

P_f is calculated final pressure (psi)

P_0 is ambient pressure (psi)

V_g is the final gas volume at Θ_{HS} (l)

V_{g_0} is the initial volume (l)

V_l is the oil volume in the tank at Θ_{HS} (l)

V_{l_0} is initial oil volume (l)

K is the solubility factor

K_{i_0} is solubility at ambient temperature

K_i is the solubility at the final temperature

$$(n \cdot Er\% \cdot cos\theta + n \cdot Ex\% \cdot sin\theta) + \frac{(n \cdot Ex\% \cdot cos\theta - n \cdot Ex\% \cdot sin\theta)^2}{200} \quad (4.3)$$

where

n is loading percentage

$Er\%$ is resistance percentage

$Ex\%$ is reactance percentage

$cos\theta$ is power factor

$sin\theta$ is the phase-shift between the current and voltage waveforms

Calculate Distribution Transformer Expected Lifetime The fall in DP is calculated using the rearranged Arrhenius equation:

$$DP_n = \frac{DP_0}{1 + DP_0 \cdot k_n \cdot \Delta t} \quad (4.4)$$

where

n is the step increase

DP_0 is 1000

DP_n is ≥ 200

k_n is $A \cdot e^{-\frac{Ea}{RT_{W_n}}}$

Δt is days since new

EL ≤ Retirement Age Any expected life in the distribution transformer beyond retirement age is unrealised utilisation, thus is discarded. Once the step increase in p.u. load results in a distribution transformer lifetime just less than or equal to expected retirement age, the optimum lifetime and utilisation point has been

reached.

$\mathbf{EL_{MAX}}$ = EL Max, Load Profile = Current Load Profile + $0.\mathrm{x}$ p.u. The new maximum load profile is increased by the proportional step increase. As a point of clarification, the step value of 0.001 p.u. is included as an example only; this value can be set at any percentage increase required.

p.u. > $\mathbf{Type_{MAX}}$ The load is checked for exceeding the p.u. limit (2.0 for Small Power Transformers and 1.8 for Medium Power Transformers).

$\mathbf{V_{Reg}}$ > LV $\mathbf{\%_{MAX}}$ The region-specific regulation is checked for exceeding the limit.

$\mathbf{V_{Reg_{MAX}}}$ = $\mathbf{V_{Reg}}$, Calculate: $\mathbf{\Theta_{HS}}$, $\mathbf{\Theta_{TOT}}$, P and $\mathbf{LOL_{org}}$ The new maximum regulation is set to calculate the temperature, pressure and loss of life values.

$\mathbf{\Theta_{TOT}}$ < 115 AND $\mathbf{\Theta_{HS}}$ AND P < $\mathbf{P_{MAX}}$ This ensures that none of the maximum limits specified in IEC Standard 60076-7:2018 [8], or the distribution transformer manufacturer in the case of P, are exceeded.

Max Load Profile = Current Load Profile The maximum overload condition has been reached. $\Theta_{TOT_{MAX}} = \Theta_{TOT}$, $\Theta_{HS_{MAX}} = \Theta_{HS}$

Complete Final Calculations $\Theta_{TOT_{Avg}}$, LOL per day, Duration above 1 p.u.

Output Optimised Values

4.4 Algorithm Validation

In this section, the algorithm is applied and verified using two cases. In the first case, the algorithm is applied to an existing distribution transformer and to a new design in the second case. In the first case, it demonstrates that a distribution transformer may have additional capacity even when the loading peaks are exceeding nameplate rating. In the second case, the algorithm is applied at design time, so the DNO is able safely to maximise the utilisation of the distribution transformer over its required lifetime.

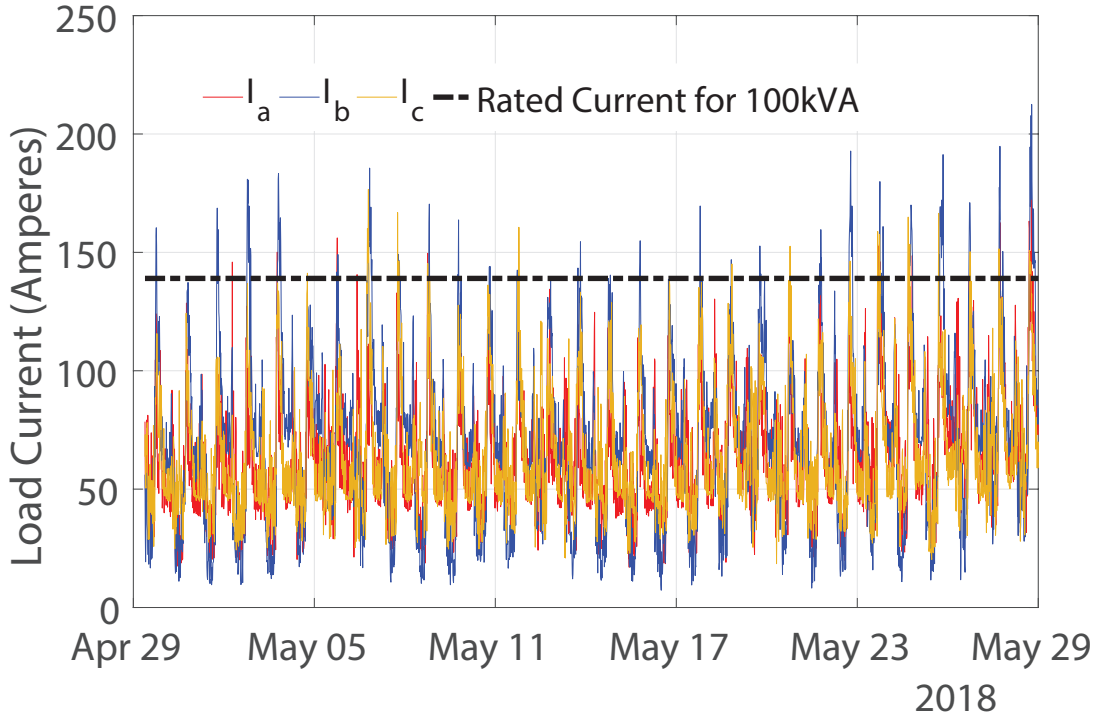

Figure 4.1: DNO-supplied Load Profile Data

4.4.1 Case One: Existing Transformer Exceeding Nameplate kVA Rating

The Problem

The DNO had concerns that the regular exceeding of the 100 kVA nameplate rating may be severely impacting the life of their distribution transformer. To this end, they sought the manufacturer's assistance to determine how severe the impact was to the transformer. The loading data in Fig. 4.1 for one month was supplied by the DNO, where all the peaks above the dotted line are where the load is exceeding the rating. In Fig. 4.2 the monthly data values of Fig. 4.1 were separated into the 24-hour daily load of the transformer and averaged to establish how much stress it was under in a typical day. This load profile is used to determine the transformer's maximum utilisation. Fig. 4.3 shows the heat-run test carried out on the same model that the manufacturer utilised

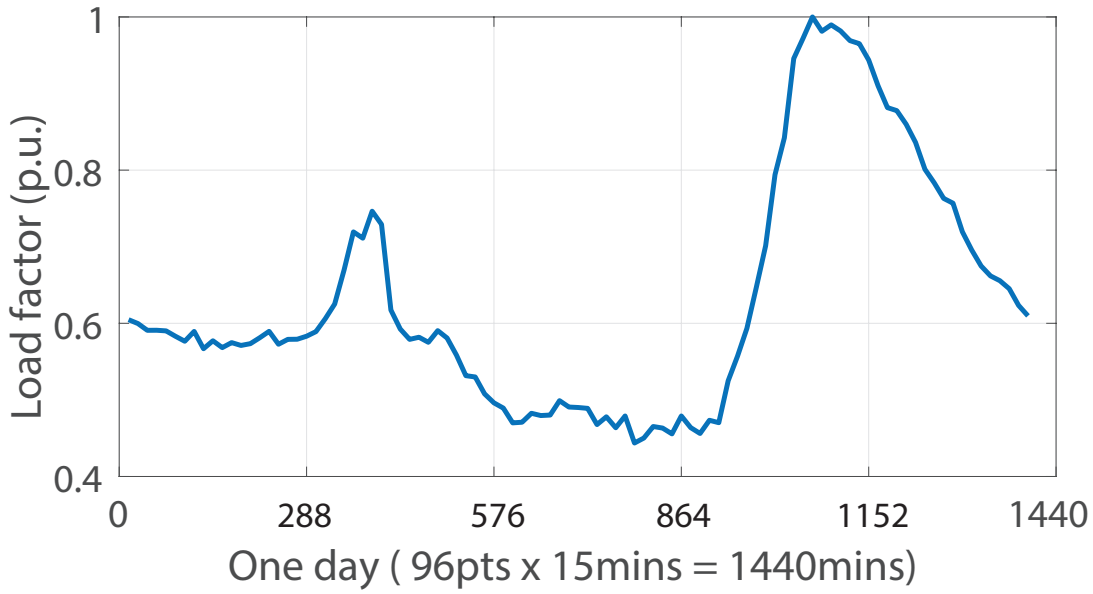

Figure 4.2: Average extracted daily load curve from Fig. 4.1

as an empirical benchmark. Using a curve fitting technique, the final long term fit parameters at rated load, are calculated as final temperature rise value = 57.84 K and τ_O = 494.28 minutes = 8.24 hours. Individual line currents were extracted to determine the duration of operation above the transformer rating. This data showed that over the month, the greatest time exceeding rated current was 285 minutes or 4.75 hours, well short of the measured thermal time constant.

Fig. 4.4 shows the rated top oil rise is calculated as 51.3 K based on the IEC standard temperature rise test criteria. It is also seen that it takes approximately 6 hours to rise from 0 to 32.32 K (0.63 × 51.3 K). The rated values are listed in Table 4.2.

In Fig. 4.5, the calculated TOT has a peak of 55 °C well below the recommended operating temperature of 80 °C. Similarly, the calculated Θ_{HS} is 71 °C, which again is well below the maximum of 110 °C.

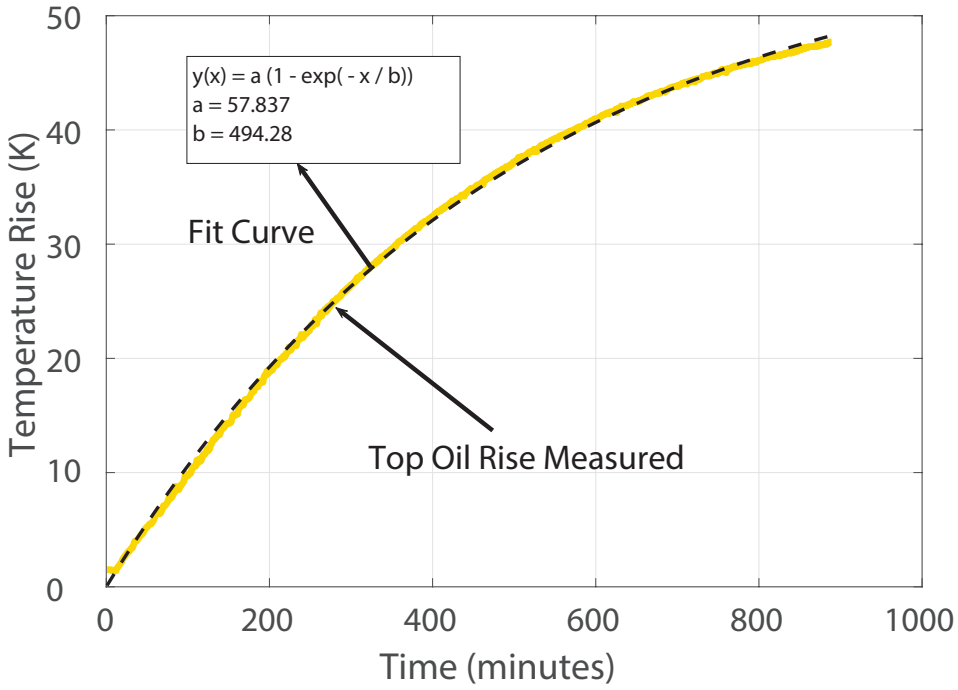

Figure 4.3: 100 kVA distribution transformer: Top oil rise test results

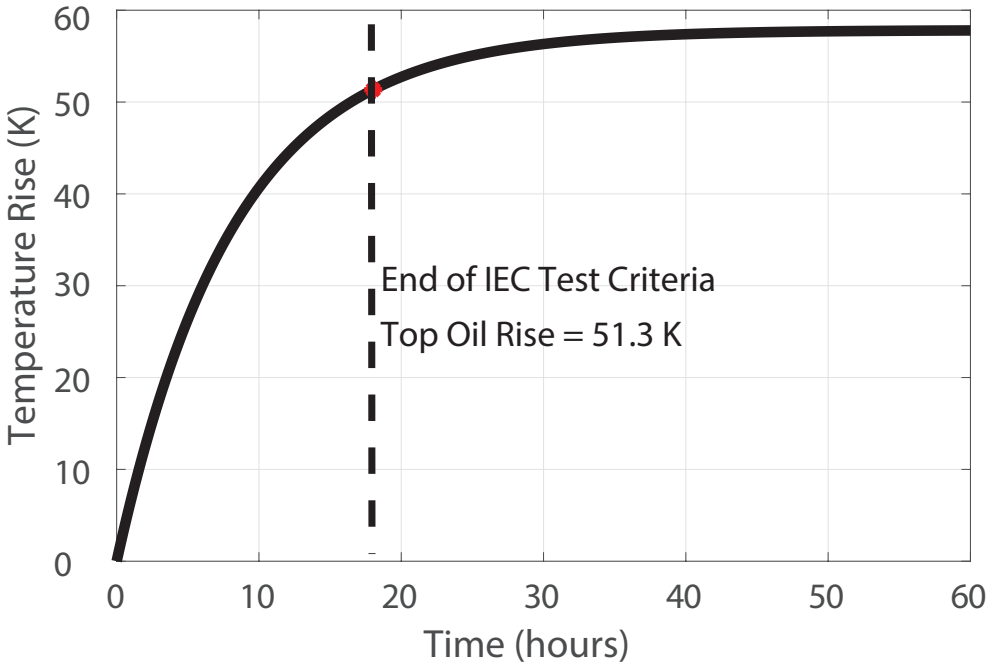

Figure 4.4: Long-term extrapolated Top Oil Rise based on Fig. 4.3

Table 4.2: 100 kVA Transformer Parameters

Number of phases	3
MV / LV Voltage	11 kV / 415 V
LV current	139.12 A
Frequency	50 Hz
Percentage resistance	1.45 %
Percentage reactance	3.95 %
Cooling method	ONAN
Top oil rise	51.3 K
Gradient	14 K
Mass Winding	32 kg (Al) 45 kg (Cu)
Mass Core	224 kg
Mass Oil	275 kg
Year of manufacture	2013

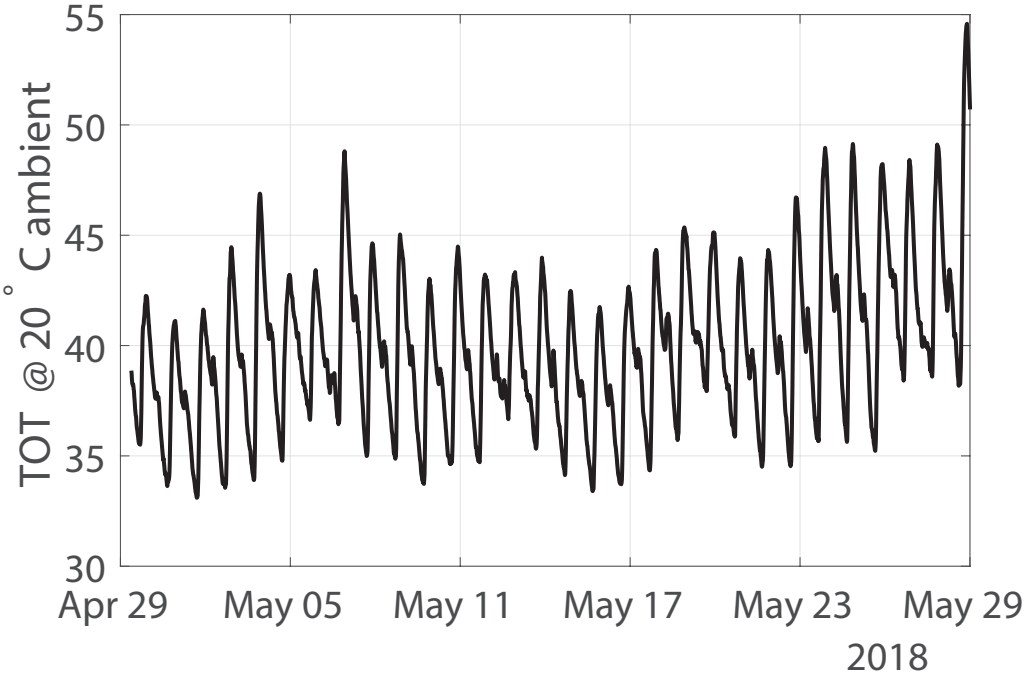

Figure 4.5: Calculated TOT

Algorithmic Utilisation Optimisation

In Fig. 4.2, the averaged 24-hour load profile scaled in p.u. shows the loading peaks at 1 p.u. and is below 0.8 p.u. for approximately 80 % of the day.

Because the transformer was manufactured under AS/NZS 60076-7:2013 [9] the distribution transformer utilisation optimisation algorithm parameters applied to the load profile were as per "Distribution Transformer" or "Small Power Transformer" in IEC 60076-7:2018 [8]. Assuming an average Θ_A of 20 °C is actually a slight overestimation for Auckland, where the annual average sits around 15 °C [139]. However, Θ_A is a significant factor in determining the safe operation of a transformer and with a Θ_A scenario of 30 °C and comparing Fig. 4.6 and Fig. 4.7, it can be seen that the blue Θ_{TOT} line and the orange Θ_{HS} lines are both 10 K higher in Fig. 4.7 than Fig. 4.6. The impact is further observed in the output where the daily safe overloading limit drops from 13 hours at 1.72 p.u. in Fig. 4.8, to 7 and 1.48 p.u. in Fig. 4.9. However, given the slight overestimation for Θ_A, it can be reasonably be assumed the transformer can be safely operated for 34 years. In Fig. 4.10 the optimised load profile, in blue, is overlaid with the supplied load profile, in orange, demonstrating the impact of applying proportional loading, rather than a linear increase. The peaks become "peakier" and the off-peak rise, while apparent, is less significant than at peak times.

4.4.2 Case Two: New Transformer Optimisation Incorporating Increased Loading

The Problem

A requirement for a distribution transformer with a known lifetime in the presence of projected load increases was presented by a DNO, to assist with reliable asset investment planning.

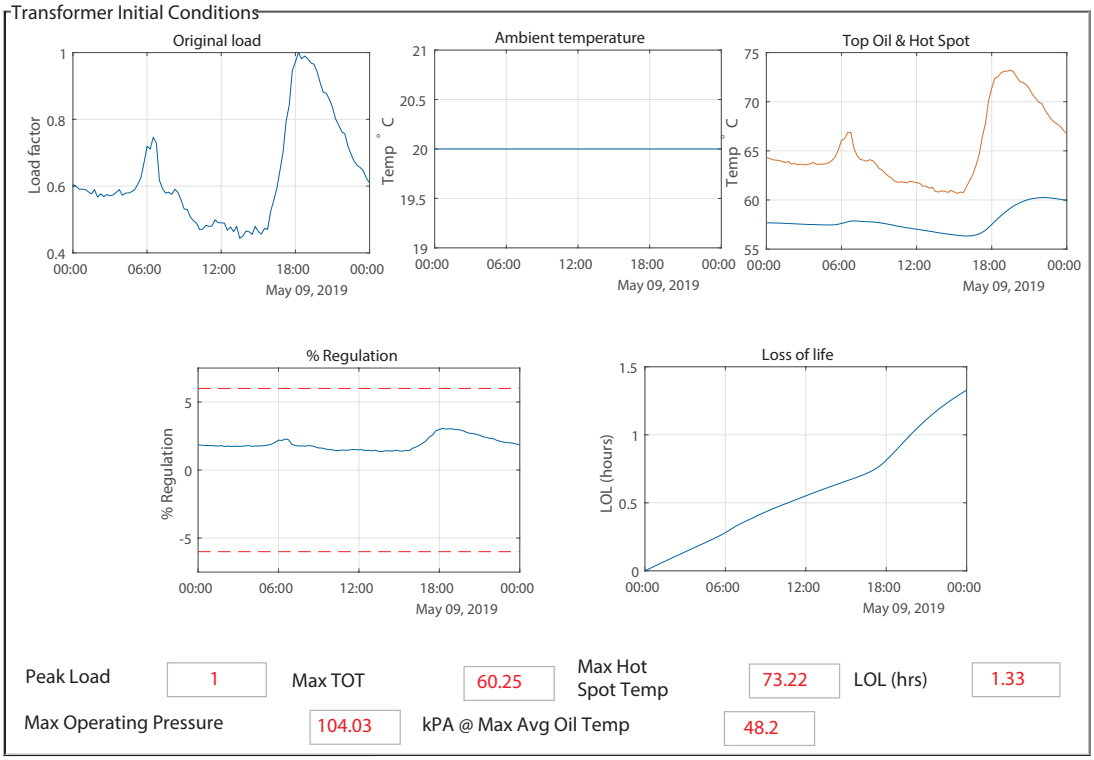

Figure 4.6: Initial Conditions (20 °C Ambient)

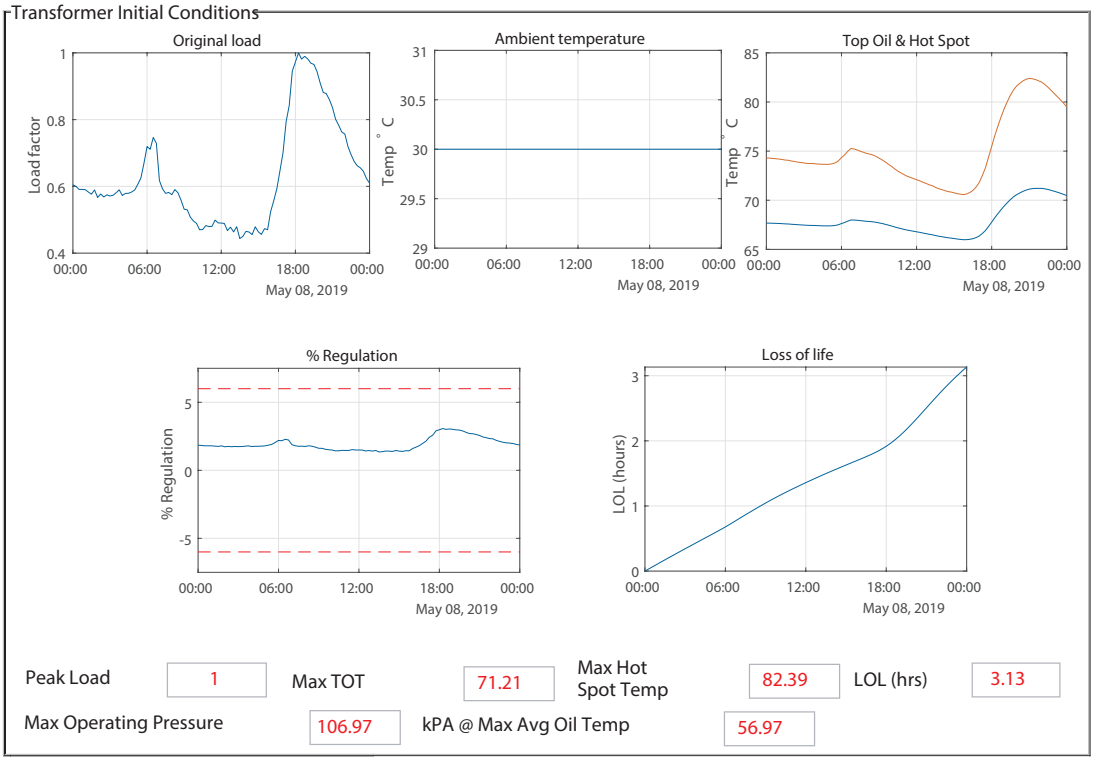

Figure 4.7: Initial Conditions (30 °C Ambient)

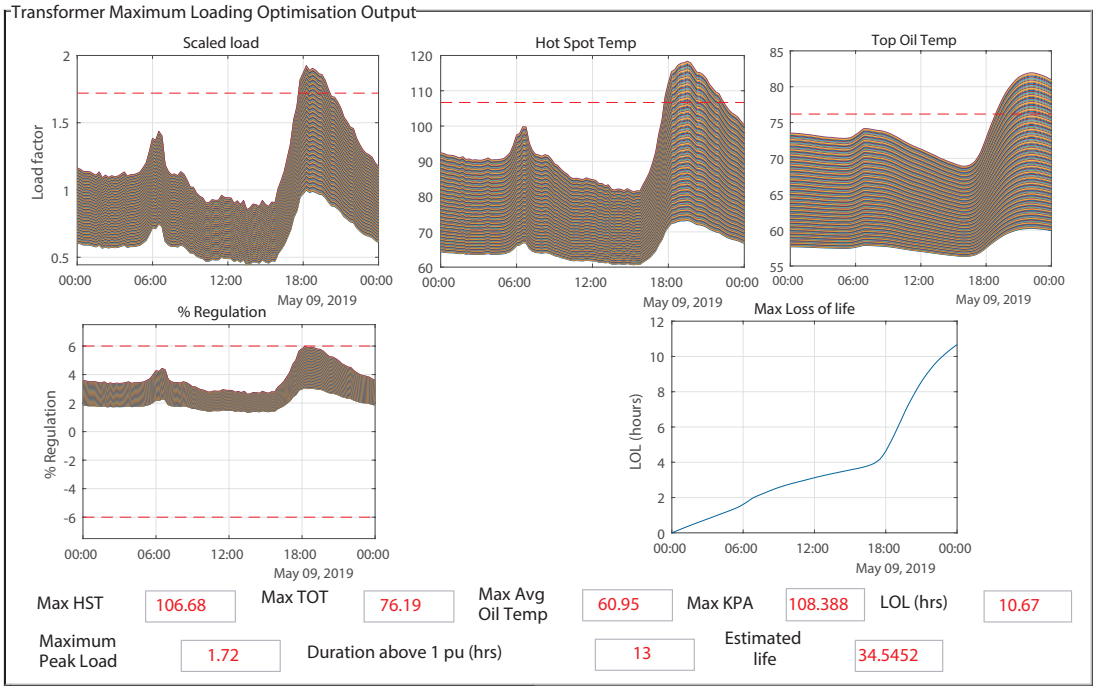

Figure 4.8: Optimisation Output (20 °C Ambient)

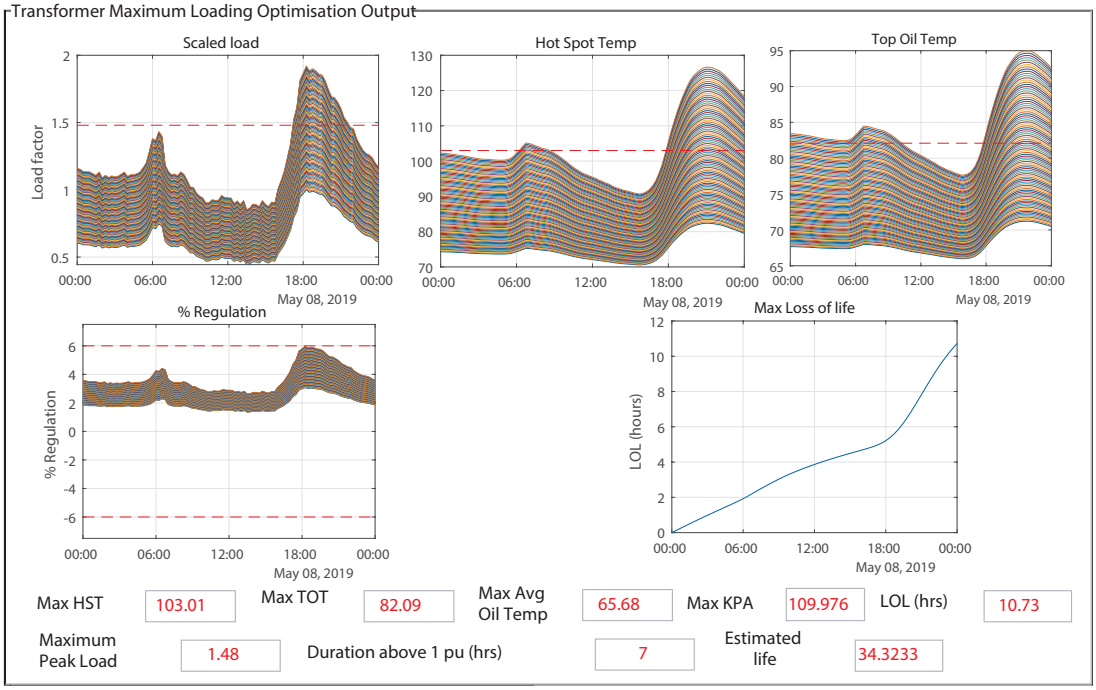

Figure 4.9: Optimisation Output (30 °C Ambient)

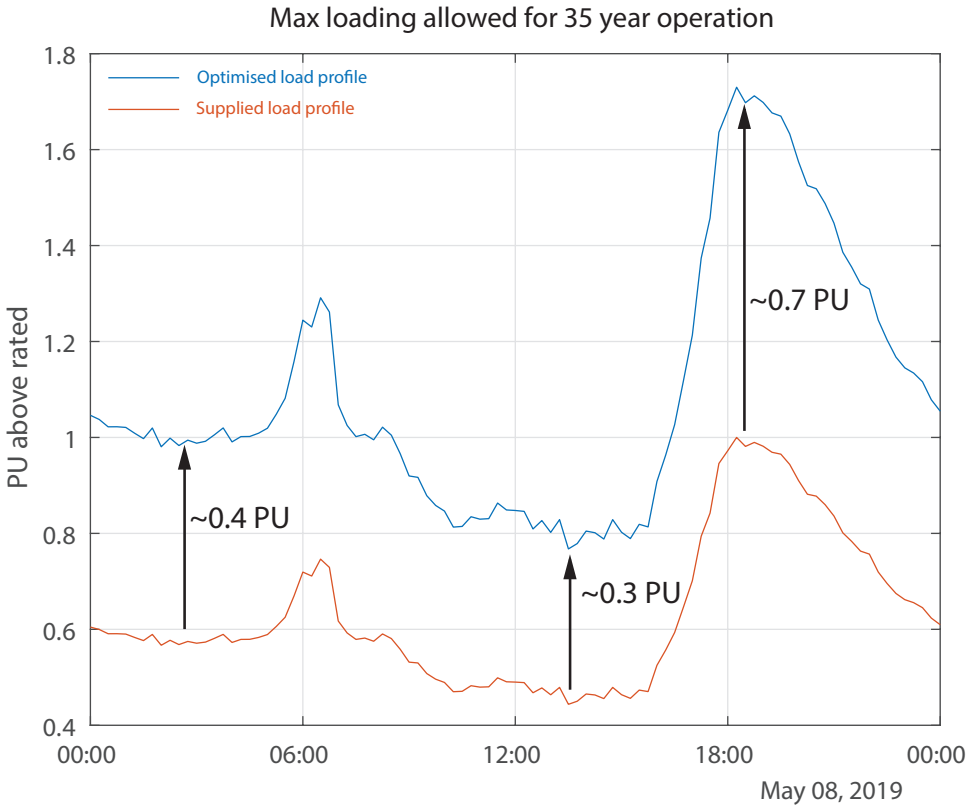

Figure 4.10: Optimised utilisation load profile vs. standard utilisation profile

Table 4.3: 630 kVA Transformer Parameters

Number of phases	3
MV / LV Voltage	22 kV / 440 V
LV current	826.66 A
Frequency	50 Hz
Percentage resistance	0.9 %
Percentage reactance	4.03 %
Cooling method	ONAN
Top oil rise	58.37 K
Gradient	14 K
Mass Winding	114 kg (Al) 128 kg (Cu)
Mass Core	886 kg
Mass Oil	620 kg
Oil time constant	369.18 mins
Winding time constant	6 mins
Year of manufacture	2018

Algorithmic Utilisation Optimisation

To validate the proposed transformer's potential to meet the DNO's prescribed specifications, a step heat run was carried out and simulated in Fig. 4.11 with an ambient temperature (Θ_A) of 20 °C. This simulated Θ_A is again higher than that of the actual heat-run which never climbed out of the teens. Another difference is that this transformer was again designed according to AS/NZS 60076-7:2013 [9], unlike in other cases, all the modelling has been carried out with the "Medium Power Transformer" modelling parameters and limits as specified by IEC 60076-7:2018 [8]. From Fig. 4.12, it can be seen that this design will achieve a lifetime close to the ideal of 35 years and support an additional load of 0.1 p.u. for 14 hours per day.

As the transformer was destined for a location where Θ_A regularly exceeds 40 °C

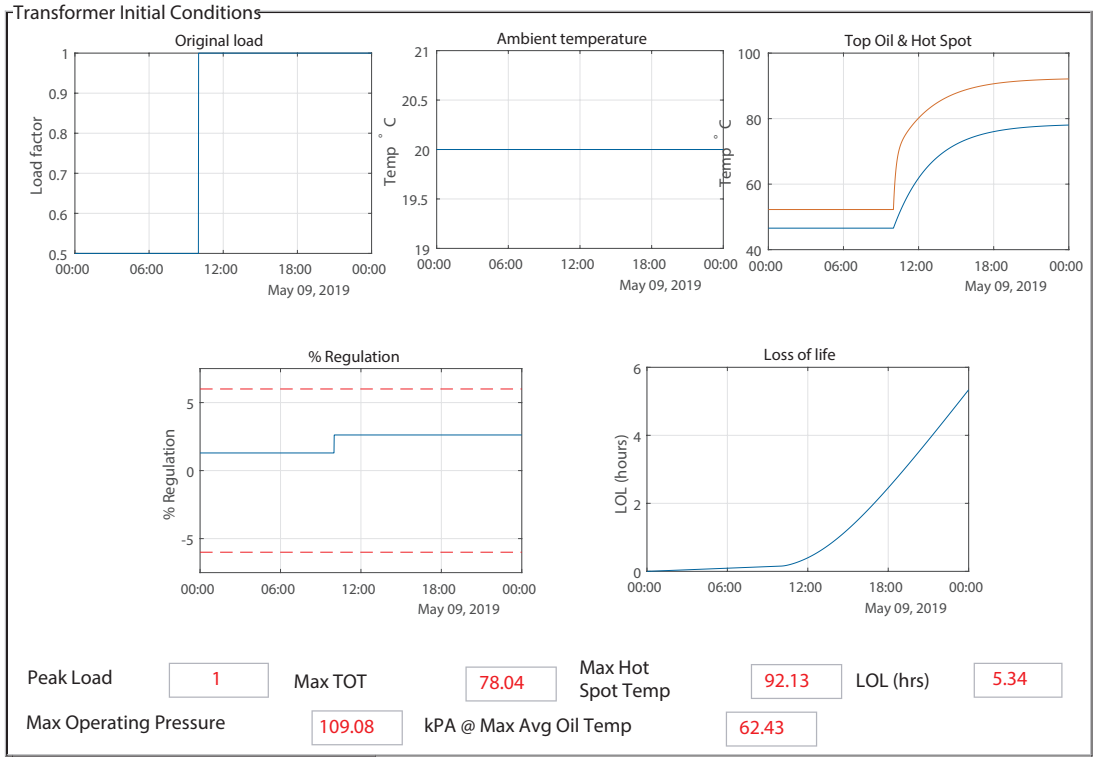

Figure 4.11: Step Increase Modelling Initial Conditions (20 °C Ambient)

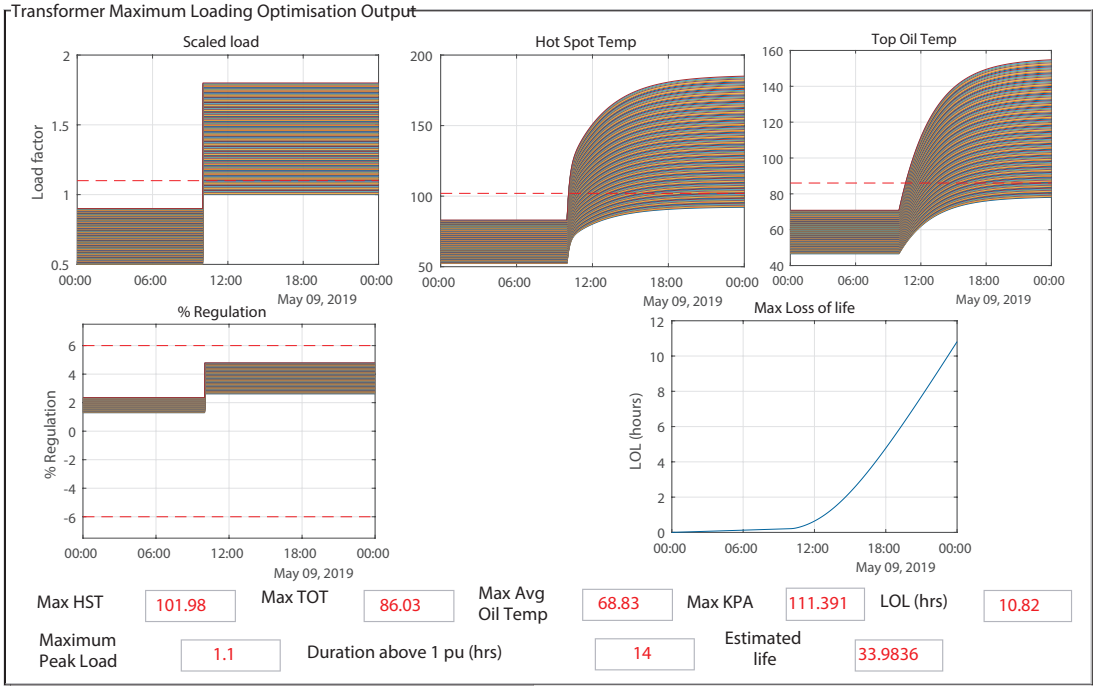

Figure 4.12: Step Increase Modelling Optimisation Output (20 °C Ambient)

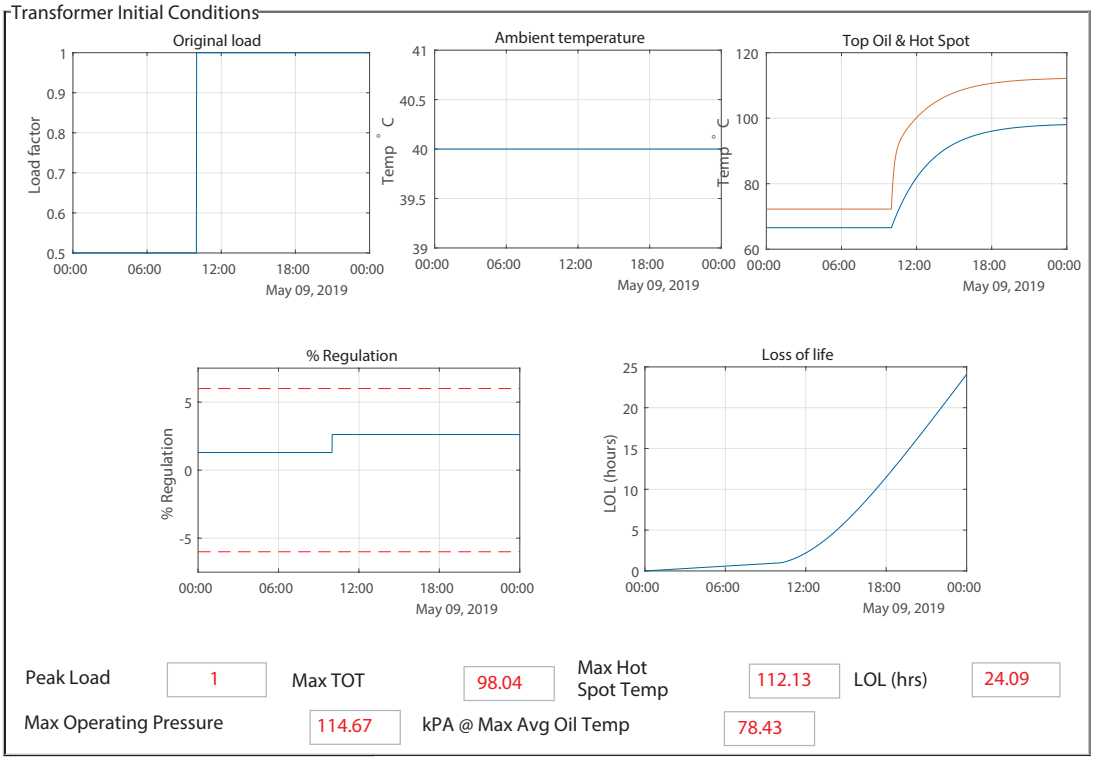

Figure 4.13: Step Increase Modelling Initial Conditions (40 °C Ambient)

the step increase modelling scenario was repeated again in Fig. 4.13, this with a Θ_A of 40 °C. From Fig. 4.14, not only would the transformer not have any capacity to overload; it would not even reach its intended design lifetime of 35 years. The step modelling demonstrated that with a Θ_A of 20 °C, the transformer design is viable, but at 40 °C it is no longer fit for purpose. To determine if the results in Fig. 4.14 are indicative as to the design's apparent lack of suitability, the final modelling scenario is based on empirical load and Θ_A data, Fig. 4.15. Running this data through the optimisation algorithm, it can be seen in Fig. 4.16, that the transformer is, in fact, fit for purpose and can support a modest overload for 2 hours per day for the duration of its 35 year life.

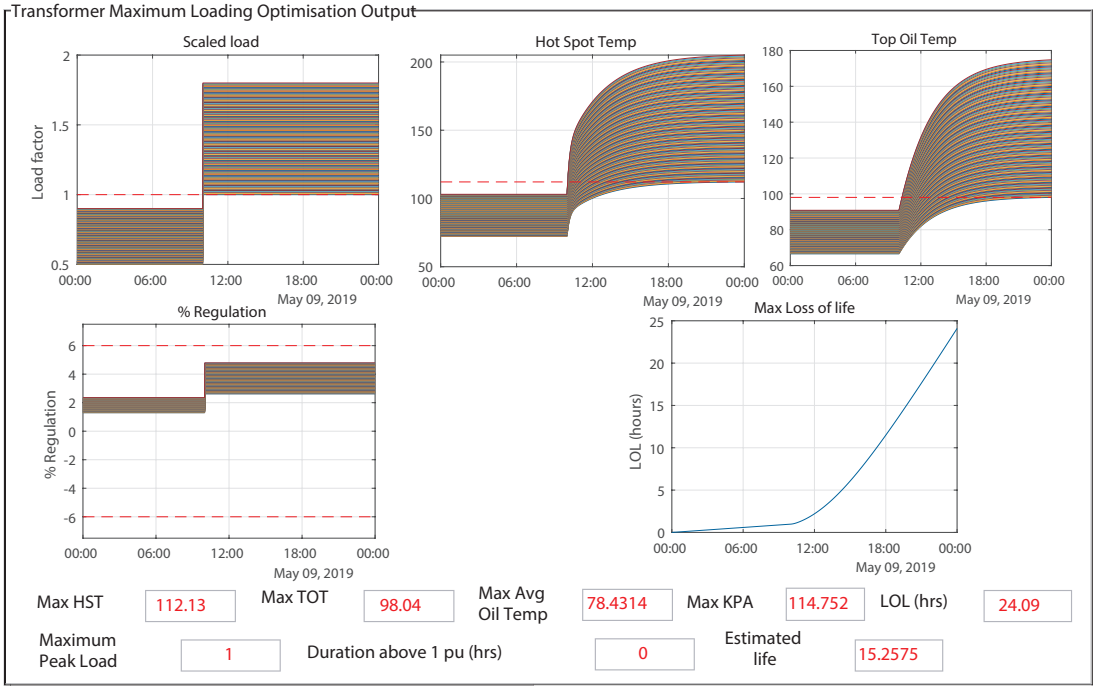

Figure 4.14: Step Increase Modelling Optimisation Output (40 °C Ambient)

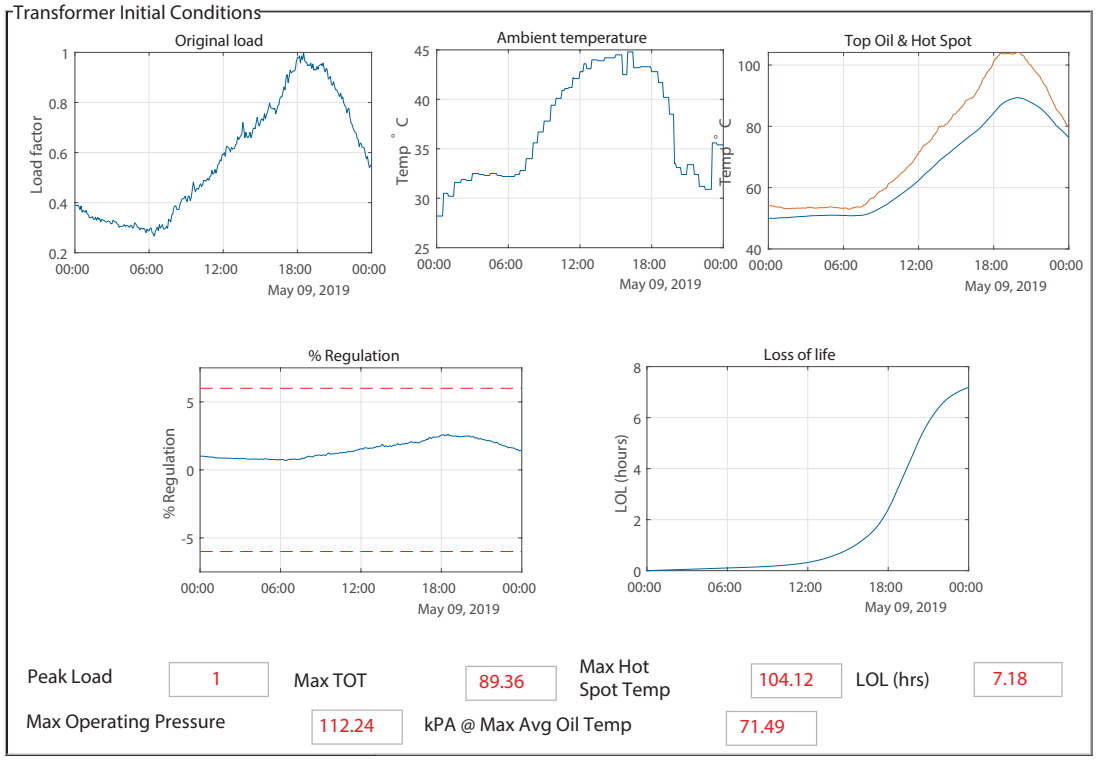

Figure 4.15: Realistic Long-Term Emergency Overloading Optimisation Initial Conditions

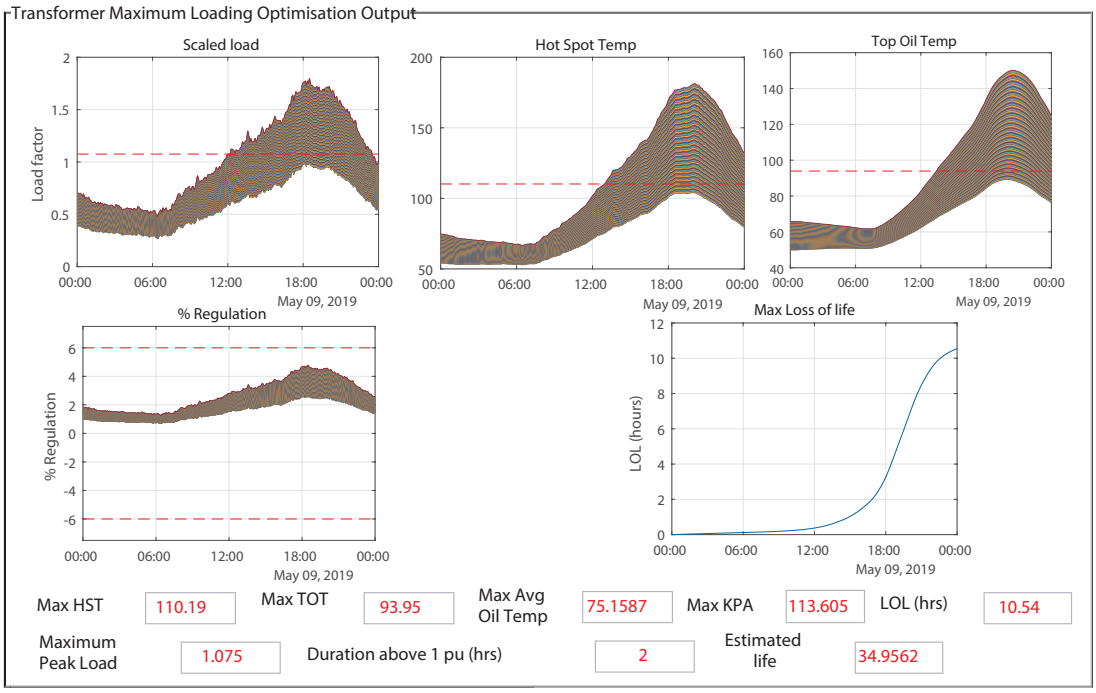

Figure 4.16: Realistic Long-Term Emergency Overloading Optimisation Output

4.5 Dynamic DP Overview

The empirical design method provides a maximum loading that the transformer can maintain over its lifetime. However, it does not calculate intermediate values where an annual forecast percentage growth in base load is expected. The dynamic DP (DDP) algorithm is designed to address this short-coming by calculating the change in distribution transformer lifetime in the presence of increasing base load. Its point-of-difference from the empirical design method, described earlier in the chapter, is the way DDP is able to recover additional lifetime accumulated by the distribution transformer in the years it takes to attain its maximum loading.

The DDP algorithm demonstrates:

1. Its suitability for determining the maximum base load a distribution transformer is capable of handling

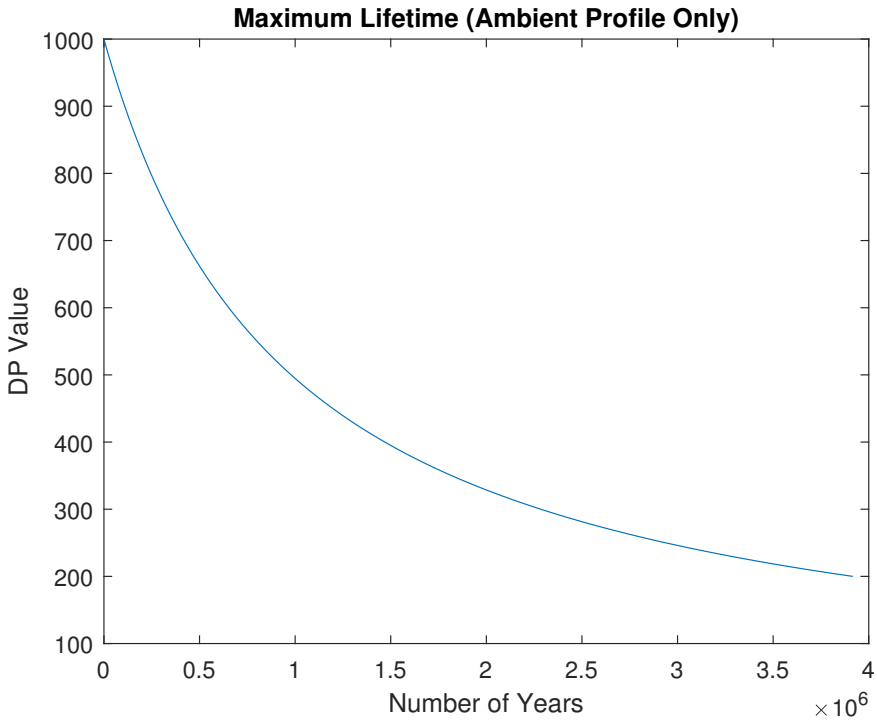

Figure 4.17: Maximum Lifetime - No Load, Ambient Temperature Only

2. What available capacity, if any, the distribution transformer has to support unplanned loading, such as plug-in electric vehicles

In section 4.5.1 the algorithmic process, Algorithm 4.2, is described and section 4.5.3 presents examples of the resulting lifetimes from the modelled parameters.

4.5.1 Algorithm Description

The DDP algorithm, shown in Algorithm 4.2, assumes that the approach employed in the empirical design method is followed and meaningful data has been collected to provide the ambient temperature, base load usage profile and the transformer parameters. These are then used to calculate Θ_{TOT} and Θ_{HS}.

The first step is determine the maximum life the transformer is capable of attaining. To achieve this, the DP fall is calculated utilising a weighted empirical ambient temperature profile, the output of which is seen in Fig. 4.17.

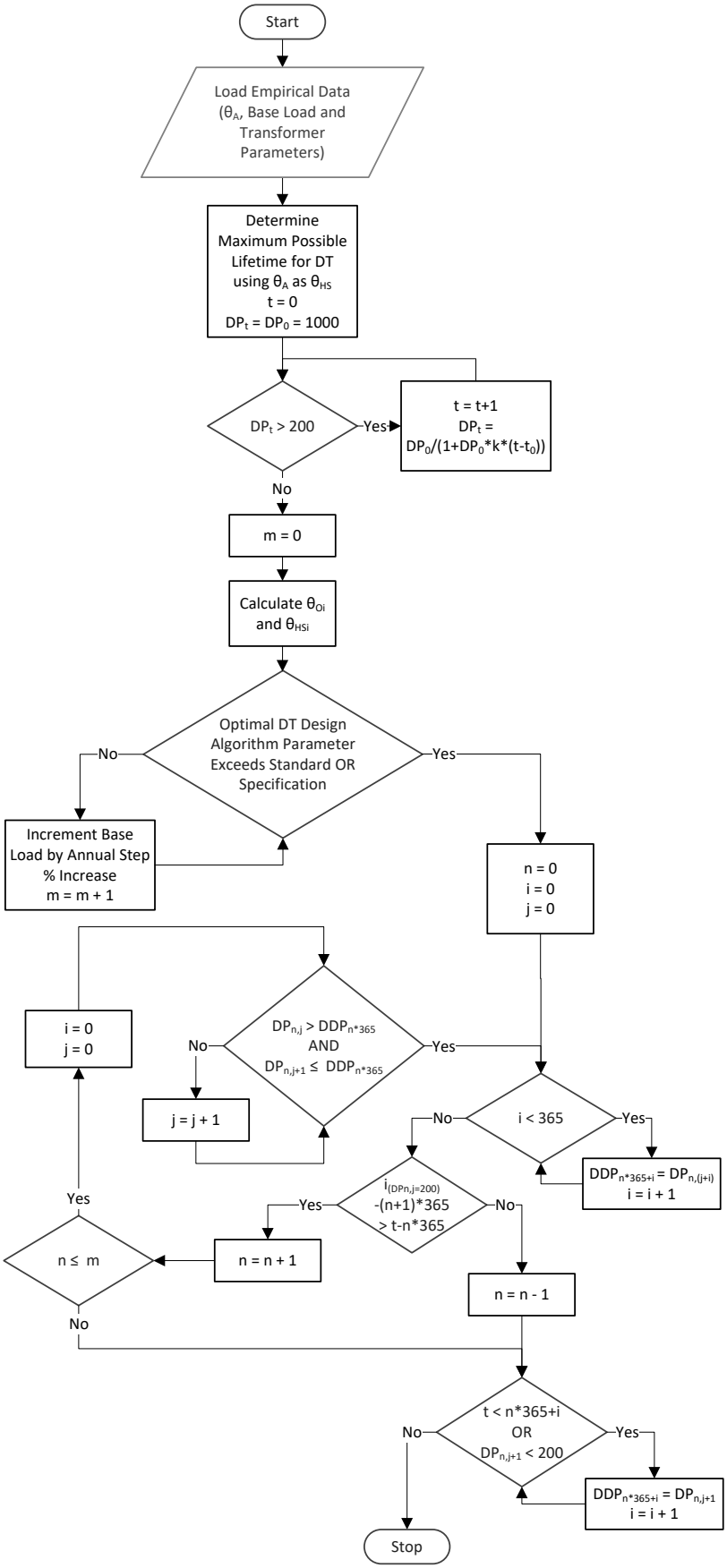

Algorithm 4.2: Logical Process for Determining Dynamic DP

Equation (4.5) calculates the weighted activation energy using Θ_{A_i} as the values for $\Theta_{HS_{0,i}}$. This is then used to calculate the weighted hot-spot temperature (T_{W_n}) in Equation (4.6). Rearranging Equation (4.7) to Equation (4.8) allows the fall in DP to be calculated using T_{W_n} from Equation (4.6).

$$E_{A_{W_n}} = \frac{\Sigma\left(\frac{-E_A}{e^{(R\cdot(\Theta_{HS_{(n,i)}}+273))}}\right)}{N} \tag{4.5}$$

$$T_{W_n} = \frac{1}{\frac{-R}{E_A \cdot ln\left(E_{A_{W_n}}\right)}} \tag{4.6}$$

$$\frac{1}{DP_{(n,i)}} - \frac{1}{DP_0} = A \cdot e^{-\frac{E_{A_{W_n}}}{RT_{W_n}}} \cdot t_{(n,i)} \tag{4.7}$$

$$DP_{n,i} = \frac{DP_0}{1 + A \cdot e^{-\frac{E_{A_{W_n}}}{RT_{W_n}}} \cdot t_{(n,i)}} \tag{4.8}$$

where N is the number of samples, DP_0 = 1000, $DP_{(n,i)}$ = DP curve value at time $t_{(n,i)}$, the molar gas constant, $R = 8.314 m^2 kg s - 2K^{-1}mol^{-1}$ and T_{W_n} is the weighted hot spot temperature in Kelvin. The environmental factor, A, depends on the quantity of dissolved oxygen and moisture content. For a hermetically sealed distribution transformer once the moisture content reaches 1.5 %, it is considered end-of-life, therefore $A = 3 \times 10^4$ [8], at rated value with no oxygen and 0.5 % moisture (the maximum allowable when the distribution transformer leaves the factory), divided by $A_r = 1.6 \times 10^4$. The activation energy, (E_A), is equal to the rated activation energy, $(E_{A_r}) = 86 kJmol^{-1}$.

At this zero-load point the available lifetime can be calculated and used a reference for determining the DP-based accelerated ageing factor.

The next phase is to determine the maximum increase in base load the distribution transformer can accommodate. Utilising the optimal distribution transformer design algorithm in [8] ensures that all boundary conditions exist within the limits set by

standards, in particular [8]. The maximum increase can be calculated relative to a required lifetime or the maximum load the distribution transformer can handle before a specified limit is exceeded.

The next step is to follow the fall in DP for the period of minimum loading and then following each fall in DP until the maximum increase has been established. It then follows the curve until the DP falls to 200. Utilising this approach takes into consideration the increase over time and "recovers" lifetime by calculating the fall in DP for each loading and starting the next fall from the previous DP value.

4.5.2 DDP Algorithm Detailed Description

his section breaks the proposed DDP algorithm down into its component parts and discusses each in detail. The algorithm has to achieve four main functions:

1. Establish initial conditions for transformer and other parameters
2. Determine distribution transformer's maximum loading based on initial conditions
3. Calculate the number of years of incremental increase that can be accommodated until maximum loading is reached based on increasing rate of loss of life (LOL)
4. Validate distribution transformer's maximum loading

With these high-level goals as a backdrop, each functional block of the algorithm, as shown in Algorithm 4.2 will be covered.

Get Data The algorithm is designed to utilise empirical data for model accuracy, and while preferred, ideal or exceptional scenarios can be investigated as well. The required inputs are:

1. Loading Data
2. Ambient Temperature
3. Retirement Age

4. Manufacturer-Supplied Transformer Parameters

Load Empirical Data (Θ_A, Base Load and Transformer Parameters) Gather all the relevant empirical data, to increase the accuracy of the calculations. Parameters gathered include, ambient temperature (Θ_A), base load profile (k), and transformer parameters, such tank dimensions and mass of oil, core and windings.

Determine Maximum Possible Transformer Lifetime using Θ_A as Θ_{HS} At this point, the transformer lifetime consumed in years (t) is initialised to zero and current fall in degree of polymerisation (DP_t) is equal to the degree of polymerisation when a transformer is brand new with zero life consumed (DP_0), which is equal to an average cellulose chain length of 1000 glucose monomers.

$\mathbf{DP_t}$ > 200 Check if DP_t is still greater than its end of life value of 200.

$\mathbf{DP_t}$ > 200 is True Increment transformer consumed lifetime (t) by a day. Calculate new DP_t using equation (4.9).

$$DP_t = \frac{DP_0}{1 + [DP_0 \cdot k \cdot (t - t_0)]} \tag{4.9}$$

$\mathbf{DP_t}$ > 200 is False Initialise percentage step increase total count (m) to zero. Each m step is calculated using the recursive equation (4.10)

$$k_m = k_{(m-1)} + k_{(m-1)} \cdot \frac{x}{100} \tag{4.10}$$

where x is the required step percentage value.

Calculate initial top oil temperature (Θ_{O_i}) and initial winding temperature (Θ_{HS_i}) based off existing base load value (k).

Optimal DT Design Parameter Exceeds Standards OR Specification Use Algorithm (4.1) to verify no design requirements, or limits have been exceeded. If valid, keep increasing the number m % steps until a manufacturer or standards limit is breached.

Transformer lifetime is not considered at this time. Once the maximum number of m steps has been determined, set number of increase years (n) to zero and initialise time index (i) and DP index (j) to zero.

Create DDP Curve The DDP Curve is built according to the iterative process described in equation (4.11).

$$DDP_{(n\cdot(365+i))} = DP_{(n,(j+i))} \tag{4.11}$$

Every k_m curve's DP values is indexed using $DP_{(n,j)}$ and the first year of the DDP curve ($\{DDP_0 ... DDP_{365}\}$) is always equal to the base load curve ($\{DP_{(0,0)} ... DP_{(0,365)}\}$). For each subsequent year, the final DP value from the previous year's curve ($DDP_{(n\cdot 365)}$) becomes the initial DP value to calculate the loss based on the fall the DP curve DP_n, and is the purpose of the DP index, j.

Find Number of Annual Increases Determine that there is more than one year of transformer life left, by finding the time index i where DP_n = 200 and subtracting the number of days until the start of the next year ($(n+1)\cdot 365$). Increase n every year, so that the difference between i and $(n+1)\cdot 365$) is greater than between the transformer end of life value (t) and the start of the year value ($n\cdot 365$), otherwise, if n is equal to the count of the number of increases, m.

Find Total Life Remaining Once the maximum number of increases has been reached, follow DP_n until its value is 200. The final value of t, i.e. the transformer lifetime, is the time index i at DP_n = 200.

4.5.3 Modelled Results

Figures 4.18 - 4.20 overview the output of the DDP process. Figure 4.18 is the initial calculation of the DP curves. Starting each curve assuming a new distribution transformer, reduces the complexity, as DP_0 is constant across all calculations. Figure 4.19

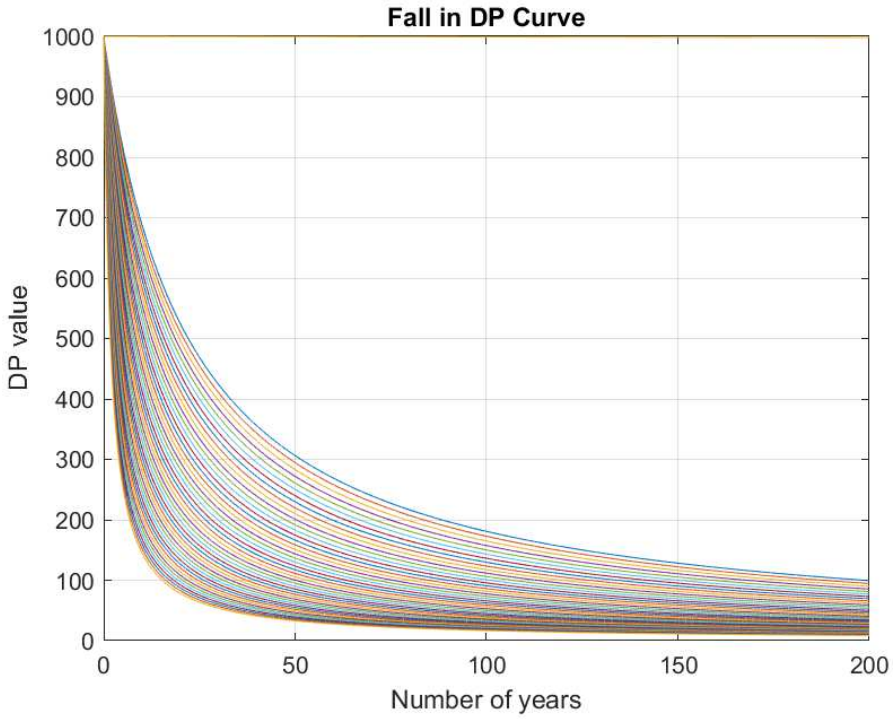

Figure 4.18: Fall in DP curves for increasing load

is the calculated loss of life (LOL) relative to the maximum lifetime determined using the Θ_A values for $\Theta_H S$. The levelling out occurs as no further increase in base loading is possible due to a specified Standard Limit being exceeded, or the required lifetime not being met. Figure 4.20 shows the calculated DDP curve which achieves the required outcome - in this case a distribution transformer lifetime of 35 years.

4.6 Discussion

4.6.1 Assumptions made regarding distribution transformer characteristics

A distribution transformer manufactured according to the same specifications, i.e. the same "type", can reasonably be assumed to yield the same behavioural characteristics as every other manufactured distribution transformer of that "type". However, it would

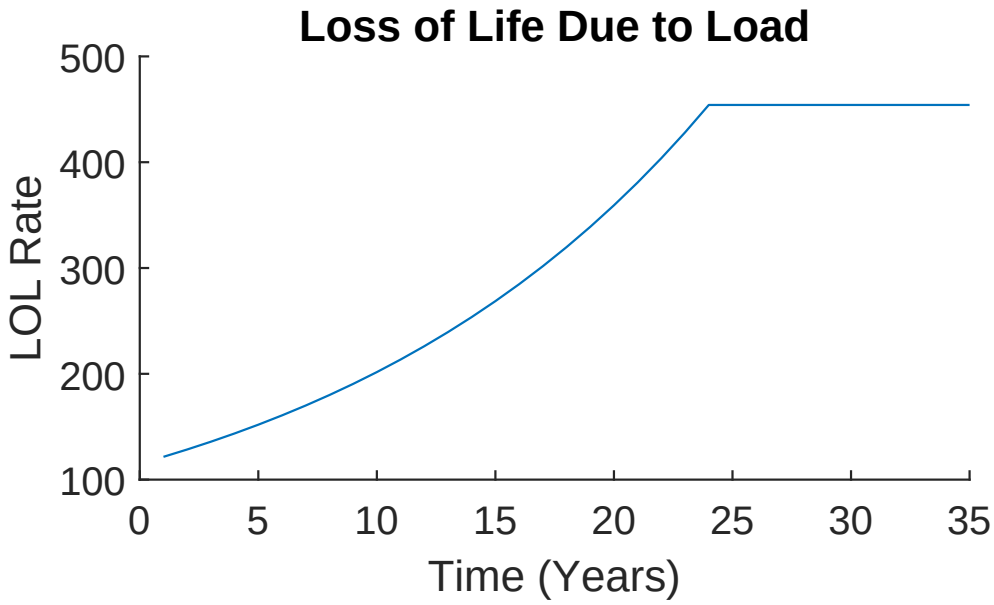

Figure 4.19: Max accelerated LOL for 35 year expected life

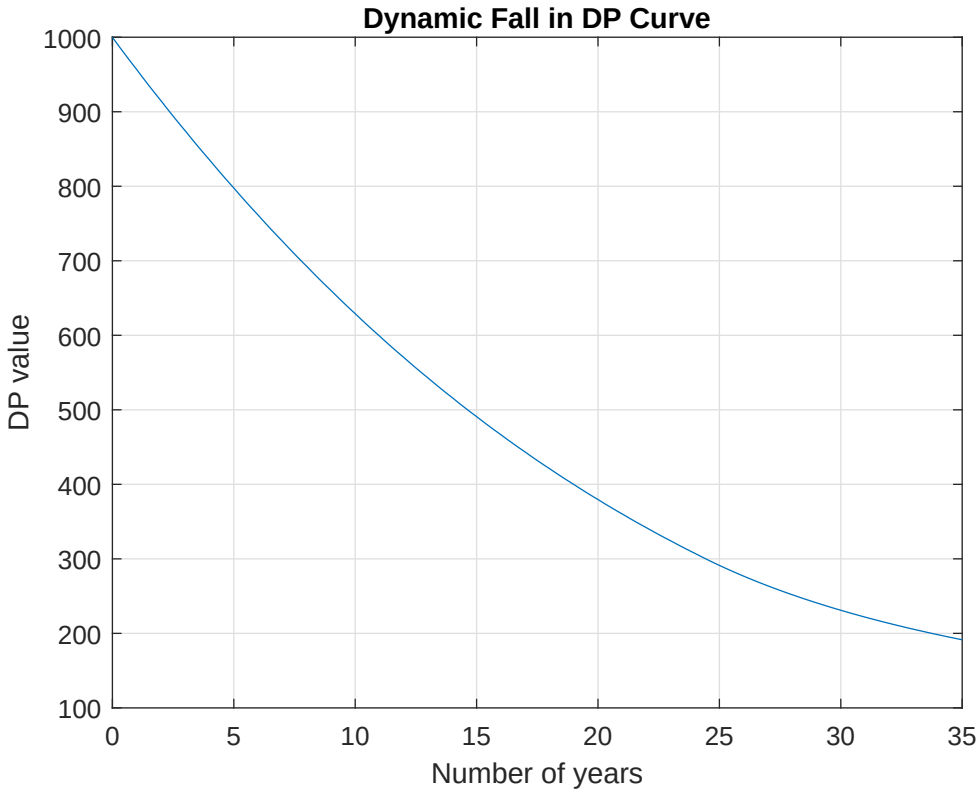

Figure 4.20: Calculated Dynamic DP Curve

be inaccurate to make assumptions about a distribution transformer's characteristics without having all relevant information. For example, both τ_W and τ_O are dependent on the mass of the core and the quantity of oil in the tank, as shown by the τ_W and τ_O equations in Annex E of [8]. If a distribution transformer manufacturer opted to standardise on a tank size that accommodated 500 kVA core coils, then there is additional space for oil with a 100 kVA core coil. This greater oil mass increases its cooling capability, resulting in an array of thermal time constants with significant variance between them.

4.6.2 Applicability to existing distribution transformers

The proposed algorithm and "designing for maximum utilisation" paradigm is primarily intended to be applied within the context of newly manufactured distribution transformers. However, it is possible to utilise the same process for existing distribution transformer as well, with one example given in section 4.4.1. This was achieved through utilising a combination of old and new design data and by carrying out a new heat run test on the same "type" assets from the same manufacturer. Utilising the assumption that all distribution transformers manufactured according to the same process, yield the same characteristics, and assuming a similar manufacturing process is used, the likelihood of shared characteristics between a 100 kVA transformer manufactured in 1999 and one manufactured in 2018, is high. By utilising these parameters and results from the new distribution transformers, the thermal characteristics for the old distribution transformers can be estimated.

4.6.3 Relevance to DNOs

For the DNO in Case One, a paradigm shift in transformer management strategies resulted as a direct consequence of seeing the output from the proposed algorithm. For

example, the DNO introduced LV monitoring for their distribution transformer and requested the distribution transformer manufacturer provide relevant design data such as core kgs, coil kgs, oil litres and heat-run test data for all new distribution transformer ranges supplied to them, so that the data from the LV monitoring could be put in context of the actual thermal loading of the distribution transformer.

For the DNO in Case Two, the collaborative effort outlined demonstrates a shift in the way manufacturers and utilities have historically interacted to produce distribution transformers, and the benefit DNOs see to "designing for maximum utilisation" in the management of their distribution transformer assets, having incorporated it at the outset.

With LV power networks becoming increasingly volatile, DDP has been developed to determine what spare capacity a distribution may have to support the increase in EV penetration within a network. The models will be further enhanced using empirical heat-run data.

4.6.4 Value Of Empirical Data

A logical extension to the value of empirical data inputs argument is that continual data collection can reduce or even remove the uncertainty inherent in estimating the current Θ_A and Θ_{HS}, for example. This assessment was also reached by the authors in [47], who acknowledged using a limited number of input sensors resulted in limited accuracy. However, they expected this to be mitigated with the introduction of smart and digital transformers, such as those found in [140, 141].

4.7 Chapter Summary

In this chapter, a distribution transformer design optimisation algorithm is presented, which is novel in both its "designing for maximum utilisation" concept and comprehensive methodology that ensures standards compliance throughout the distribution

transformer's lifetime. The case was made for accurate modelling, which is best achieved with as many empirical inputs as possible. This was seen in the second case study (Case 2) in Section 4.4.2, where laboratory testing scenarios left the distribution transformer's suitability for purpose in doubt. The algorithm also provides an indicator for existing distribution transformers on their suitability to accommodate additional loading without compromising SAIDI and SAIFI. Such a scenario was presented in Section 4.4.1, where the distribution transformer that was regularly exceeding its nameplate rating was shown to be operating well within its design parameters. This was achieved through the empirical design method's unique approach of not relying on one factor to determine the degree of overloading, and consequently remains standards compliant at all times. Addition benefits of improved distribution transformer utilisation are reductions to losses and costs, an improved return on investment and network reliability, again reliant on empirical inputs.

Chapter 5

A Thermally-Based Approach for Dynamic Load Management

A limitation exists with algorithms utilising thermal ageing acceleration factors to establish a distribution transformer's remaining lifetime. In [37], an algorithm that examines the transformer winding hot-spot (Θ_{HS}), relative to the top-oil temperature (Θ_{TOT}), and the ambient temperature (Θ_A), was used to ensure Θ_{HS} never exceeds 110 °C. However, as a means to establish the present mechanical strength of a distribution transformer's insulation and therefore its remaining lifetime, this approach is not ideal. The reason is that the cellulose chain length that corresponds to its remaining mechanical strength and measured as a fall in the degree of polymerisation (DP), has a normalised lifetime of 17.2 years according to the IEC [8] or 20.5 years according to the IEEE [66]. Therefore, by adopting this approach, the minimum lifetime will be either 17.2 or 20.5 years. However, how much life is available in addition to this? The acceleration factor equation for thermally upgraded Kraft paper insulation (5.1) is the same for both the IEC and IEEE, except that it is described as V by the IEC and F_{AA} by the IEEE. However, which of the two normal lifetimes is more accurate? Therefore, the approach taken in this research is to examine the fall in DP directly, rather than rely

on competing definitions of the "normal" lifetime.

$$V = e^{\left(\frac{15000}{110+273} - \frac{15000}{\Theta_{HS}+273}\right)} \tag{5.1}$$

This chapter proposes a thermally-based dynamic (TD) approach, which aims to balance the demands of consumers for desired levels of EV charging power as quickly as possible, with those of network operators, who are concerned with limiting transformer load levels relative to nameplate ratings. Implementing such an approach can avoid or postpone the need for a transformer upgrade and suits the nature of EV charging loads. The TD approach allows for the loading of transformers beyond nameplate ratings to achieve a desired transformer insulation lifetime with knowledge of forecasted demand, present loading levels and thermal time constants. This is realised by allowing for the dynamic determination of when, to what level, and how long a transformer can be overloaded without compromising key transformer overload parameters. Further, the approach is customised to individual transformers because it is based on measured transformer thermal time constants.

The remainder of the chapter is organised as follows. Section 5.1 describes the TD approach, including the key overload parameters, Section 5.5 describes the experimental measurement of transformer thermal time constants and Section 5.6 shows the effectiveness of applying the approach through a case study for an EV car park under realistic conditions.

5.1 The TD Approach

Operating a transformer beyond its nameplate rating is allowed for by IEEE [66] and IEC [8] standards. The TD Approach seeks to take advantage of this allowance by determining acceptable overload durations based on transformer empirical measurements.

The TD approach concept is shown in Fig. 5.1. When an EV arrives, a request is made for supply, and the TD approach algorithm assesses the impact this additional load will have on key parameters affecting the transformer. The parameters are the transformer winding and top-oil temperatures ($Temp$), remaining lifetime ($Life$), voltage regulation (V_{reg}), and oil pressure (kPa). The impact assessment is used to create the dynamically determined daily load-cycle capacity profile, which uses knowledge of past, present, and predicted transformer loading levels to ensure that the limits for the key parameters are not exceeded. If the loading is within the profile, the EV is allowed to charge. Otherwise, the request is queued until there is available capacity.

Checking the impact of additional loading using a load cycle determined on a daily basis is integral to the TD approach, as cellulosic breakdown of the insulation does not happen instantly and is best determined using a weighted average across the day [48]. In addition, the TD approach requires knowledge of a transformer's thermal inertia, as this impacts on the rate of a transformer's internal temperature rise. Using thermal inertia allows the TD approach to account for the impact of past loading. For example, a transformer operating at 0.2 p.u. can sustain an overload longer than one operating close to 1 p.u. because the internal temperature has up to 60 K temperature rise before the loading temperature is equivalent to that at 1 p.u [8, 66]. This allows transformer capacity to be unlocked without compromising on transformer lifetime, effectively realising additional capacity.

A means of collectively assessing each of the key transformer parameters in Fig. 5.1 is provided by adapting the empirical design method (EDM) algorithm introduced in [70] for use with the TD approach, is described in the next section.

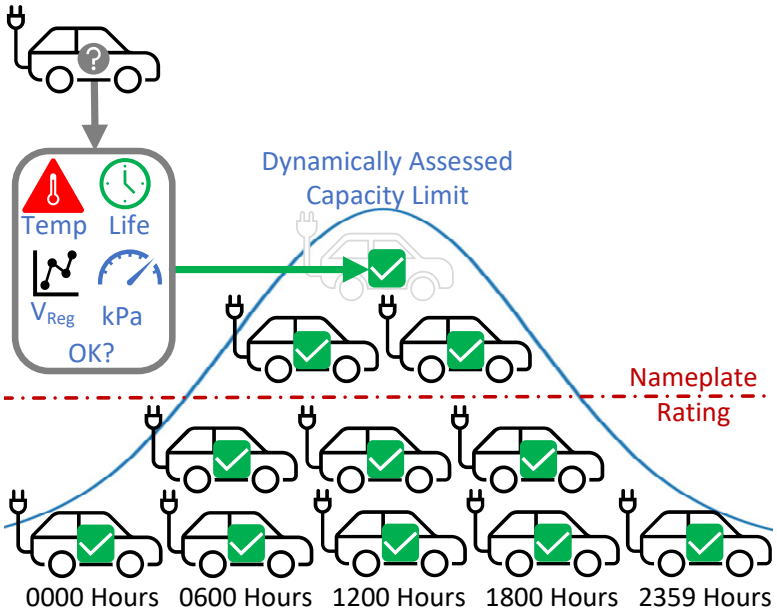

Figure 5.1: Concept diagram for transformer using TD approach for EV charging

5.2 TD Approach Parameter Assessment Metrics

For distribution transformers, a winding insulation material commonly used is thermally upgraded Kraft paper (TUK). The tensile strength of TUK can be related to its degree of polymerisation (DP) [8,66]. A DP of 1000 corresponds to the tensile strength when new, and 200 is approximately 35 % retained tensile strength, which is considered so poor that it represents the insulation's end of life. The primary accelerators of insulation (and therefore transformer) lifetime loss are heat, oxygen, and moisture [8,66]. Additional moisture release is minimal for hermetically sealed transformers constructed with insulating paper that is adequately dried before installation, as additional moisture is excluded from the system until the seal is broken. Therefore, this leaves heat as the primary lifetime loss acceleration mechanism. This is accounted for using a weighted daily temperature, T_W (K), described in Section 5.2.1.

5.2.1 Weighted Temperature

To account for the kinetics affecting the fall in DP, a weighted daily temperature, T_W, in Kelvin, is calculated using (5.2) [48]:

$$T_W = \left[\frac{-R}{E_a} \cdot ln \frac{\sum e^{-E_a/RT_i}}{n} \right]^{-1} \tag{5.2}$$

where R is the molar gas constant, 8.314 $Jmol^{-1}K^{-1}$, E_a is the empirically derived activation energy, 111 $kJmol^{-1}$, T_i is the sample point temperature in K, and n is the number of sample points taken across the day. T_W is then incorporated into the Arrhenius relationship as described in Section 5.2.2, to determine the expected transformer lifetime.

5.2.2 Calculate Lifetime

The expected transformer lifetime, t_{life} (years), is calculated using (5.3) from [8].

$$t_{life} = \frac{\frac{1}{DP_f} - \frac{1}{DP_0}}{A \times 24 \times 365} \cdot e^{E_a/RT_i} \tag{5.3}$$

where DP_f is 200, DP_0 is 1000, and A is $6.92 * 10^7$ $hours^{-1}$, an empirically derived environmental factor [142]. As T_W affects t_{life}, the ability to use T_W to accurately predict t_{life} is dependent on the internal transformer oil temperature, which is also a key overload parameter that affects the transformer lifetime, described in Section 5.2.3.

5.2.3 Calculate Oil Temperature

Oil temperature affects multiple factors, in addition to transformer lifetime, so the instantaneous top and average oil temperatures must also be assessed. Top-oil is calculated using the differential equations from [8], with average oil temperature calculated

as $0.8 \cdot \Theta_O$. There are additional challenges associated with calculating hot-spot temperature and these are described in Section 5.2.4.

5.2.4 Calculate Hot-Spot Temperature

The results of the empirical testing that will be presented in Section 5.5, show that the hot-spot rise is not dependent solely on the τ_W, but instead reaches a maximum gradient that once reached is not exceeded. Therefore, additional rise in Θ_{HS} is limited to the rate of increase in Θ_O which is dependent on τ_O. As no existing model is capable of calculating this gradient value, empirical measurement is required to determine its value. Calculating Θ_{HS} without considering this limiting factor will result in an over-estimation of Θ_{HS} for any calculations longer than τ_W. Therefore, all the Θ_{HS} calculations are limited to the empirically-determined value of $20\ K$ above Θ_O. Additionally, 140 °C was chosen as an appropriate upper limit for the maximum operating temperature, as bubbles of water are ejected from the TUK insulation above this temperature [8]. In hermetically sealed transformers, internal pressure is another factor that needs to be assessed, and is described in Section 5.2.5.

5.2.5 Calculate Internal Pressure

Internal pressure, P_{int}, is calculated according to (5.4) from [50]. However, to make an accurate assessment, the physical characteristics of the transformer need to be known. As the nature of the loading is intended to be more dynamic, the expansion co-efficient of the tank material is also included, so that the internal pressure calculation allows for the additional volume created by the thermal expansion of the tank.

$$P_{int} = 0.145 \cdot P_0 \left(\frac{\Theta_{HS}}{\Theta_A}\right)\left(\frac{V_{l0}}{V_l}\right)\left[\frac{SF_0 + \left(\frac{V_{g0}}{V_{l0}}\right)}{SF_i + \left(\frac{V_g}{V_l}\right)}\right] \tag{5.4}$$

where P_0 is ambient pressure (psi), V_g is the final gas volume at Θ_{HS} (l), V_{g0} is the initial volume (l), V_l is the oil volume in the tank at Θ_{HS} (l), V_{l0} is initial oil volume (l), SF_0 is solubility factor at ambient temperature, and SF_i is the solubility factor at the final temperature. If P_{int} becomes too high, the tank structure, and in particular the cooling fins are vulnerable to failure [143]. The final aspect to be considered is the voltage regulation limits for the local jurisdiction, which is described in Section 5.2.6.

5.2.6 Calculate Voltage Regulation

The voltage regulation on the LV side of the transformer is not a risk to the operation of the transformer itself, but to the network of which it is a part. Local network regulations, for example AS/NZS 3000 [45], impose limits as to how much the voltage is allowed to droop as a percentage of the nominal voltage, and is calculated according to [138]

$$\begin{aligned}\%_{Reg} = &\left(K_{EV(t)} - \%Res \cdot cos\theta + K_{t(t)} - \%X \cdot sin\theta\right) + \\ &\frac{\left(K_{t(t)} - \%X \cdot cos\theta - K_{t(t)} - \%X \cdot sin\theta\right)^2}{200}\end{aligned} \tag{5.5}$$

where $K_{EV(t)}$ is the instantaneous load in p.u., $\%Res$ and $\%X$ are the respective percentage resistive and reactive components of the transformer, $cos\theta$ is the power factor and $sin\theta$ is the phase-shift between the current and voltage waveforms.

How all of these parameters are collectively assessed and utilised in the implementation of the TD approach, is further explained in Section 5.2.7.

5.2.7 The Implementation of the TD Approach

The assessment process to determine the impact each additional load has on the daily load cycle is described by equation (5.6).

$$K_{TD} = K_{TD(X)} + \sum_{n=1}^{N} K_{EV(n,t)} + \sum_{n=1}^{N} K'_{EV(t(n,Y))} + K_{B(T)} \tag{5.6}$$

where

K_{TD} is the daily load profile

K_{EV} is the instantaneous EV charging load

K'_{EV} is the forecast additional charging load

K_B is the existing daily base-load profile

N is the total number of EVs currently charging

$T = \{t \in \mathbb{Z}_+ \mid t < 86400\}$

$X = \{x \in T \mid x < t\}$

$Y = \{y \in T \mid t < y \leq t + d\}$

Over this 24-hour period, K_{TD} is generated equal to the sum of the current load from the load cycle's initialisation point ($K_{TD(t=0)}$) to the present time step, t. This in turn is added to $K'_{EV(Y)}$ from time step index $t + 1$ to $t + d$, where d is the charging duration for the EV from 0 % state of charge (SoC). Any existing base load the transformer is required to accommodate is described by K_B, and is assessed throughout the day from $t = 0$ to $t = |T|$. At $t = 0$, $K_{TD} = \sum_0^N C_{R(n)} \cdot K_{EV(0)} + \sum_0^N C_{R(n)} \cdot K'_{EV(Y)} + K_B$, where N is equal to the number of EVs charging, C_R is the charging rate, and K_B is the 24-hour base or existing building load.

Initialisation of K_{TD} is timed to coincide with minimum transformer loading, typically midnight for businesses and midday for residential locations. $K_{TD(X)}$ is the historical empirical load from the start of the daily load cycle to the present time. Therefore, K_{TD} output from the TD approach is almost entirely daily base load, K_B, at

the time of initialisation, and becoming more dynamically assessed output throughout the day as the current EV charging load, $K_{EV(t)}$, and the forecast EV charging load, $K'_{EV(Y)}$, are added. $K_{EV(t)}$ and $K'_{EV(Y)}$ are automatically decreased as EVs finish charging, or depart. However, they are only allowed to increase after having passed the TD approach algorithmic assessment process, shown in the flow diagrams for Algorithms 5.1-5.4.

5.3 TD Approach Algorithm Description

This section describes each step of the TD approach top-level algorithm shown in Algorithm 5.1. Section 5.3.1 explains the process for a first-time initialisation when applying the TD approach. Section 5.3.2 explains how additional loading is allowed. How the TD approach utilises the wait queue $EV_{(Wait)}$ to assist in minimising wait time and maximising the charging rate when the transformer's capacity limit is reached is explained in Section 5.3.3.

5.3.1 Initialisation Process

The first step in implementing the TD approach is to establish K_B, as any EV load must be additional and not interrupt existing loading. Ideally this determination is based on empirical loading data. Assuming the base load is below the nameplate rating, there will be available capacity to utilise. Using an algorithm such as that proposed in [70] allows this to be quantified. However, this algorithm only determines the amount the base load can safely be increased, not how much dynamic load can be accommodated. Having established the baseline, assessment using the TD approach can begin. If there are any EVs already charging prior to initialisation, they should be added to the base for the duration of a full charge. While using the duration of a full charge in the assessment does have a slight impact on available capacity, this approach limits computational

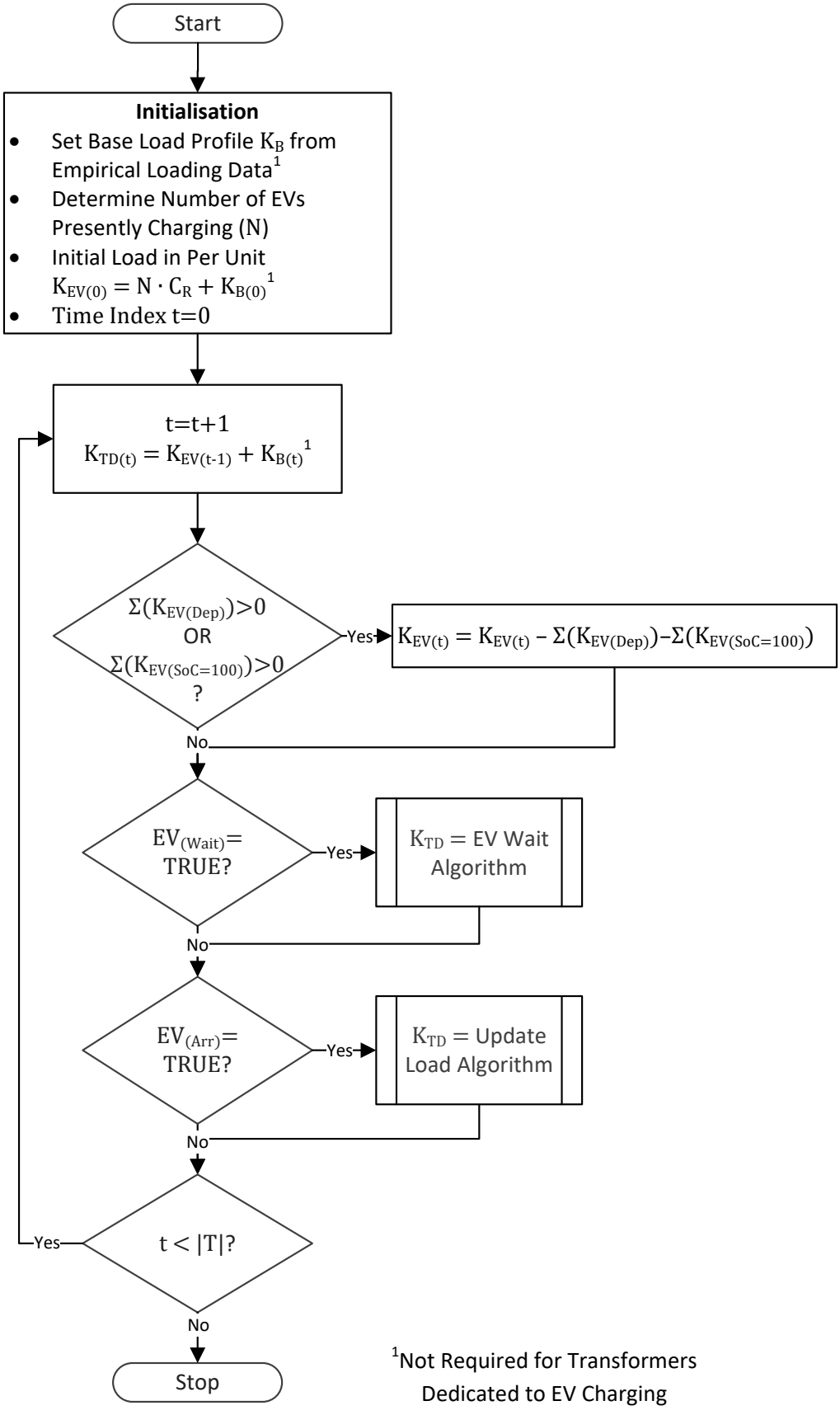

Algorithm 5.1: TD approach load management Process algorithm

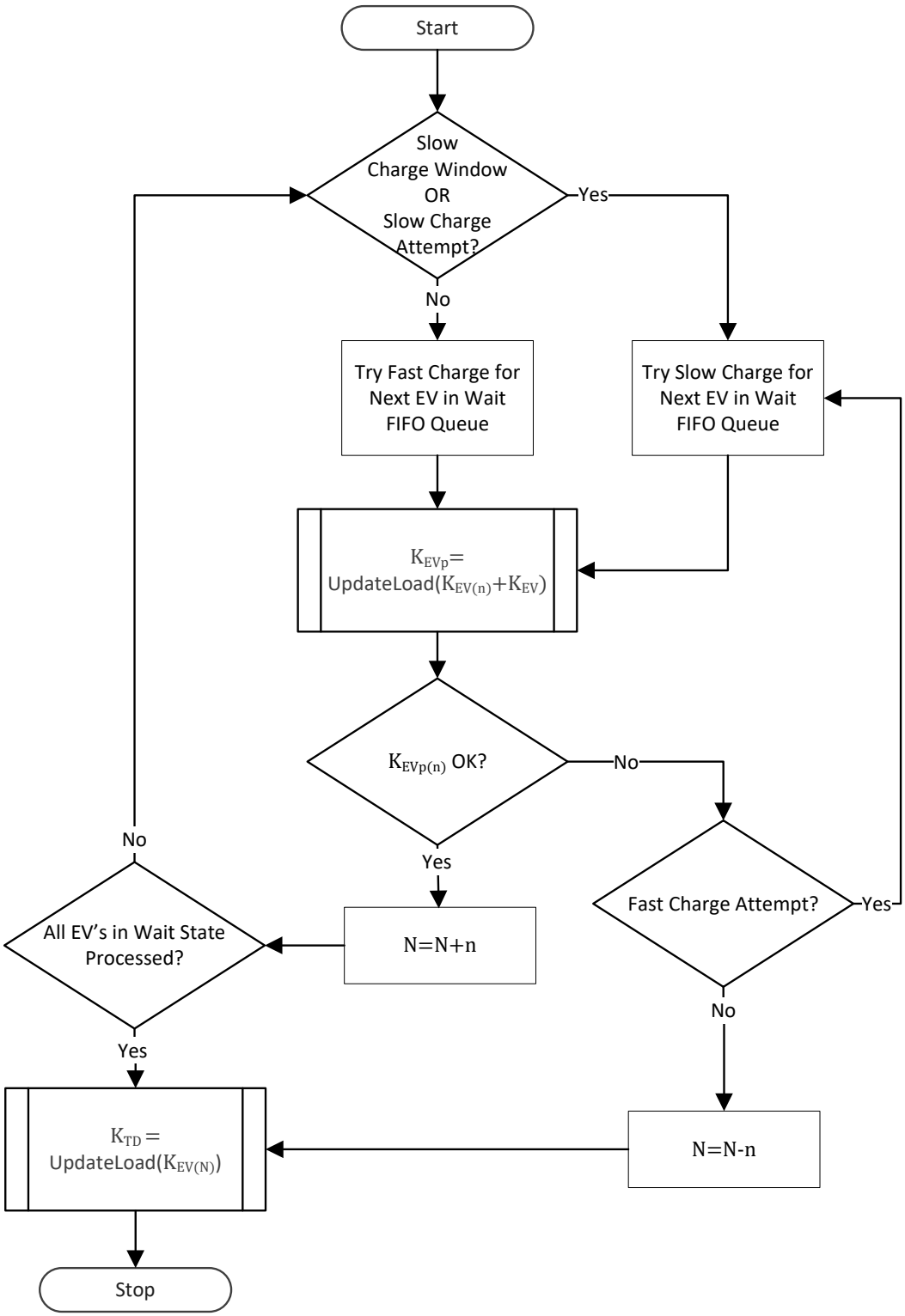

Algorithm 5.2: TD approach load management EV Wait algorithm

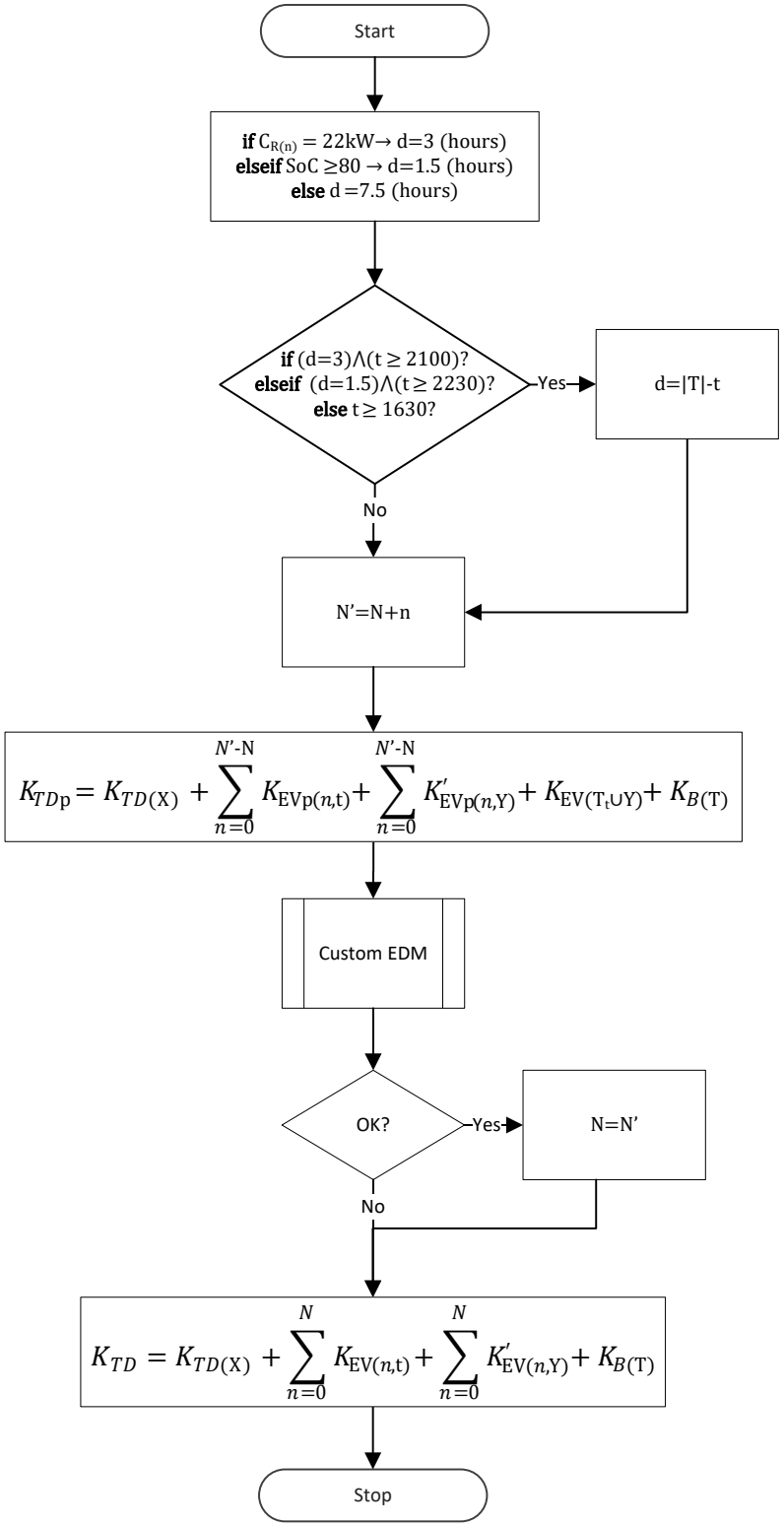

Algorithm 5.3: TD approach load management Update Load algorithm

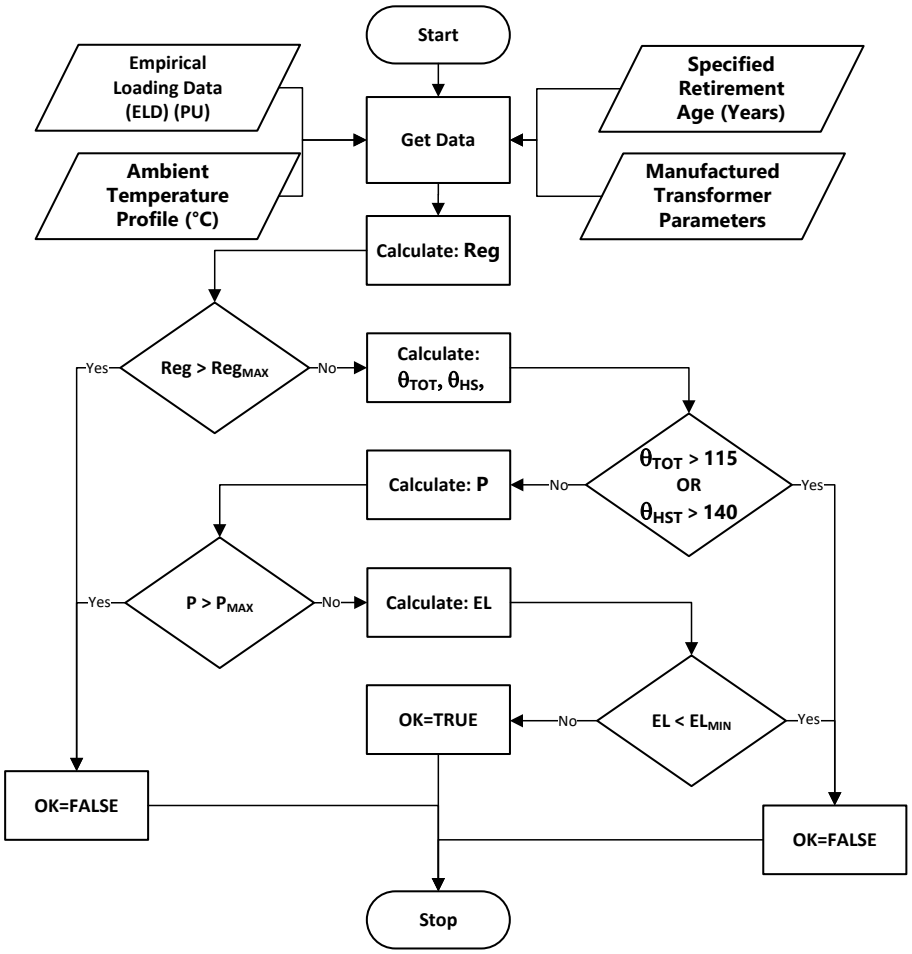

Algorithm 5.4: TD approach load management customised EDM algorithm

effort and adds a slight buffer in that the transformer's capacity cannot be exceeded. To determine whether an additional load is allowed on the transformer, along with the level and duration of loading beyond nameplate rating the TD approach utilises the Update Load algorithm (Section 5.3.2).

5.3.2 Update Load Algorithm

The update load algorithm is used to assess newly arrived EVs ($EV_{(Arr)}$) and determine whether waiting vehicles ($EV_{(Wait)}$) are allowed to charge and at what rate. The algorithm always attempts to apply the maximum charging rate, only dropping it back after determining the transformer cannot handle the additional load, outputting the new value of $K_{EV(t)}$ and $K'_{EV(Y)}$.

The Update Load algorithm is able to provide all the analysis for each $EV_{(Arr)}$. However, processing each $EV_{(Wait)}$ in the first-in first-out (FIFO) queues requires its own algorithm, the EV Wait Algorithm, explained in Section 5.3.3.

5.3.3 EV Wait Algorithm

The EV Wait Algorithm uses the Update Load Algorithm to assess how many EVs can be added for charging at any time. Which EVs are added is determined using prioritised FIFO queues. The highest priority queue is for vehicles forcibly slowed to allow charging, followed by vehicles awaiting a charge and then the low priority queue is for vehicles that have already received an 80 % or greater charge. This approach assumes that 22 kW 3-phase a.c. charging points have been supplied to 80 spaces in the car park. Once the vehicle has received at least 80 % charge, along with reduced charging rate, it is designated as low-priority, which is eligible to have its pausing charged when capacity is required for higher priority loads.

The number of EVs that can be added depends on the available capacity taking

into account transformer loss of life factors, and standard requirements. The EV Wait Algorithm assumes that the fastest charge rate possible will be applied, so prior to processing checks that the maximum charge rate will at no time exceed 1.8 p.u. It then calls the Update Load algorithm to assess whether all the EVs in the FIFO queue can be added to $K_{EV(t)}$. The process keeps looping until shedding the EVs from the end of the FIFO queue reducing the load to be added. If no EVs can be added at the fast charge rate, the algorithm runs again using a slow rate until no additional load can be added.

5.4 Detailed Description for TD Approach Algorithms

This section breaks the proposed algorithms down into their component parts and discusses each in detail. Because of the complexity of the task, the TD approach is not addressed by a single algorithm, but four to achieve its function. The first algorithm is the process algorithm, Algorithm 5.1 and is described in subsection 5.4.1.

5.4.1 Process Algorithm

Initialisation The function of the Initialisation process is to take the base load profile, K_B and ensure that it is in per unit. Set the time index, t back to zero. The time at which this occurs is not dependent on the calendar time, but rather the daily load cycle, which is what is relevant for the assessment carried out as in the TD approach. The per unit load from any vehicles already charging prior to implementation is added using $K_{EV}(0) = N \cdot C_R + K_B$ where K_B is the set of all values of K_B throughout the daily process.

$\mathbf{t = t + 1}$ $\mathbf{K_{TD(t)} = K_{EV(t-1)} + K_{B(t)}}$ This step iterates $\mathbf{t}$ and updates the instantaneous value of $\mathbf{K_{EV}}$ by bringing forward the load from the previous time step $(t - 1)$, and creating a zero reference for any changes positive or negative relative to that value.

$\mathbf{\Sigma(K_{EV(Dep)}) > 0}$ **OR** $\mathbf{\Sigma(K_{EV(SoC=100)}) > 0}$ This step checks for any decrease in the load due to any vehicles that have departed while they were still charging, or if an EV's SoC has reached 100 % and if so, sets the charging value to zero.

$\mathbf{K_{EV(t)} = K_{EV(t)} - \sum_{n=0}^{n_{Dep}} K_{EV(Dep)} - \sum_{n=0}^{n_{SoC=100}} K_{EV(SoC=100)}}$ This equation processes the decrease in load determining the new instantaneous value of $K_{EV(t)}$ by subtracting $\sum_{n=0}^{n_{Dep}} K_EV(Dep)$ and $\sum_{n=0}^{n_{SoC=100}} K_EV(SoC = 100)$, where Dep and $SoC = 100$ are the index values for the EV chargers.

$\mathbf{EV_{(Wait)}}$ = $\mathbf{TRUE}$? This checks the flag for EV vehicles connected to a charger, but not yet allowed to receive a charge, due to the assessed capacity limit having been reached.

$\mathbf{K_{TD}}$ = **EV Wait Algorithm** If the flag is set, call the EV Wait Algorithm to assess if the vehicle can now be allowed to charge.

$\mathbf{EV_{(Arr)}}$ = $\mathbf{TRUE}$? This checks if the newly arrived vehicle flag has been set, for a vehicle that has connected to an empty charging location and is request a charge.

$\mathbf{K_{TD}}$ = **Update Load Algorithm** Calls the Update Load Algorithm to assess whether there is available capacity and allow or deny the EV charging based on this assessment.

$\mathbf{t < |T|}$ Checks if the time index is still within the 24-hour daily load-cycle window, by comparing the time index value, t, to the cardinality of the set T. If so, continue the assessment process. If not, this 24-hour assessment is complete.

5.4.2 EV Wait Algorithm

Slow Charge Window OR Slow Charge Attempt? This step checks if the slow charge flag has been set. The TD approach allows for a slow-charge window to be specified, for example a car parking building may wish to offer slow-rate charging to those availing themselves of "early-bird" parking rates, and will be parked all

day, so the rate is not so important to them. The flag is also set for those vehicles requesting a charge, but the assessed capacity limit does not allow for a full-rate charge to be supplied. The last set of vehicles this applies to are those whose state of charge (SoC) has reached 80 %, as their charging rate is already limited to preserve the battery lifetime.

Try Fast Charge for Next EV in Wait FIFO Queue This step sets the EV charging rate value flag, C_R to "fast" for the Update Load Algorithm.

Try Slow Charge for Next EV in Wait FIFO Queue This step sets the EV charging rate value flag, C_R to "slow" for the Update Load Algorithm.

$\mathbf{K_{EVp}}$ = **UpdateLoad(**$\mathbf{K_{EV}(n) + K_{EV}}$**)** This calls the Update Load Algorithm and passing the requested potential load,K_{EVp} through for assessment. The actual loading already provided is not affected by this step.

$\mathbf{K_{EVp}OK}?$ Assesses the status of the load OK flag which indicates the outcome of the assessment, whether or nor the new loading request is to be allowed.

$\mathbf{N = N + n}$ Increases count of the number of EVs allowed to charge, N, by the number of EVs assessed as being OK for loading, n.

All EVs in Wait State Processed? Checks the status of the FIFO Wait Queue, and if it is not empty repeats the process. If all EVs have been processed, call the Update Load Algorithm to finalise the new load value.

Fast Charge Attempt? Examines if the attempt at at charging was at the fast or slow rate. If it was at the fast rate, try again at the slow rate.

$\mathbf{N = N - n}$ This decrement of the number of EVs charging, relates only to the provisional request to allow the charging, the number of vehicles already allowed to charge is not impacted.

$\mathbf{K_{TD}}$ = **UpdateLoad(**$\mathbf{K_{EV(N)}}$**)** Call the Update Load Algorithm to process the finalised load using the final value of $K_{TD(t \cup Y)}$ for this time step.

5.4.3 Update Load Algorithm

if $\mathbf{C_R}$... elseif SoC... else... This step initialises the duration, d for the charging. This value always assumes an initial SoC of 0, ensuring that required duration is always less than or equal to d.

if $C_{R(n)} = 22\ \text{kW} \rightarrow d = 3$ (hours)

Sets d to the fast charging duration of 3 hours.

elseif $SoC \geq 22\ \text{kW} \rightarrow d = 1.5$ (hours)

Sets d to 20 % of the slow charging duration of 7.5 hours.

else $d = 7.5$ (hours)

Sets d to the slow charging duration of 7.5 hours

if d... elseif d... else... This step determines whether actual duration, d, can be used.

if $(d = 3) \wedge (t \geq 2100)?$ (hours)

Checks if t is greater than or equal to the relative time of 2100 since the assessment began for the fast charging value of d.

elseif $(d = 1.5) \wedge (t \geq 2230)?$ (hours)

Checks if t is greater than or equal to the relative time of 2230 since the assessment began for the 20 % slow charging value of d.

else $t \geq 1630?$ (hours)

Checks if t is greater than or equal to the relative time of 1630 since the assessment began for the slow charging value of d.

$\mathbf{d} = |\mathbf{T}| - \mathbf{t}$ This adjusts the value of d relative to the cardinality of the 24-hour window, shortening it by the difference between t and the remaining number of steps.

$\mathbf{N'} = \mathbf{N} + \mathbf{n}$ This step increases of the virtual N value, N' which only applies to the potential loading, K_{EVp}, and, K'_{EVp}.

$\mathbf{K_{TDp}}$ **=...** This calculates the new potential load profile in preparation for passing to the Custom EDM for assessment.

$\mathbf{K_{TD(X)}}$ Is the array of calculated TD values from T_0 to $T_(t-1)$ as described by being indexed by the set X.

$\sum_{\mathbf{n=0}}^{\mathbf{N'-N}} \mathbf{K_{EVp(n,t)}}$ Sums all the EVs requesting charge, at the current instant in time, T_t, from 0 to $N' - N$ as this is a delta variable.

$\sum_{\mathbf{n=0}}^{\mathbf{N'-N}} \mathbf{K'_{EVp(n,Y)}}$ Sums the forecast load for all the EVs requesting charge from 0 to $N' - N$, from the time $T_(t+1)$ to $T_(t+1+d)$, as described by being indexed by the set Y.

$\mathbf{K_{EV(t\cup Y)}}$ Is any existing EV charging load from the current time T_t to the end of the forecast load, as indicated by its index, $T_t \cup Y$. As this load has already been assessed, the only change is any EVs that leave early or finish their charging within this window. However, as this is an unknown, the potential $EV_{(Dep)}$ and SoC = 100 EV loads must be included until this occurs.

$\mathbf{K_{B(T)}}$ Is the existing base load for the entire 24-hour period, as evidenced by its index set T.

Custom EDM Calls the Custom EDM Algorithm to assess if the new load can be added without compromising transformer lifetime, thermal considerations, pressure and regulation limits.

OK? Processes the OK flag

$\mathbf{N = N'}$ If OK, the number of EVs charging is increased to N'.

$\mathbf{K_{TD}}$ =**...** Is the final load. If assessed as OK, this includes the newly added load. Otherwise, the load remains unchanged from when the assessment request was made.

$\mathbf{K_{TD(X)}}$ Is the array of calculated TD values from T_0 to $T_(t-1)$ as described by being indexed by the set X.

$\sum_{\mathbf{n=0}}^{\mathbf{N}} \mathbf{K_{EV(n,t)}}$ Sums all the assessed EVs, at the current instant in time, T_t, from 0 to N.

$\sum_{\mathbf{n=0}}^{\mathbf{N}} \mathbf{K'_{EV(n,Y)}}$ Sums the forecast load for all the assessed EVs from 0 to N, from the time $T_(t+1)$ to $T_(t+1+d)$, as described by being indexed by the set Y.

$\mathbf{K_{B(T)}}$ Is the existing base load for the entire 24-hour period, as evidenced by its index set T.

5.4.4 Detailed Description of Custom EDM Algorithm

The approach taken by the models is to determine the hotspot as a rise over top-oil temperature. While this does make sense, as top oil has always been easier to measure than the windings, it is a backwards process. The core and the windings are trying to heat up and it is the oil that is inhibiting that rise. The TD approach exploits this fact, as the level of cooling may be such that the load placed on the transformer is not enough to overcome this and the core, windings and oil are held to the ambient temperature. Examining the thermal behaviour by starting with the assumption that the oil drags and inhibits the temperature rise, better explains what has been observed in the experimental results in section 5.5.1.

Some modifications incorporated into the algorithms below are the limiting of the value of the hot-spot temperature relative to the top-oil temperature, accounting for the thermal expansion of the tank in the pressure calculations, using an empirically derived oil thermal time constant, τ_O, rather than one provided by the standards or calculation based on transformer parameters.

Get Data The algorithm is designed to utilise empirical data for model accuracy, with the required inputs:

Empirical Base Loading Data (p.u.) A representative base load is required to determine whether there is any scope to add additional load to the transformer. If this initial assessment shows that the loading is such that the

transformer is already compromised, then the TD process stops at that point.

Ambient Temperature (°C) The degree to which a distribution transformer can be operated beyond nameplate rating is best determined with using a representative daily ambient temperature profile (Θ_A). This is particularly relevant when Θ_A exceeds 20 °C, as this has the potential for the thermal limit to be reached before the maximum p.u. is reached. Similarly, a lower ambient creates greater scope for operation beyond nameplate rating.

Specified Retirement Age (Years) The minimum or required operational life of the distribution transformer in years, as specified by the utility.

Manufacturer Transformer Parameters These are the parameters such as tank and core-coil size and weight and heat-run test data, which improve the accuracy of the lifetime calculation.

Manufacturer-Supplied Transformer Parameters

Calculate Reg This is calculated prior to the other parameters, as its only variable is loading according to equation (5.7).

$$(n \cdot Er\% \cdot cos\theta + n \cdot Ex\% \cdot sin\theta) + \frac{(n \cdot Ex\% \cdot cos\theta - n \cdot Ex\% \cdot sin\theta)^2}{200} \quad (5.7)$$

where

n is loading percentage

$Er\%$ is resistance percentage

$Ex\%$ is reactance percentage

$cos\theta$ is power factor

$sin\theta$ is the phase-shift between the current and voltage waveforms

Reg > $\mathbf{Reg_{MAX}}$ Tests to see if the calculated value Reg exceeds the limit specified by local standards, for example $\pm 6\%$ of nominal from AS/NZS 3000:2018 [45]. If the test is true, the additional load cannot be accommodated and no further

testing is carried out. However, if $Reg < Reg_{MAX}$ the process is passed to the next parameter test.

Calculate Θ_{TOT}, Θ_{HS} This uses a customised version of of the differential model in [8]. For example, as the measured $\Delta\Theta_{HS}$ was never more than 20 K above Θ_{TOT} it was limited to rise at the rate of Θ_{TOT}, as the impact of the the winding time constant tau_W was not observed beyond the transient stage, at which time the rate of rise of both Θ_{HS} and Θ_{TOT} was governed by the oil time constant τ_O.

$(\Theta_{TOT} > 115) \vee (\Theta_{HS} > 140)$? If either of these situations is true, then the load cannot be added and no further parameters are assessed. If neither case is true, the calculated Θ_{TOT} and Θ_{HS} are passed to the next stage.

Calculate: P This calculates the internal tank pressure. However, the equation differs from the equation in [50], not only that it scales to kPa, but it also accounts for tank thermal expansion and is calculated according to equations (5.8)-(5.10).

$$\Delta\Theta_{O_{avg}} = \Theta_{O_{avg(MAX)}} - \Theta A_{avg} \tag{5.8}$$

where ΘA_{avg} is the average ambient temperature for the transformer tank assembly location, in this case the value is 15 °C, as this is a sensible average for Auckland [139]. $\Theta_{O_{avg(MAX)}}$ is the maximum average oil temperature, with the average oil temperature calculated according to $0.8 \cdot \Theta_{TOT}$

$$\begin{aligned} V_{g_n} =& (L_{Tank} + (\Delta L_{Tank} \cdot \Delta\Theta_{O_{avg}})) \cdot (W_{Tank} + (\Delta W_{Tank} \cdot \Delta\Theta_{O_{avg}})) \\ & \cdot (H_{Cushion} + (\Delta H_{Cushion} \cdot \Delta\Theta_{O_{avg}})) \cdot 1000 \end{aligned} \tag{5.9}$$

where

V_{g_n} is the gas volume at Θ_{HS} for any value of V_g (l)

V_{oil} is the volume of oil (l)

L_{Tank} is the tank length (m)

ΔL_{Tank} is the thermal expansion in tank length calculated according to $1.3 * 10^{-5} \cdot L_{Tank}$

W_{Tank} is the tank width (m)

ΔW_{Tank} is the thermal expansion in tank width calculated according to $1.3 * 10^{-5} \cdot W_{Tank}$ (m)

$H_{Cushion}$ is the air cushion height (m)

$\Delta H_{Cushion}$ is the thermal expansion in the cushion height calculated according to $1.3 * 10^{-5} \cdot H_{Cushion}$. If the $H_{Cushion} = 0$ then this would be calculated relative to the change in tank height ΔH_{Tank}, as this could contribute to creating a cushion.

$$P_f = 0.145 \cdot P_0 \left(\frac{\Theta_{HS}}{\Theta_A}\right)\left(\frac{V_{l_0}}{V_l}\right)\left[\frac{K_{i_0} + \left(\frac{V_{g_0}}{V_{l_0}}\right)}{K_i + \left(\frac{V_g}{V_l}\right)}\right] \tag{5.10}$$

where

P_f is calculated final pressure (psi)

P_0 is ambient pressure (psi)

V_g is the final gas volume at Θ_{HS} (l)

V_{g_0} is the initial volume (l)

V_l is the oil volume in the tank at Θ_{HS} (l)

V_{l_0} is initial oil volume (l)

K is the solubility factor

K_{i_0} is solubility at ambient temperature

K_i is the solubility at the final temperature

$\mathbf{P > P_{MAX}}$ If the calculated pressure exceeds the maximum allowable internal pressure, no further testing is carried out. Otherwise, the process is passed to the next

parameter test.

Calculate: EL The transformer lifetime is determined relative to the fall in degree of polymerisation (DP). This approach differs slightly from the EDM approach in Chapter 4 as it makes a daily assessment assuming that the transformer's DP is zero and then calculates the lifetime based on the loading for the day. If the projected increase in load would cause the lifetime to drop below the required lifetime, it is disallowed. The TD approach will maximise load, to ensure that as close as possible required lifetime and transformer end-of-life coincide. This approach does require an index is maintained separately for the number of years that the transformer has been in use, otherwise, it is evident that the x year lifetime would continue ad infinitum.

EL < $\mathbf{EL_{MIN}}$ If the minimum required lifetime would not be met, the proposed additional load is rejected and the algorithm returns $FALSE$ for the OK flag. Otherwise, the OK flag returns $TRUE$

5.4.5 Practical Consideration

In this section, the process that the TD approach uses to assess loading levels has been described. However, for a practical implementation the rate at which the transformer's internal temperature changes needs to be determined. This requires knowledge of the transformer thermal time constants. Accordingly, the experimental method used to establish transformer thermal time constants is described in Section 5.5.

5.5 Thermal Time Constant Determination

The TD approach achieves operation beyond nameplate rating with knowledge of thermal inertia. As shown in [70, 87, 92, 144, 145], τ_O can be longer than the values specified in [8, 66] for a transformer fitted with external radiators for cooling. This

Table 5.1: 300 kVA Example Transformer Parameters

Parameter	Value
Nameplate Rating	300 kVA
MV / LV Voltage	11 kV / 415 V
LV Current	417.4 A
Per Unit Impedance (Resistive / Reactive)	0.96 / 4.21 (%)
Maximum Rated Pressure	155 kPa

means that measurements assure the accurate determination of values of τ_O. Therefore, in this section, the experimental setup used to determine the transformer thermal time constants and the results of the experimental work are described. The work is based on a 300 kVA transformer fitted with a Fibre-Bragg Grating (FBG) temperature-sensing system installed in the LV windings, as well as thermocouples installed to measure oil temperatures. The specifications of the transformer are listed in Table 5.1. It is identical to a production type, except that it is not hermetically sealed to allow for observation and adjustment of the fibres of the FBG system and the thermocouples.

5.5.1 Experimental Process

To determine the thermal time constants of the transformer the LV windings are shorted, and a low-voltage high current is supplied to the HV windings. This allows for loading to various levels. Fig. 5.2 shows the experimental setup, including supply leads to the HV winding bushings. The shorted LV windings are on the far side of the transformer.

To measure the ambient temperature two thermocouples are used, one in free air and the other in oil. These are external to the transformer, on the same side as the LV terminals.

An additional thermocouple is placed to measure top-oil temperature. These are indicated in Fig. 5.2. Other equipment indicated in Fig. 5.2, is used for processing the

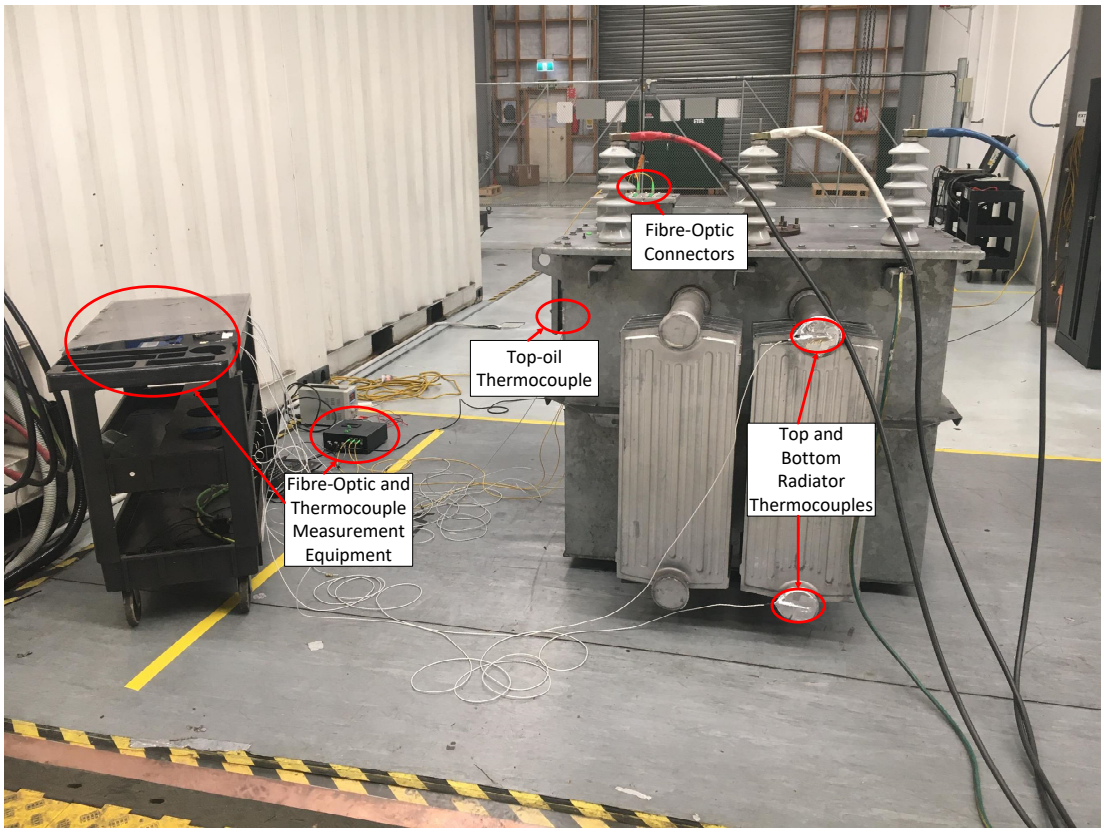

Figure 5.2: 300 kVA transformer experimental setup

thermocouple and FBG system signals.

In previous work such as [146], 28 measurement points were used. However, previous experimentation for the development described in [44], determined the appropriate location for individual fibres to measure the hot-spot temperature and was adopted in this work. Similarly, findings of much shorter values of τ_O in [146] is consistent with the findings in this work, as those transformers had no external cooling.

A load profile designed to stress the transformer and assess its behaviour above 1 p.u. is implemented, as shown in Fig. 5.3. Using this load profile, measurements are taken and then averaged. This includes the temperature measurements from within the windings, in the top-oil and of the ambient temperature

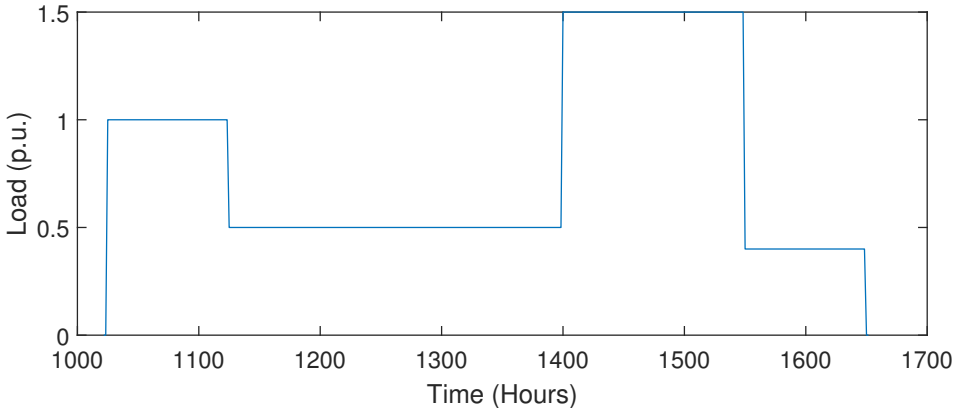

Figure 5.3: 300 kVA example transformer input: Per unit load profile

5.5.2 Experimental Results

In Fig. 5.4, the 3 °C ambient temperature rise over the duration of the experiment can be seen, and Fig. 5.5 shows the experimental results. The measured Θ_A is subtracted from Θ_{HS} and Θ_O to derive $\Delta\Theta_{HS}$ and $\Delta\Theta_O$, respectively. The $\Delta\Theta_{HS}$ for each winding is then overlaid onto $\Delta\Theta_O$ by offsetting the values, so the comparative rise times can be determined. This result shows that the initial rise in $\Delta\Theta_{HS}$ is not a static value but does appear to be related to τ_W. However, after this initial rise, the rate at which $\Delta\Theta_{HS}$ increases follows the rate of rise of $\Delta\Theta_O$. Therefore, for periods greater than τ_W it validates the assertion that Θ_{HS} is dependent on τ_O, as the rise times of $\Delta\Theta_{HS}$ correlate with those of $\Delta\Theta_O$. The slope of $\Delta\Theta_O$ indicates that τ_O is 481 minutes. The experiment was modelled using a τ_O of 481 minutes, where the rise in $\Delta\Theta_O$ correlated with the empirical measurements, Fig. 5.6. This value of τ_O is applied in the EV charging case studies presented in Section 5.6.

5.6 Validation Case Study

The case study presented compares the performance of the TD approach to the traditional approach of limiting the transformer loading to its nameplate rating. The case study

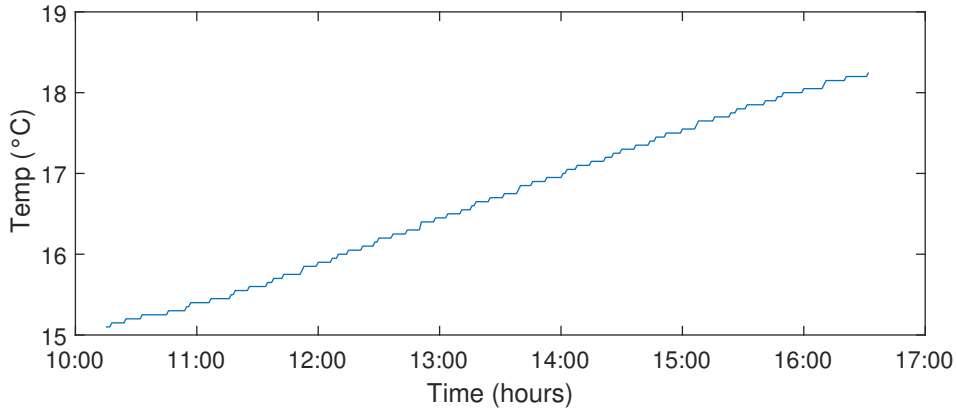

Figure 5.4: 300 kVA example transformer input: Ambient temperature profile

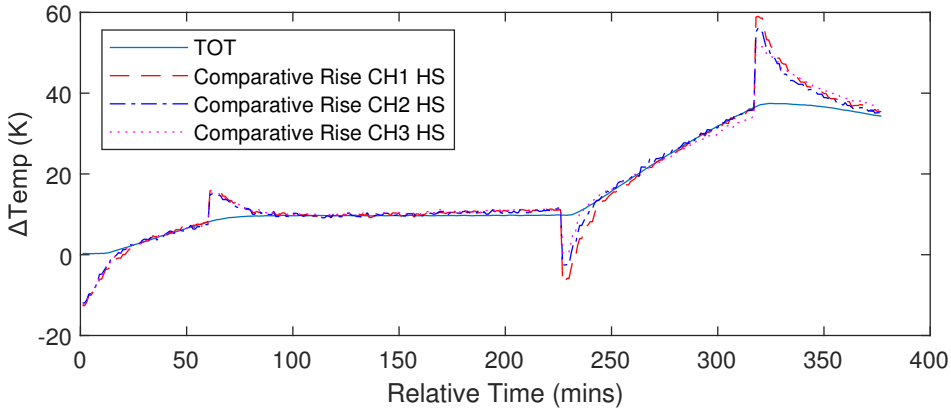

Figure 5.5: 300 kVA offset winding and TOT rise comparison

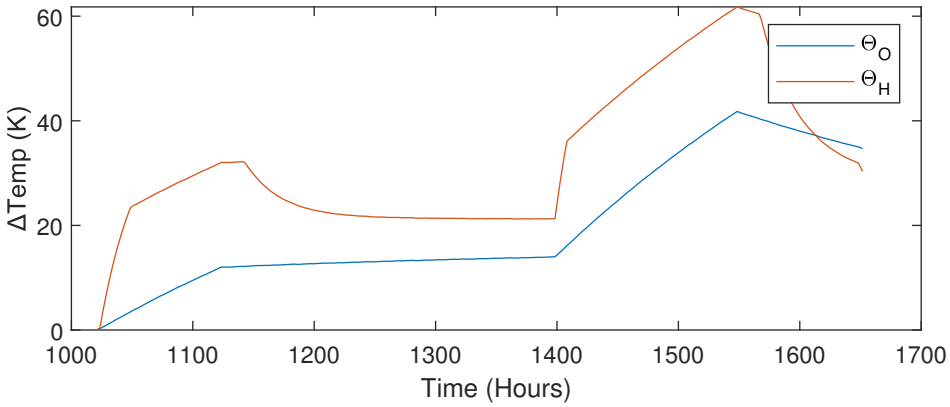

Figure 5.6: 300 kVA modelled output

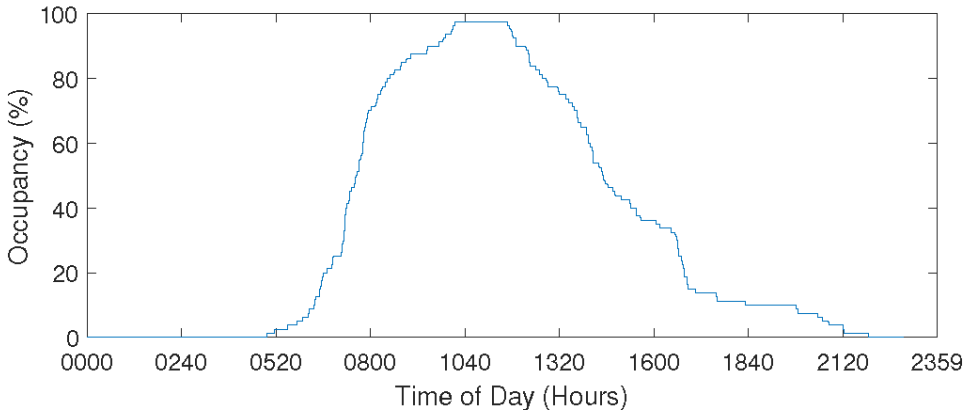

Figure 5.7: Car park occupancy profile

assumes that 22 kW, 3-phase a.c. charging points have been supplied to each of the 80 spaces in the car park, with a goal of supplying at least 80 % charge to the vehicles. Once an EV has received at least 80 % charge, its maximum charging rate is limited to 7 kW, and it is designated as low-priority. The low-priority designation means it is eligible to have its pausing charged when capacity is required for higher priority loads. The motivation behind choosing this case study is explained in Section 5.6.1.

5.6.1 Case Study Motivation

It is common for university campuses, business parks, and high-rise buildings to be furnished with a dedicated transformer designed for an expected load that does not include EV charging. This case study examines the feasibility of implementing 3-phase EV charging infrastructure, given that peak charging is likely to coincide with peak base loading. Furthermore, there is limited scope to valley-fill or load-shift to periods of low utilisation, such as late night, or early morning, as the EV charging demand only exists during the workday. The case study simulation parameters are summarised in Table 5.2. An explanation of the parameters used for each scenario is provided in Section 5.6.2.

Table 5.2: Simulation Parameters

Parameter	Value
Expected Load Power Factor	0.9
Local Voltage Regulation Limit	$\pm 6\ \%$
Maximum Θ_{HS} Temperature	$140\ ^{\circ}C$
Maximum Θ_{O} Temperature	$115\ ^{\circ}C$
EV Fast Charge Power	$22\ kW$
EV Fast Charge Duration	$3\ Hours$
EV Slow Charge Power	$7\ kW$
EV Slow Charge Duration	$7.5\ Hours$
Lifetime Tolerance	$\pm 10\ \%$
Thermal Expansion Zero	$15\ ^{\circ}C$
Voltage Regulation Simulation Limit	$\pm 5\ \%$
Pressure Safety Margin	$+2\ \%$
Thermal Limit Safety Margin	$+10\ \%$

5.6.2 Case Study Parameters

Fig. 5.8 presents the potential loading scenario when no load management approaches are taken. Such a load is impossible to accommodate without some method to limit the maximum loading. Similar to load-shifting and valley-filling, the TD approach incorporates queuing, which imposes a slight delay to the addition of loading. However, the TD approach incorporates the loading as soon as there is available capacity. This is distinct from load-shifting and valley-filling approaches where the intent is to move the entire EV charging load to a period of low-utilisation. The loading the transformer is capable of using the TD approach methodology is contrasted with loading limited to the nameplate rating of the transformer.

The case study investigates this performance contrast by examining how capable an existing 300 kVA transformer in south Auckland is to power the EV charging infrastructure for an outdoor car park, in addition to its existing load, supplying the

university campus building beside the car park. The ambient temperature profile used is a generalised average across a year, see Fig. 5.9. Parking profiles for 80 car park spaces are generated based on Fig. 5.7. As cars could arrive, depart or finish charging at any time, the simulation runs over 86,400 seconds (24 hours) enabling it to check if there has been a change every second and complete the relevant processes accordingly. The scenario assumes the chargers are compliant with IEC 62196, support simple level-based communication which allows them to supply fast, slow or no charging. The chargers are all 3-phase, supplying up to 22 kW a.c., and are available at each of the 80 car parks. The chargers only supply fast-charging up to 80 % state of charge (SoC) and a 7 kW maximum from 80–100 %. In this scenario, and even assuming a base load of zero, only a maximum of thirteen EVs can be fast-charged simultaneously before the nameplate limit is exceeded. The case study scenario has a maximum car park occupancy of 100 % around 1200 hours, with the results detailed in Section 5.6.3.

5.6.3 Case Study Results

Fig. 5.10 provides an example of a mid-cycle output generated using the TD approach. The assessed load is also comprised of the highlighted forecasted load and the base load for the remainder of the load-cycle. The final output from the TD approach and nameplate-limited (NL) analyses are presented in Fig. 5.11. These results demonstrate that both the TD approach and NL support EV charging in addition to the base load without compromising it. However, the TD approach allows for higher peak loading during the day, whereas using NL requires an effort to support EV charging load for an extended period throughout the day. The improvement that the TD approach offers compared with NL is quantified in Table 5.3.

The highlighted results presented in Table 5.3 demonstrate that on average, the TD approach has reduced the EV wait time for a charge by more than 66 %, increased

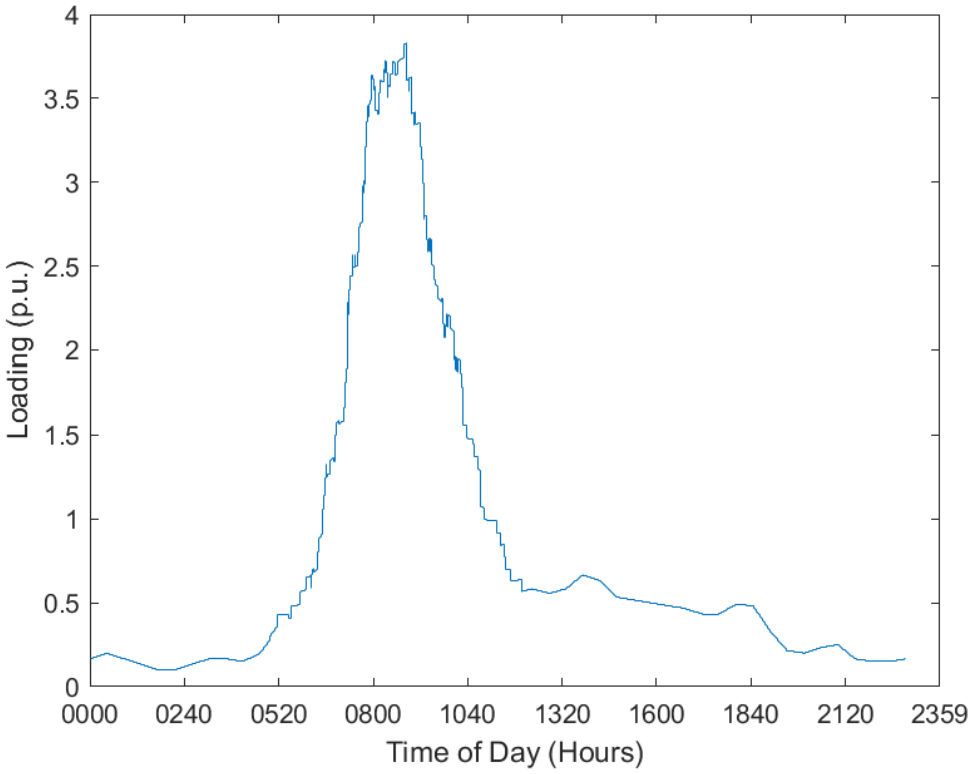

Figure 5.8: Maximum potential load for case study scenario

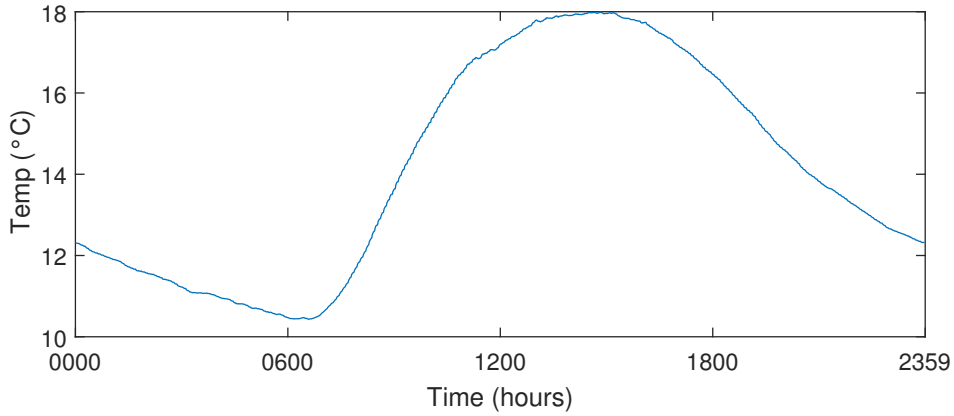

Figure 5.9: 300 kVA Case study: Ambient temperature profile

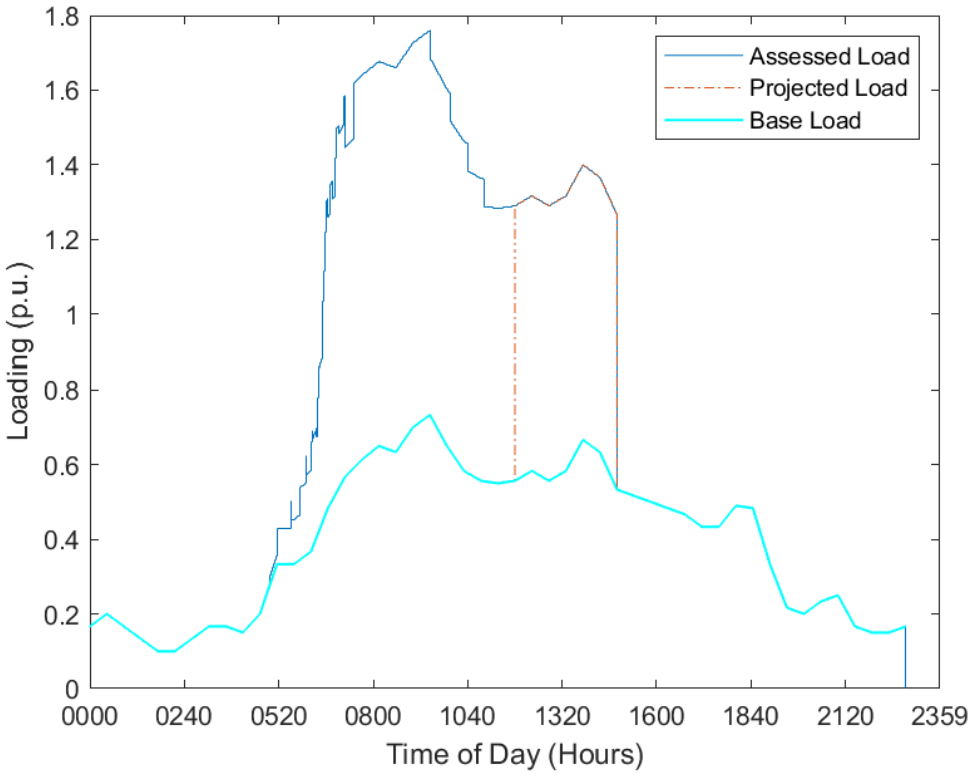

Figure 5.10: TD approach assessed scenario load output at 1230 hours showing existing and projected loading overlaid on base loading

Table 5.3: Scenario Comparative Analysis:
TD Approach vs. Nameplate Rating

Performance Metric	TD Approach	Nameplate Rating
Max. Top Oil Temperature	91.4 °C	62.18 °C
Max. Hot Spot Temperature	111.4 °C	75.03 °C
Max. Internal Pressure Reached	113.4 kPa	104.8 kPa
Remaining Lifetime	36 Years	> 100 Years
Average Wait Duration	74 mins	219 mins
Average Charge per EV	45.8 kWh	25.3 kWh
EVs Receiving 80%+ Charge	93.8 %	61.3 %
EVs Receiving 0% Charge	3.75 %	38.75 %

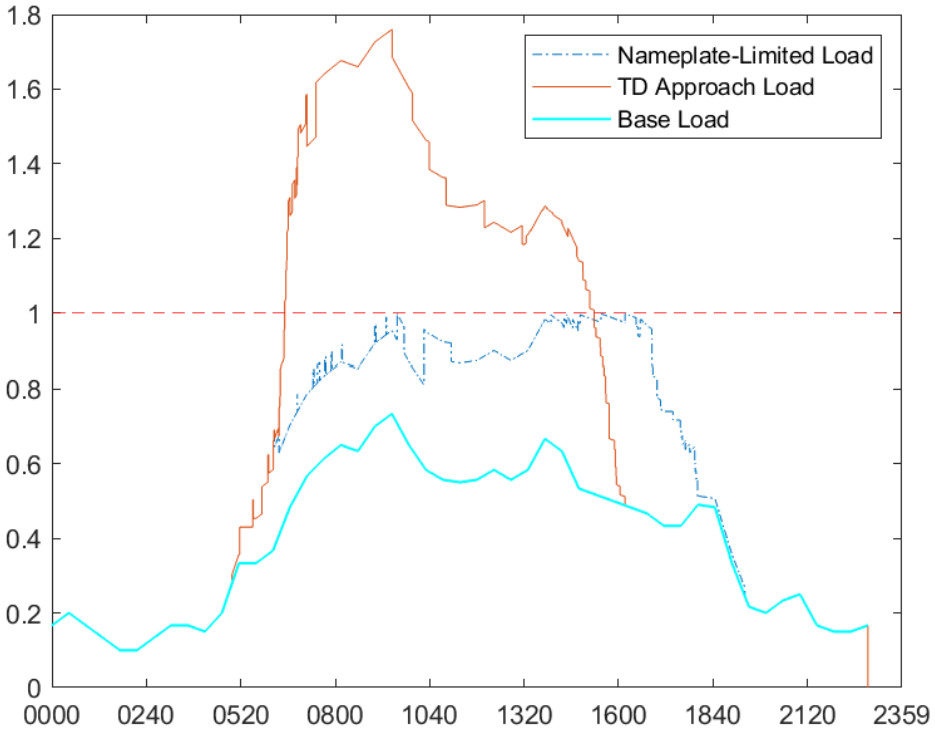

Figure 5.11: TD approach output for scenario vs. nameplate rating overlaid on base loading

the energy supplied to each EV by more than 20 %, and for the scenario 32.5 % more vehicles departed with an SoC or 80 % or greater. Furthermore, the minimum lifetime requirement of 35 years was maintained, and maximum oil and winding hot-spot temperatures were kept below 115 °C and 140 °C, respectively.

The assessed lifetime of more than 100 years from the nameplate-limited loading results demonstrates that methods, such as the TD approach, are required to allow the retirement age to coincide with the transformer's expected lifetime.

5.7 Chapter Summary

This chapter introduced the TD approach, a novel thermally-based solution for managing dynamic loading on a transformer. By using knowledge of thermal inertia, it was shown that with a dynamic load profile a transformer can operate for periods in excess of its nameplate rating. This was achieved, without exceeding any relevant IEEE or IEC standards, manufacturer's specifications, or user-provided parameters. Therefore, the TD approach balances the requirement to meet high charging load demands, due to rapid EV uptake, and existing infrastructure constraints. The operation of the TD approach was presented and described. The two case studies showed that while existing approaches can support EV charging on top of the base load, avoiding the immediate expense of upgrading the site's distribution transformer, utilising the TD approach is an improved methodology, reducing waiting time and increasing average charge per EV without exceeding IEEE and IEC limits.

Chapter 6

Use of Fibre Bragg Grating for Direct Temperature Measurement

6.1 Introduction

The nature of electrical distribution grids is rapidly changing. Existing networks were designed for one-way power flow and not bi-directional, as is the case with solar installations in the low voltage (LV) network. The increased uptake in electric vehicles (EVs) also add significant challenge as they alter the traditional load profile and can themselves consume one or more household's worth of electricity. Therefore, improved distribution transformer design and monitoring approaches are required to minimise lifetime costs and future capital expenditure. Traditionally, the determination of the health and life of a distribution transformer, has relied on modelled rather than measured data, which can lead to inaccurate assessment of transformer health and non-optimised transformer utilisation. To address some of these concerns, this research has already developed multiple algorithmic solutions:

i. An empirical design method for distribution transformer utilisation optimisation

ii. A dynamic degree of polymerisation algorithm for lifetime optimisation

iii. A thermally-based dynamic (TD) approach for load management with unknown potential loads

However, incorporating real-time feedback with these solutions, particularly the TD approach, means the algorithm could be adapted to deal with situations that add model complexity, such as unbalanced loading, or with emergency conditions, such as an unexpected temperature rise due a tank rupture. Therefore, direct measurement can both complement and enhance the algorithmic solutions proposed. This chapter examines such solutions and discusses their suitability for supporting these algorithms.

This chapter examines the "Smart Supervisory System", which is introduced later in the chapter, and developed in conjunction with our industry partner, ETEL, is an example of such a suitable platform.

6.2 Rationale For Fibre-Based Winding Measurement

Direct winding measurement utilising fibre optic technology is not a new concept and has been proposed for use in power transformers since the early 1980s [147]. However, such fibre-based systems were not cost-effective [148], and therefore not suitable for use in distribution transformer. However, the authors in [148] have highlighted the following as likely future trends for the industry:

Restructuring The electricity market is expected to experience an extended period of continued restructuring.

Asset Optimisation Incentivisation measured expected for optimised asset use, incorporating diagnostics and monitoring systems.

Analytics A shift to occur from sensor development to analytics

Research Universities to focus on the physics needed for interpretation, preferably in collaboration with manufacturers and utilities.

On-line Diagnostics Development of on-line diagnostic methods, avoiding the need to take transformers out of service.

New Diagnostics Increase in transformer utilisation resulting in the development of new diagnostic techniques.

System Integration The transformer will be seen less as a separate item, but as a contributor to the system as a whole.

Technology Cost-effectiveness Price-drops for technology will contribute to the up-take of diagnostics.

Many of these assertions are in agreement with assertions made in this thesis, and the idea to improve the thermal understanding of transformer behaviour is not new. The authors in [149] noted a specific disadvantage of the TOT method they were describing, was that it avoided direct winding temperature measurement (DWTM). However, they reasoned that the perceived risks and complications, associated with DWTM, precluded it as a viable option at that time. While [149] makes the case that top-oil temperature measurement is an improvement over the purely modelled system that preceded it, an additional limitation was highlighted in [150]. In this study, the author placed thermocouples into the winding to investigate the accuracy of the thermal models for transformer windings. These results showed improvements to the models were required, for which the author included new equations that he had generated. The author also referenced an industrial survey into state of the art DWTM techniques carried out in 1990 by a Cigré Working Group, which recommended that DWTM be encouraged [151]. However, this recommendation still has not received meaningful adoption, and even with DWTM, there are transformer failure factors it cannot protect against, such as poor quality repairs, improper earthing, and loose connections, as highlighted in Fig. 6.1 [44].

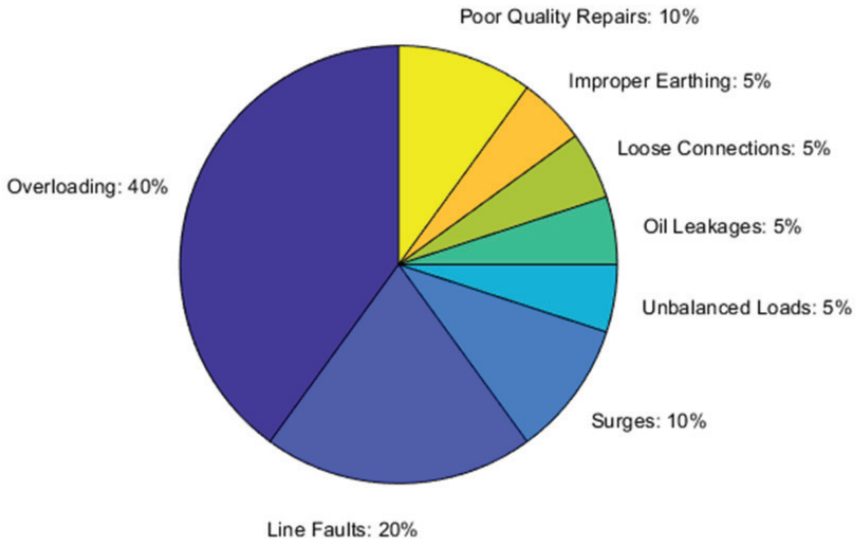

Figure 6.1: Causes of distribution transformer failures from [44].

However, there are other potential causes of failure that an advanced DWTM transformer monitoring system can sense and apply direct protection measures. In particular, overloading which was found to be the cause of 40 % of the total failures is a scenario that can be guarded against. The following subsections examine these scenarios and a solution presently in the market is contrasted with our industry partner's intended solution utilising fibre Bragg grating (FBG) sensors.

6.2.1 Overload Protection

Because the operational life of a transformer is effectively the life of its insulating paper, and the paper's life is dependent on its mechanical strength derived from the number of monomer units per chain, its degree of polymerisation (DP), any process that accelerates chain breakdown is of concern. Pyrolysis is such a factor and is the sole determination in IEC and IEEE loading guides, specifying a normal operating temperature for thermally

upgraded Kraft paper at 110°C, yielding a transformer lifetime of 17.2 years and 20.5 years respectively [8,66]. Operational loading such that the internal temperature remains below the normal temperature slows ageing, extending its lifetime and operation at temperatures above accelerate ageing. Furthermore, extreme heat results in charring of the cellulose [152], and other potential risks are [8]:

i. Winding and oil temperatures increase, possibly to unsafe levels.

ii. Winding leakage flux density increases, providing additional heating to metallic parts linked by the flux.

iii. Additional heating promotes increased moisture content in the paper and oil.

iv. Higher stresses are placed on the bushings, tap-changers and cable-end connections.

However, there are three different overloading scenarios allowed for in [8]:

Normal cyclic loading loading where a higher ambient temperature or higher-than-rated load current is experienced during part of the cycle, but relative to the thermal ageing model, is equivalent to the rated load at normal ambient temperature.

Long-time emergency loading where an extended period of excess loading occurs due to unavailability of other assets and a new higher steady-state has been reached and will be maintained until the excess loading is removed.

Short-time emergency loading where a period of excess loading occurs due to unavailability of other assets and a new higher steady-state has not yet been reached before the excess loading is removed.

In each of these scenarios, the required load may be maintained, subject to the limits specified in Table 6.1 [8].

Table 6.1: IEC 60076-7 – Maximum Overloading Limits

	Normal	Emergency	
Parameter	Cyclic	Long-time	Short-time
Current	1.5 (p.u.)	1.5 (p.u.)	1.8 (p.u.)
Winding Hot Spot	120 °C	140 °C	160 °C
Top Oil	105 °C	115 °C	115 °C

6.2.2 Non-Linear Loading Assessment

Non-linear loads cause harmonic currents in the network, resulting in harmonic voltages. This combination increases both no-load and on load losses. The harmonic order and corresponding magnitude determine the effect of these harmonics. Transformers subjected to heavy harmonic loading may experience higher hot spot temperature and increased core losses [153], and the IEEE advise the automatic lowering of the VA rating of liquid-filled DT in the presence of harmonics according to equation (6.1) [154]:

$$I_{max} = \sqrt{\frac{P_{(LL-R)}}{1 + F_{HL} \cdot P_{(EC-R)}}} \tag{6.1}$$

where

I_{max} is the maximum permissible RMS non-sinusoidal load current under rated conditions in $p.u.$

$P_{(LL-R)}$ is the per-unit load loss under rated conditions in $p.u.$

F_{HL} is the harmonic loss factor for winding eddy currents

$P_{(EC-R)}$ is the per-unit winding eddy-current loss under rated conditions in $p.u.$

However, a case is made in [155] that automatic derating may not always be necessary and provide a flowchart, presented in Fig 6.2, which details the process for determining whether derating is required when Θ_{HS} is known. This demonstrates that through measuring Θ_{HS} the effect of harmonics on the life of the transformer is

automatically factored in.

6.2.3 Online Dissolved Gas Assessment

Dissolved gas is an indicator to the current state of a transformer's health and is generated due to three causes:

i. Chemical reaction – produced by stray gassing

ii. Localised overheating or hot spot

iii. Partial discharge (PD)

There are nine gases generated inside a liquid-filled transformer: Hydrogen, methane, acetylene, ethylene, ethane, carbon monoxide, carbon dioxide, nitrogen, and oxygen, for which hydrogen can serve as the primary indicator of a transformer's health [156], therefore, sensing only hydrogen is sufficient.

Moisture lowers the dielectric strength of oil and the solid insulation, increasing the risk of breakdown of the paper insulation. Moisture increases the likelihood of bubble formation and accelerates the thermal ageing of the paper insulation. Even a leak free transformer releases water as a by-product of its normal ageing process. An ageing method which takes into account the effects of moisture is included in equations (6.2) and (6.3) [48]:

$$\frac{1}{DP_T} - \frac{1}{DP_0} = A \cdot e^{-\frac{E_A}{RT}} \cdot t \tag{6.2}$$

where

DP_0 is the initial DP value.

DP_T is the value the final DP value for the range being examined.

R is the Molar gas constant and is equal to $8.314 m^2 kg s^{-2} K^{-1} mol^{-1}$.

T is winding hot spot temperature Θ_{HS} in degrees Kelvin.

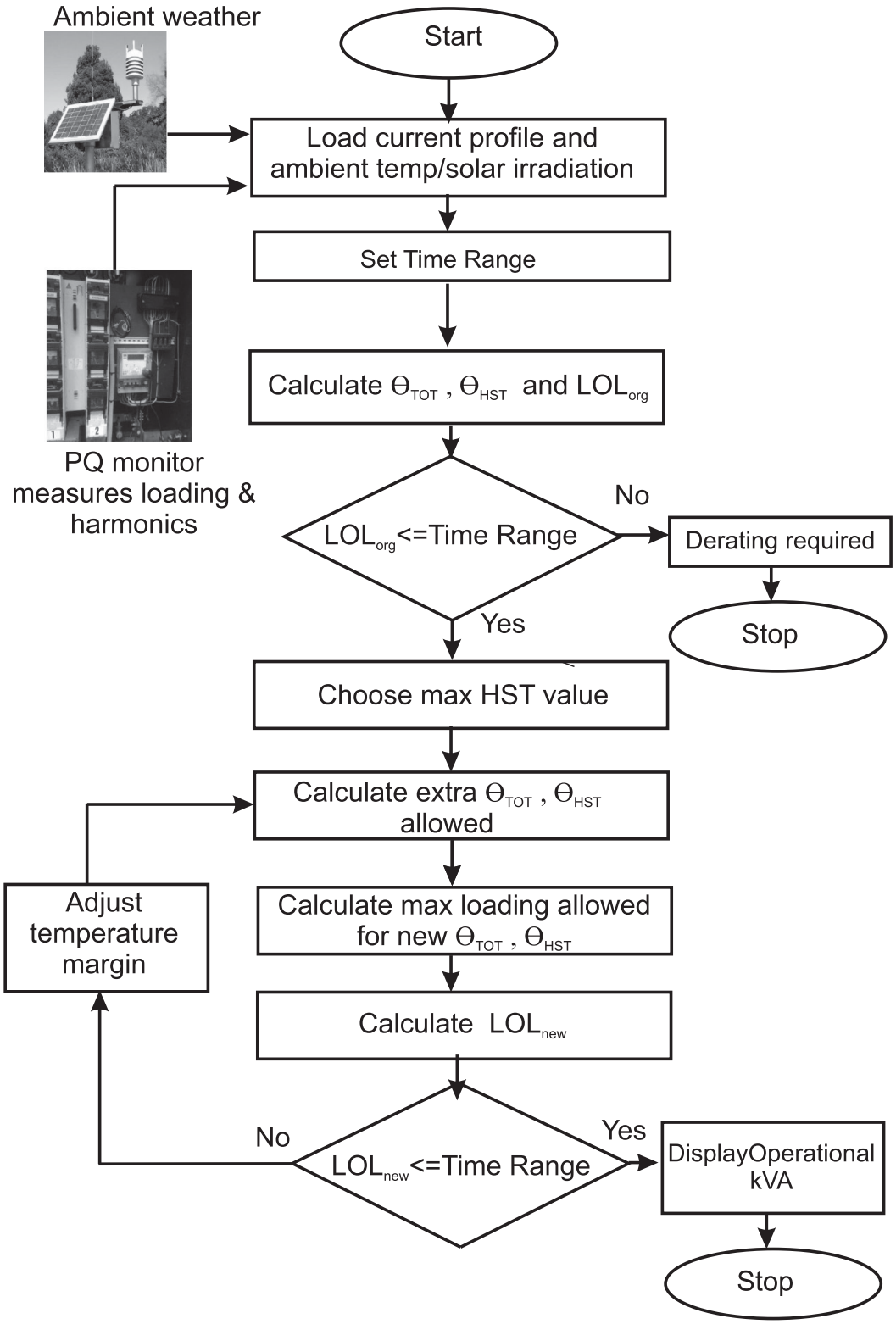

Figure 6.2: Flowchart for determining whether derating is required in the presence of harmonics from [155].

Table 6.2: Equations for Calculating A[1]

Oxygen Level (ppm)	Equation
Low < $7,000$	$(1.78 \times 10^{12})w^2 + (1.10 \times 10^{10})w + 5.28 \times 10^7$
Medium $7,000 < 14,000$	$(2.07 \times 10^{12})w^2 + (5.61 \times 10^{10})w + 2.31 \times 10^8$
High > $16,500$	$(2.29 \times 10^{12})w^2 + (5.61 \times 10^{10})w + 3.86 \times 10^8$

[1]where w is the water content of the paper expressed in a decimal fraction [48]

A is the environmental factor and is equal to 6.92×10^7. However, its value depends on the quantity of dissolved oxygen and moisture content and can be determined using the relevant equation from Table 6.2.

E_A is the activation energy and is equal to $110\ kJmol^{-1}$.

In operational transformers, it is expected that the moisture content will increase over its life, and is a significant factor in non-hermetically sealed transformers. While less of a factor in hermetically sealed transformers, increased heating does release additional moisture from the insulating paper, so its effect should be considered, and therefore, a revised calculation for transformer ageing rate (V) is used [8]:

$$V = A \cdot e^{\left(\frac{1}{R}\right)\cdot\left(\frac{EA_T}{383} - \frac{E_A}{T+273}\right)} \tag{6.3}$$

For the purposes of loss of life (LOL) calculations for hermetically sealed distribution transformers, no oxygen and 1.5% moisture scenario is considered to represent the worst case. Due to the varying nature of Θ_{HS}, the weighted Θ_{HS_W} and weighted activation energy E_{A_W} are calculated according to equations (6.4) and (6.5) [48]:

$$\Theta_{HS_W} = \frac{1}{\frac{-R}{E_A} \cdot \ln \frac{\Sigma\left(\frac{-E_A}{e^{R\times\Theta_{HS}+273}}\right)}{n}} \tag{6.4}$$

$$E_{A_W} = \frac{\Sigma\left(\frac{-E_A}{e^{R\times\Theta_{HS}+273}}\right)}{n} \tag{6.5}$$

where

n is the number of interval steps for the LOL calculation

E_{A_W} is the value used to calculate the time required for DP_0 = 1000 to fall to its end of life value, DP_{final} = 200.

From the equations above, it can be seen that the inclusion of moisture and oxygen sensing, in addition to Θ_{HS} and TOT measurements, will improve the determination of the DT lifetime. Although, the moisture content and health of the oil, cannot be ascertained by direct temperature measurement, because hydrogen is a primary indicator gas, the moisture and oxygen can be determined through DGA, utilising a hydrogen sensor.

6.2.4 Fault Impact Minimisation

For severe faults and voltage surges, protection against immediate and catastrophic failure is the responsibility of external protection devices. However, lower fault and voltage levels can create weak points within the transformer structure, which eventually grow to the point of becoming a catastrophic failure. Through sensing of Θ_{HS}, this can be indirectly detected, due to the localised heating.

Indirect sensing can also be used to detect oil leakage. Sealed transformers maintain a consistent relationship between oil temperature and pressure. They are designed to withstand the internal pressure variation resulting from the expansion and contraction of the air space above the oil due to temperature changes. Any lowering of pressure and oil level relative to the norms will be indicative of leaks. This could be measured directly, or indirectly through Θ_{HS}, which will provide abnormal temperature readings for the load conditions.

6.3 Fibre Bragg Grating Sensors

Due to the relative low cost and being inert to electrical and magnetic fields, fibre Bragg grating (FBG) has the potential lower the cost to market and create the market for transformer monitoring that did not previously exist. In this next section, the potential for FBG-based sensing is explored.

6.3.1 Examples of FBG Implementations in Research

A comparison of FBG-based sensing to the use of thermocouples in [157] resulted in favourable outcome for the suitability of FBG sensors. The thermocouple temperature was found to waver, whereas the FBG sensors appeared to produce more consistent results. The multiple sensors also demonstrated significant temperature variance from top to bottom of the winding. Similar stability findings were made from the measurements over a two month period in [158], with a reported FBG temperature resolution of ±0.6 °C, with similar findings also made in [159, 160]. This aligns with our industrial partner's expectation for an accuracy of ±0.5 °C.

6.3.2 FBG Implementations in Industry

The only commercial implementation of a transformer incorporating FBG sensors is that described in section 6.4. To this end it is assumed that such implementations are primarily the preserve of research and the rest of the section will examine what is being done in industry to support distribution transformer real-time monitoring and analytics, hereby referred to as "intelligent" transformers.

6.3.3 Intelligent Transformers in Industry

Although distribution transformers, have not traditionally incorporated on-line monitoring equipment due to the cost and lack of a suitable technology [148], for reasons cited in Section 6.2, and other pressures such as the increasing demand from EV charging, sensor-infused transformers development and release is now underway. For example, the original smart transformer prototype that the "smart supervisory system" development described in Section 6.4 has built upon was realised in 2016 for a 2026 commercial release by our industrial partner, ETEL [5, 140], and their market competitor, ABB, first reported their commercially available intelligent distribution transformer in 2017 [141, 161]. However, they have taken a very different approach to implement "smart" or "intelligent" transformers, as outlined in the following side-by-side comparison.

6.3.4 Initial Platform Development: ETEL

The smart transformer (ST) concept was initially presented at the 2016 EEA Conference and Exhibition. The key benefits summarised for utilities were: enhanced asset capacity (rating), extended transformer life, avoiding failures, faster restoration of supply post-fault, optimisation of planned maintenance, optimisation of control room operations, improved planning and network design, health and safety issues dealt with pre-emptively, demand-side management and reduction in electrical losses [140]. At the time of publication, they were presenting their Generation 2 (Gen 2) mode, and did not include any comparison with the Generation 1 (Gen 1) model. This was covered in their second publication [5], in which they revealed that their ST development programme began in 2010, and both Gen1 and Gen2 had been in field trials for two years. They also asserted that maintenance philosophies are also changing from reactive in the 1980s to proactive in the 1990s to diagnostic/analytic in the 21st century, and their ST is one such example

Table 6.3: Side-by-Side Comparison of Intelligence Gathering Techniques: ABB and ETEL

ABB [141]	ETEL
Ambient Temperature	Ambient Temperature (Thermistor-based)
Top-Oil Temperature	FBG Winding Temperature
Levels	Levels
Pressure	Pressure
Moisture	FBG Moisture Sensing[1]
Voltage	LV Power Sensing[1]
Current	–
Hydrogen	FBG Hydrogen Sensing[1]
Position (GPS)	–
Local Analytics	Local Analytics
Consumed Transformer Lifetime	Expected Lifetime Calculation[2]
–	Regulation
Total Harmonic Distortion	Harmonics
Built-in WiFi – data download only	Serial – RS232[3]
Wired Ethernet – including DNP3 and IEC 61850 support	Wired Ethernet – including DNP3 and IEC 61850 Support[4]
300 kVA+	100 kVA+

[1]Sensor partially developed – yet to be integrated

[2]Potential for algorithmic enhancement

[3]Capability can be extended through the use of external protocol converters

[4]Proposed - unspecified time frame

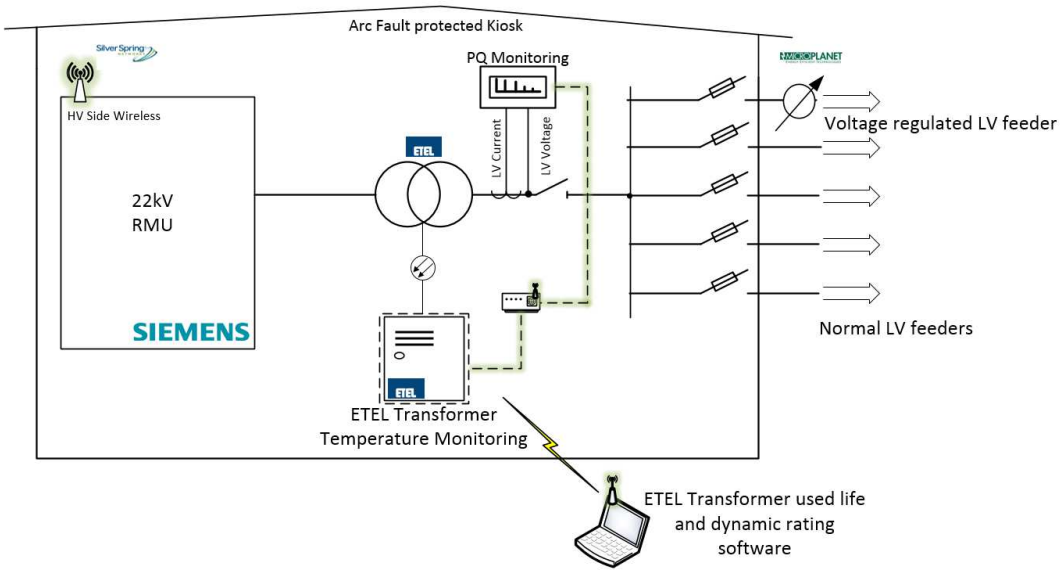

Figure 6.3: Concept diagram of the Smart Transformer kiosk [140]

of a tool that can contribute to realising this philosophy.

Table 6.4 below summarises the features of each generation [3].

Although they have yet to formally implement a Generation 3 variant, ETEL collaborated with us to develop a "smart supervisory system" incorporating monitoring, self-protection, and communications features of a DT designed for industrial use was developed in collaboration with them for a customer based in Australia. In Section 6.4, a solution overview and description of the implemented system.

6.4 Smart Supervisory System Solution Overview

Fig. 6.5 is a block diagram of the smart supervisory integration system for utilities that already have a Modbus TCP supervisory control and data acquisition (SCADA) network in place, and wish to integrate the monitoring functions into it. Fig. 6.6 is an alternative design for utilities that require a stand-alone system. The diagram in Fig. 6.6 still retains the same functionality as that shown in Fig. 6.5. However, the software incorporates alarm functionality should the set-point Θ_{HS} values be exceeded.

Table 6.4: Smart Kiosk Features

Features	Details	Gen 1	Gen 2
Modularity	Kiosk based	✓	✓
	Oil bund	–	✓
	Arc fault	–	✓
LV Monitoring	LV Power Logging	✓	✓
LV Regulation	(Single Phase)	–	✓
	Buck-boost	–	✓
Fault response	Blown fuse	✓	✓
	Overload response	✓	✓
	Short-circuit response	✓	✓
	Earth fault response	✓	✓
	Detailed fault indication	–	✓
Transformer monitoring	Oil temperature	–	✓
	Winding temperature	–	✓
	Kiosk ambient temperature	–	✓
Asset management	Used life analysis	–	✓
	Health index analysis	–	✓
	Maintenance reporting	–	✓
HV monitoring	Remote control	✓	✓
	HV power logging	–	✓
	Fault indication	✓	✓
Communication	Radio/3G	✓	✓
Reactive power	Capacitor bank	✓	–

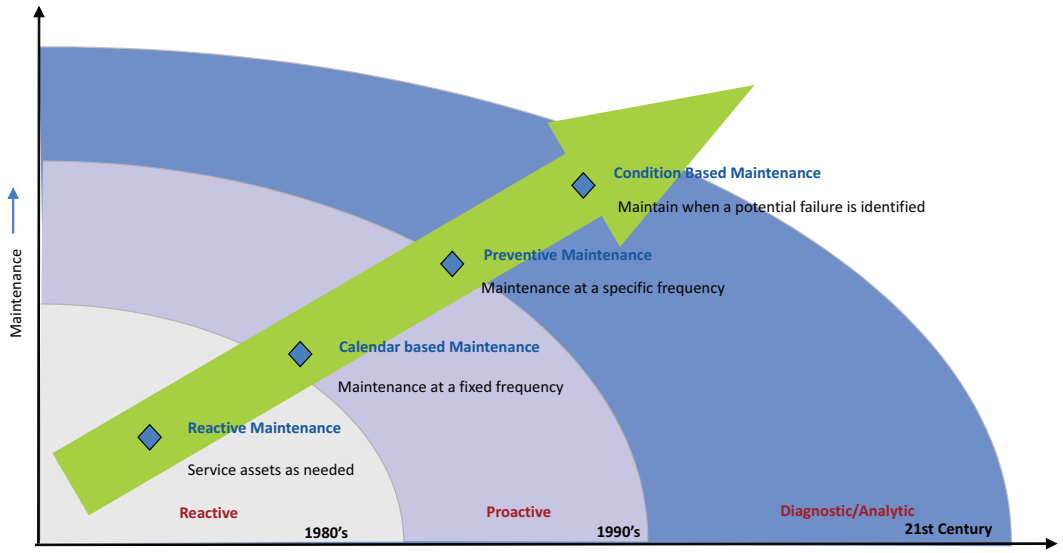

Figure 6.4: Transformer maintenance strategies over the years [5]

Overload protection for both solutions is provided through the MV switchgear for the MV to low voltage (LV) step-down transformer. This switchgear receives signals directly from the Θ_{HS_W} sensors forming part of the monitoring section of the system. This realises a transformer that can disconnect itself from the load, if any Θ_{HS} reaches 140°C, the near bubbling threshold for the oil. Manual re-connection is required after a trip. External signals can also be applied to trip MV switchgear, which are not shown for clarity.

The monitoring section includes TOT and hydrogen sensing, in addition to the fibre-optic Θ_{HS} sensors, but these cannot directly operate the MV switchgear. This is justified on the basis that changes in Θ_{HS} occur at a faster rate than changes in TOT and hydrogen levels, and the direct and critical effect of Θ_{HS} on DT lifetime.

The integration design, shown in Fig. 6.5, has low-speed serial data from all sensors captured by a protocol converter capable of aggregating the relevant information to a single Modbus TCP interface. The system collects data automatically, ready to be polled by the remote-monitoring station, which contains the Modbus TCP Master. For the standalone solution, shown in Fig. 6.6, each sensor has a dedicated protocol converter

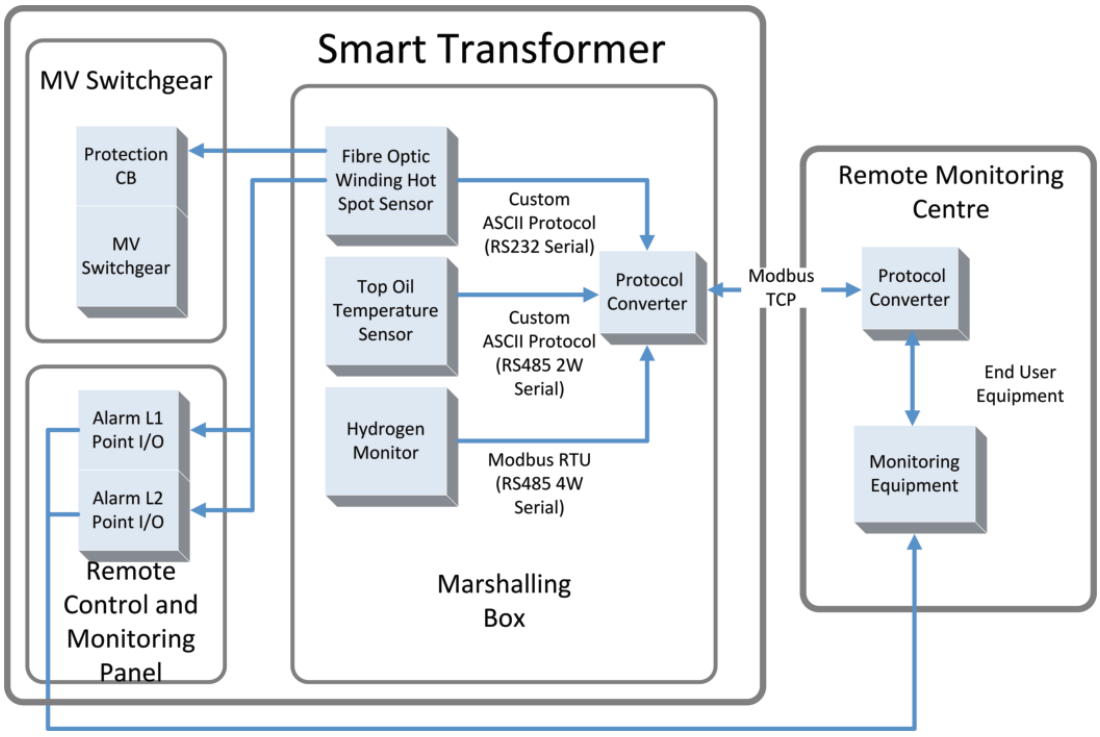

Figure 6.5: Industrial DT Functional Block Diagram (Integration Solution).

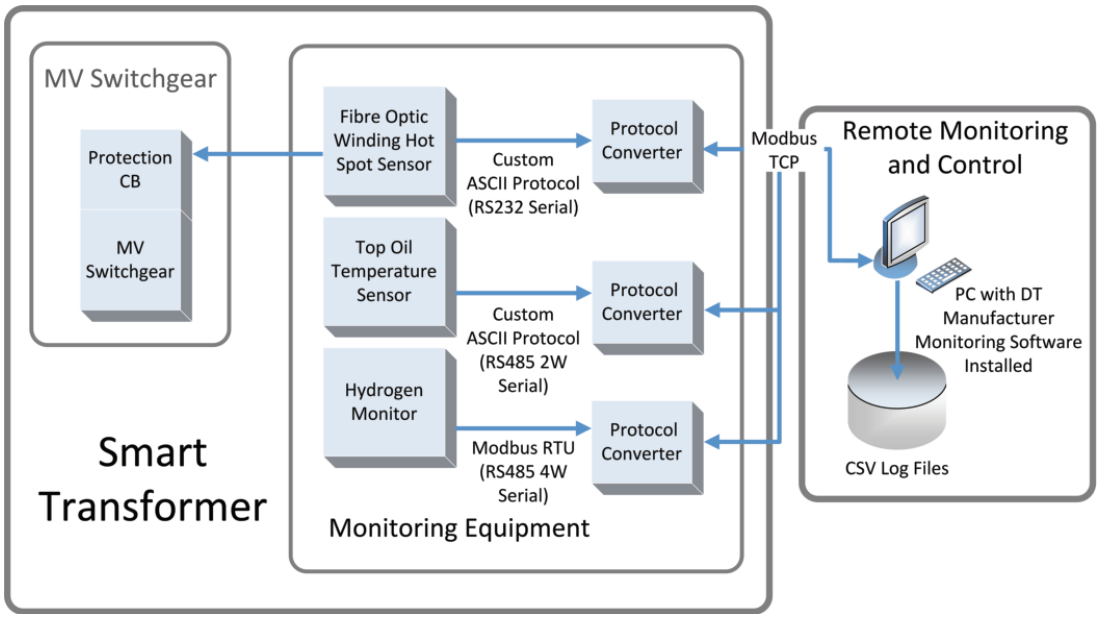

Figure 6.6: Industrial DT Functional Block Diagram (Standalone Solution).

to translate the low-speed serial data to Modbus TCP. The remote-monitoring station incorporates a PC running software, custom developed by the manufacturer, which aggregates the sensor data and functions as the Modbus TCP Master and data-logger. The remote-monitoring station in Fig. 6.5 also receives signals from the remote control and monitoring panel section of the "smart supervisory system". This section comprises two alarm outputs,which are each set to activate at different and factory pre-settable temperature levels. Input to the alarms comes solely from the fibre-optic hot-spot sensors. The remote-monitoring station in Fig. 6.6 can still receive the alarm notifications. However, alarm notifications are also incorporated into the custom monitoring software.

6.5 Implemented Smart Supervisory Systems

In Section 6.4 two developed solutions were presented along with their respective functional block diagrams, and use cases Fig. 6.5 and Fig. 6.6. This section overviews what was built and presents results gathered from a heat-run utilising the system in Fig. 6.6.

6.5.1 Fibre-Optic Measurement

These systems both utilise one fibre per winding to measure Θ_{HS_W} and IEC 60076-7 discusses temperature sensing using fibre-optic probes, and the temperature gradients that may exist within a winding structure. Further, it is stated, *"Hence, it is unlikely that the insertion of, for example, one to three sensors will detect the real hot spot". The need for multiple hot-spot sensors per winding can impact significantly on cost. However, through accurate loss and thermal calculations, as well as winding modelling, the need for multiple sensors can be overcome."* However, an alternative approach, [5], allows Θ_{HS} measurement utilising only one fibre per winding.

Figure 6.7: Physical Implementation of Marshalling Box in Fig. 6.5.

6.5.2 Communications

Fig. 6.7 shows the inside of the DT's marshalling box. The fibre-optic sensor is located in the top-left of the figure. The two connections in the top are RS-232 and power. The grey box with the pink and grey cables exiting from underneath is the TOT sensor, communicating with 2-wire RS-485. The hydrogen sensor is not visible, as it is plugged directly into the tank of the DT. However the 4-wire RS-485, used for monitoring parameters and the RS-232, used for debugging and parameter-setting, are located under the red protocol converter.

The protocol converter polls each of the sensors, collecting the information, which is then presented to a single Modbus TCP slave port. The fibre-optic and TOT sensors both utilise a custom ASCII protocol and the hydrogen monitor utilises the industry standard Modbus RTU for monitoring. The protocol converter has to poll each device according to its own communication standard and has a dedicated communications

port for each sensor. The RS-232 interface for the hydrogen monitor is primarily for diagnostics and configuration, so is not included in the monitoring solution.

6.5.3 Protection

In Fig. 6.7 the three connections on the left of the fibre-optic sensor are the connections to the alarm monitoring and MV CB. When the various set-point temperatures are exceeded, the relevant relays within the box engage, either for an alarm or to trip the MV CB. The stand-alone solution in Fig. 6.6 also has this capability, however the alarms can also be viewed within the software.

6.5.4 System Validation

Fig. 6.6 was an extension to custom monitoring software, previously designed for the Generation 2 kiosk detailed in [5], which communicated via a PC serial port to the fibre-optic reader. This revision removed the serial port communication from the software and replaced it with Modbus TCP and incorporated TOT and hydrogen data logging. The heat-run data presented in Fig. 6.8 and Fig. 6.9 were captured utilising this system. In Fig. 6.8 blue line represents the raw temperature (RT) measurement, including ambient temperature (AT), the red line is AT, and the yellow is RT less AT. The values in Fig. 6.9 are RT less AT. The AT measurement was an external device, and is not part of this solution. In Fig. 6.9 the Phase B temperatures are consistently higher than Phases A and B. This phenomenon is unique to a heat-run scenario, where a perfectly balanced load is drawn across all three windings. Thus, resulting in the central winding, Phase B, being subjected to additional heating from the windings either side.

In practice the inherent levels of unbalance in the phases results in a more even heating across the phases, except where extreme unbalanced loads are applied to the DT.

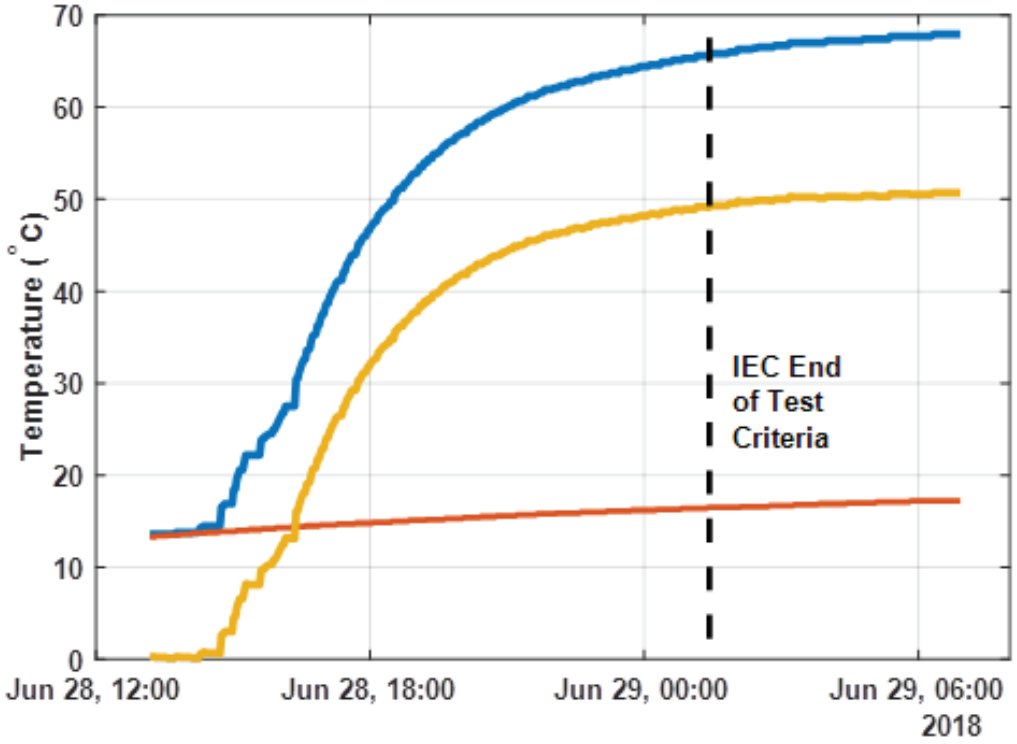

Figure 6.8: TOT Heat-Run Data.

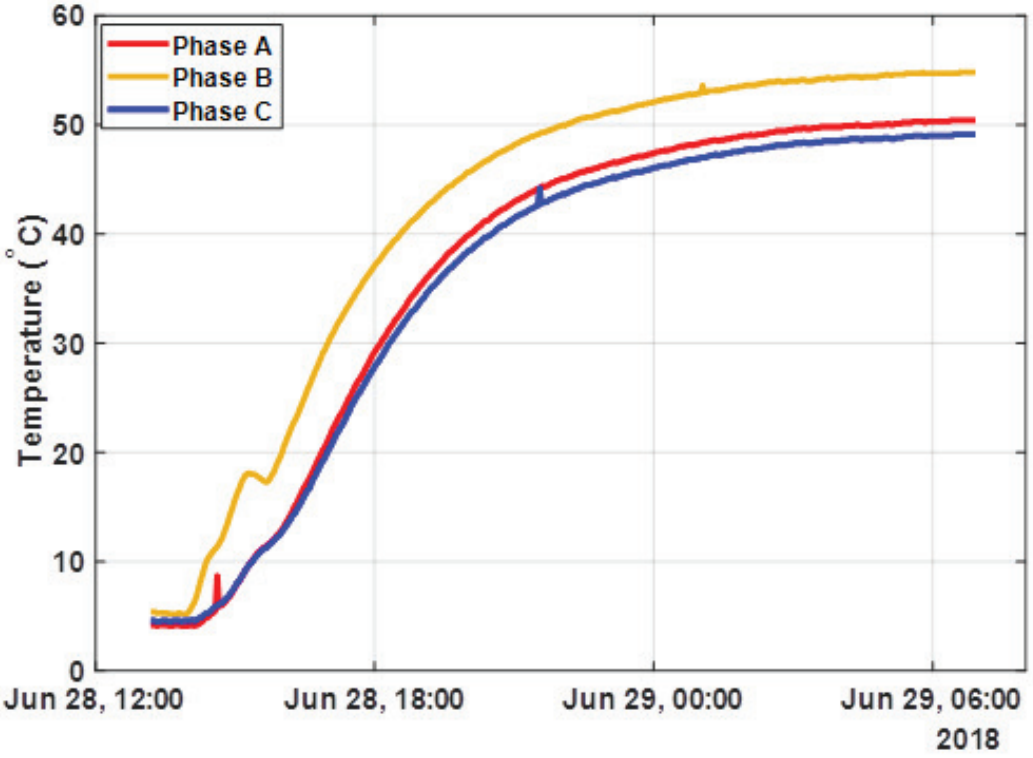

Figure 6.9: Θ_{HS} Heat-Run Data.

The TOT values presented in Fig. 6.8, were captured by a commercially available TOT sensor and validates the accuracy of the DT manufacturer's fibre-optic Θ_{HS} sensor.

6.6 Chapter Summary

This chapter examined the suitability for FBG sensing and its potential realised through the presented development of a transformer "smart supervisory system" for industrial use. The system incorporated remote monitoring utilising Modbus TCP. Self-protection was made possible through integration with the MV switchgear protection circuit breaker. Considerations for determining what DT parameters to monitor to assess health and DT lifetime were discussed. This chapter recommended Θ_{HS}, TOT and DGA as the metrics required to determine both health and lifetime. The actual implementation was discussed and heat-run results presented.

Chapter 7

Conclusion

This thesis examined transformer utilisation, contrasting the impacts of low-utilisation and early retirement with novel strategies to balance the competing requirements of transformer safety and uncompromised lifetime, such as the empirical design method, dynamic DP, and the thermally-based dynamic load management approach.

7.1 Summary of Contributions

In Chapter 4, the empirical design method (EDM) was presented that allows for the design of a distribution transformer whose retirement age coincides with its end of life. The EDM algorithmic process inherently designs for a required transformer lifetime based on the fall of the insulation paper's degree of polymerisation, removing its dependence on accelerated lifetimes based on differing definitions of normal between the IEC and IEEE. Furthermore, EDM has established a range of competing factors from the transformer manufacturer, the operator and IEEE and IEC standards. Because the EDM approach allows for operation above nameplate rating, utilisation is improved, reducing losses and retirement age transformer end-of-life better correlate. Furthermore, the dynamic degree process (DDP) provided both an alternative and enhanced methodology

to determine lifetime in the presence of a predicted increase in base loading.

In Chapter 5, the thermally-based dynamic load management (TD) approach to transformer load management was proposed for the forecasting and processing of unknown loading in a real-time scenario, which allows for the dynamic loading of the transformer beyond nameplate rating without compromising the required lifetime. Experimentation presented showed the initial rise in the hot-spot temperature, Θ_{HS}, was not dependent on the oil time constant, τ_W. However, once the steady-state condition was reached in the windings, the rise was entirely dependent on τ_W. Therefore, the behaviour of the IEC differential thermal model was modified so that the results more accurately reflected the empirical measurements.

7.2 Potential Directions for Future Research

7.2.1 EDM and DDP

Both the EDM and DDP require further investigation to determine whether the processes are best to remain separate use-cases or if they could be streamlined into a single optimal design and in-service assessment process.

There are a number of scenarios that were outside the scope EDM and DDP, such as an optimised strategy and methodology for fittings, such as bushings and switchgear when incorporating them into this new paradigm. All of the strategies presented assumed a fixed-tap setting and focused on the demand, not distributed generation. Voltage rise issues are also problematic, and the algorithms can be further enhanced by including a dynamic voltage management solution such as through the use of an on-load tap changer.

7.2.2 The TD Approach

The TD approach focuses on EV charging, which is presently the most extreme case for dynamic loading. However, it is possible that with further development, the TD approach can assist in managing other loading scenarios, such as reverse power flow and unbalanced loading. This assumes that it is incorporated alongside a sensor-based system, such as the "smart supervisory system" discussed in Chapter 6. The development of such a solution would allow the TD approach to deal with increasingly complex loading and emergency scenarios. For example, if there was a sudden temperature rise due to an oil leak or a severe case of unbalanced loading or reverse power flow.

The TD approach in its current form is only suitable for 3-phase supply, as unbalanced loading is has a level of complexity beyond the time constraints of this research. To ascertain how capable the TD approach is to manage dynamic loading to single-phase chargers, further investigation is required to determine the scope of enhancements to the algorithm or whether it is better served using a more generic approach.

Any future inclusion alongside a transformer monitoring system requires the TD approach to be adapted, so the algorithm is able to extract and process the temperature in real-time to forecast its rise for both the thermal hot-spot and the oil.

7.2.3 Nano and Microgrid Support

All the approaches presented have the potential to incorporate enhanced capabilities to support nano and microgrids. For example, while not explicitly addressing nano and microgrids, a proposal in [162] demonstrated that integrating a battery energy storage system (BESS) into a dynamic loading scenario is a viable concept. Citing the empirical design method and including a customised version of it provided the base for the algorithmic solution to facilitate a BESS-supported dynamic grid. However, the authors acknowledge that cost is a limiting factor for the wide-scale adoption of BESS solutions

in distribution grids. Whereas, for the niche situations offered by nano and microgrids, with BESS often included to facilitate islanding, it is worth examining the benefits such a collaboration between the TD approach and BESS could afford. For example, the TD approach demonstrates how transformers can deal with increased loading. However, they are not capable of sinking voltage rise when loading is low, whereas batteries are ideal in light-loading scenarios. Furthermore, this could be extended to investigate methods for coordination to limit the effects of unbalanced loading and reverse power flow.

The communication between each of the components in nano and microgrids is another significant aspect of consideration for any future development process. Furthermore, if the capability of the transformer monitoring system is such that it can also function as a controller for the nano or microgrid, additional aspects require consideration, as the unit has now effectively become an intelligent electronic device (IED). Such aspects are implementing an appropriate safety integrity level (SIL), ensuring functional safety, according to IEC 61508, long-term reliability, and incorporating control features of IEC 61850, such as generic object-oriented substation event (GOOSE) protocol. However, even if the transformer is not tasked with controlling the grid, providing a meaningful benefit to the system still requires collaboration between the microgrid controller, or in the case of nanogrids, possibly a building management system.

7.2.4 FBG Sensor Enhancement

One final avenue for future work is that presently, only the FBG sensors measuring temperature have any degree of maturity in their development. Therefore, the potential exists for further development of the smart supervisory system to dispense with third-party sensors. For example, the hydrogen monitor included in the existing smart supervisory system, while very capable, is also quite expensive. Our industrial partner,

ETEL, already has prototype hydrogen and moisture FBG sensors developed outside this research. However, significant additional development is required to bring them to a stage where they are suitable for inclusion in a future generation of the monitoring system. In addition, a more compact and integrated solution could be realised utilising FBG fibres as additional fibres take up only a tiny area on a monitoring box. The cost of microcontrollers relative to their performance means there is a wide range of powerful yet inexpensive processors to drive the sensors and compute the algorithms, and the FBG fibres themselves are relatively low cost. This confluence of close integration and lowered-cost technology presents the opportunity to realise a cost-effective, comprehensive load-control and transformer, health and lifetime monitoring system.

References

[1] S. Jeszenszky, "History of transformers," *IEEE Power Engineering Review*, vol. 16, no. 12, pp. 9–, Dec 1996.

[2] J. Coltman, "The transformer [historical overview]," *IEEE Industry Applications Magazine*, vol. 8, no. 1, pp. 8–15, 2002.

[3] S. K. Salman, *Introduction to the Smart Grid : Concepts, Technologies and Evolution*. Stevenage, UNITED KINGDOM: Institution of Engineering and Technology, 2017.

[4] IEEE, "IEEE guide for smart grid interoperability of energy technology and information technology operation with the electric power system (EPS), end-use applications, and loads," *IEEE Std 2030-2011*, pp. 1–126, 2011.

[5] B. P. Das and R. Gopalan, "ETEL smart transformer initiative," in *2016 IEEE Innovative Smart Grid Technologies - Asia (ISGT-Asia)*, Nov 2016, pp. 1031–1036.

[6] B. P. Das, "ETEL smart distribution transformer for electric vehicle applications," in *2018 Condition Monitoring and Diagnosis (CMD)*, Sep. 2018, pp. 1–6.

[7] M. Bunn, B. Seet, C. Baguley, and B. Das, "A smart supervisory system for distribution transformers," in *2018 Australasian Universities Power Engineering Conference (AUPEC)*, Conference Proceedings, pp. 1–6.

[8] IEC, "Power transformers - part 7: Loading guide for mineral-oil-immersed power transformers," *IEC 60076-7:2018*, 2018.

[9] AS/NZS, "Power transformers - part 7: Loading guide for oil-immersed power transformers," *AS/NZS 60076.7:2013*, 2013.

[10] B. Dibner, "Ten founding fathers of the electrical science: I. William Gilbert: On magnets and on electrics," *Electrical Engineering*, vol. 73, no. 4, pp. 306–307, April 1954.

[11] ——, "Ten founding fathers of the electrical science: II. Otto von Guericke: And the first electric machine," *Electrical Engineering*, vol. 73, no. 5, pp. 396–397, May 1954.

[12] R. Gerhard-Multhaupt, "Biographies of contributors to the early investigation of electrical phenomena," *IEEE Transactions on Electrical Insulation*, vol. 26, no. 1, pp. 85–130, Feb 1991.

[13] B. Dibner, "Ten founding fathers of the electrical science: III. Benjamin Franklin: And the universal nature of electricity," *Electrical Engineering*, vol. 73, no. 6, pp. 506–507, June 1954.

[14] I. Falconer, "Charles Augustin Coulomb and the fundamental law of electrostatics," *Metrologia*, vol. 41, no. 5, pp. S107–S114, sep 2004.

[15] R. Cecchini and G. Pelosi, "Alessandro Volta and his battery," *IEEE Antennas and Propagation Magazine*, vol. 34, no. 2, pp. 30–37, April 1992.

[16] B. Bowers, "Volta and the continuous electric current," *Proceedings of the IEEE*, vol. 89, no. 4, pp. 574–576, April 2001.

[17] B. Dibner, "Oersted and the discovery of electromagnetism," *Electrical Engineering*, vol. 80, no. 5, pp. 321–325, May 1961.

[18] C. E. Magnusson, "The centennial of the discoveries of Oersted, Arago, and Ampère," *Journal of the American Institute of Electrical Engineers*, vol. 39, no. 12, pp. 1031–1033, Dec 1920.

[19] R. S. Elliott, "The history of electromagnetics as Hertz would have known it," *IEEE Antennas and Propagation Society Newsletter*, vol. 30, no. 3, pp. 5–18, June 1988.

[20] A. Savini and B. Bowers, "From Oersted to Ampere: 1820, annus mirabilis for the electric sciences [historical corner]," *IEEE Antennas and Propagation Magazine*, vol. 62, no. 5, pp. 138–142, Oct 2020.

[21] M. Guarnieri, "The development of ac rotary machines [historical]," *IEEE Industrial Electronics Magazine*, vol. 12, no. 4, pp. 28–32, Dec 2018.

[22] O. Darrigol, *Electrodynamics from Ampère to Einstein*. OUP Oxford, 2003.

[23] J. C. M. F.R.S., "XIV. on physical lines of force," *The London, Edinburgh, and Dublin Philosophical Magazine and Journal of Science*, vol. 23, no. 152, pp. 85–95, 1862.

[24] O. M. Bucci, "From electromagnetism to the electromagnetic field: The genesis of Maxwell's equations [historical corner]," *IEEE Antennas and Propagation Magazine*, vol. 56, no. 6, pp. 299–307, Dec 2014.

[25] D. Gooding, "Faraday, Thomson, and the concept of the magnetic field," *The British Journal for the History of Science*, vol. 13, no. 2, p. 91–120, 1980.

[26] C. C. Chesney and C. F. Scott, "Early history of the a-c system in America," *Electrical Engineering*, vol. 55, no. 3, pp. 228–235, March 1936.

[27] A. Allerhand, "Early ac power: The first long-distance lines [history]," *IEEE Power and Energy Magazine*, vol. 17, no. 5, pp. 82–90, Sep. 2019.

[28] M. Guarnieri, "The beginning of electric energy transmission: Part one [historical]," *IEEE Industrial Electronics Magazine*, vol. 7, no. 1, pp. 50–52, March 2013.

[29] C. Sulzberger, "Triumph of ac - from Pearl Street to Niagara," *IEEE Power and Energy Magazine*, vol. 1, no. 3, pp. 64–67, May 2003.

[30] A. A. Halacsy and G. H. von Fuchs, "Transformer invented 75 years ago," *Electrical Engineering*, vol. 80, no. 6, pp. 404–407, June 1961.

[31] M. Guarnieri, "Who invented the transformer? [historical]," *IEEE Industrial Electronics Magazine*, vol. 7, no. 4, pp. 56–59, Dec 2013.

[32] H. Willis, *Power Distribution Planning Reference Book, Second Edition*. CRC Press, 2004.

[33] B. Suechoey, J. Ekburanaway, N. Kraisnachinda, S. Banjongjit, and M. Kando, "An analysis and selection of distribution transformer for losses reduction," in *2000 IEEE Power Engineering Society Winter Meeting. Conference Proceedings (Cat. No.00CH37077)*, vol. 3, Conference Proceedings, pp. 2290–2293 vol.3.

[34] Vector, "EV network integration (Green Paper)," Vector Ltd., https://bit.ly/EVGreenPaper, 2019.

[35] A. Sbravati, M. H. Oka, J. A. Maso, and J. Valmus, "Enhancing transformers loadability for optimizing assets utilization and efficiency," in *2018 IEEE Electrical Insulation Conference (EIC)*, Conference Proceedings, pp. 144–149.

[36] M. Lachman, P. Griffin, W. Walter, and A. Wilson, "Real-time dynamic loading and thermal diagnostic of power transformers," *IEEE Transactions on Power Delivery*, vol. 18, no. 1, pp. 142–148, Jan 2003.

[37] M. Humayun, M. Z. Degefa, A. Safdarian, and M. Lehtonen, "Utilization improvement of transformers using demand response," *IEEE Transactions on Power Delivery*, vol. 30, no. 1, pp. 202–210, 2015.

[38] M. R. Dorostkar-Ghamsari, M. Fotuhi-Firuzabad, A. Safdarian, A. S. Hoshyarzade, and M. Lehtonen, "Improve capacity utilization of substation transformers via distribution network reconfiguraion and load transfer," in *2016 IEEE 16th International Conference on Environment and Electrical Engineering (EEEIC)*, Conference Proceedings, pp. 1–6.

[39] A. Bracale, G. Carpinelli, M. Pagano, and P. De Falco, "A probabilistic approach for forecasting the allowable current of oil-immersed transformers," *IEEE Transactions on Power Delivery*, vol. 33, no. 4, pp. 1825–1834, 2018.

[40] M. Djamali, S. Tenbohlen, E. Junge, and M. Konermann, "Real-time evaluation of the dynamic loading capability of indoor distribution transformers," *IEEE Transactions on Power Delivery*, vol. 33, no. 3, pp. 1134–1142, June 2018.

[41] G. C. Jaiswal, P. A. Venikar, M. S. Ballal, H. M. Suryawanshi, and D. R. Tutakne, "Smart transformers for industrial applications," in *2017 IEEE Transportation Electrification Conference (ITEC-India)*, Conference Proceedings, pp. 1–4.

[42] M. S. Ballal, G. C. Jaiswal, D. R. Tutkane, P. A. Venikar, M. K. Mishra, and H. M. Suryawanshi, "Online condition monitoring system for substation and service transformers," *IET Electric Power Applications*, vol. 11, no. 7, pp. 1187–1195, 2017.

[43] K. C. Schneider and R. F. Hoad, "Initial transformer sizing for single-phase residential load," *IEEE Transactions on Power Delivery*, vol. 7, no. 4, pp. 2074–2081, 1992.

[44] N. M. Rao, R. Narayanan, B. R. Vasudevamurthy, and S. K. Das, "Performance requirements of present-day distribution transformers for smart grid," in *2013 IEEE Innovative Smart Grid Technologies-Asia (ISGT Asia)*, Conference Proceedings, pp. 1–6.

[45] AS/NZS, "Electrical installations - known as the Australian/New Zealand wiring rules," *AS/NZS 3000:2018*, 2018.

[46] ANSI, "Electric power systems and equipment - voltage ratings (60hz)," *ANSI C84.1-2016 Standard*, 2016.

[47] C. Z. El-Bayeh, I. Mougharbel, D. Asber, M. Saad, A. Chandra, and S. Lefebvre, "Novel approach for optimizing the transformer's critical power limit," *IEEE Access*, vol. 6, pp. 55 870–55 882, 2018.

[48] D. Martin, Y. Cui, C. Ekanayake, H. Ma, and T. Saha, "An updated model to determine the life remaining of transformer insulation," *IEEE Transactions on Power Delivery*, vol. 30, no. 1, pp. 395–402, 2015.

[49] B. Das, T. S. Jalal, and F. J. S. McFadden, "Comparison and extension of IEC thermal models for dynamic rating of distribution transformers," in *2016 IEEE International Conference on Power System Technology (POWERCON)*, Sep. 2016, pp. 1–8.

[50] T. Oomnen, "Gas pressure calculations for sealed transformers under varying load conditions," *IEEE Transactions on Power Apparatus and Systems*, vol. PAS-102, no. 5, pp. 1278–1284, 1983.

[51] AS/NZS, "Guide to the protection of structural steel against atmospheric corrosion by the use of protective coatings - part 1: Paint coatings," *AS/NZS 2312.1:2014*, 2014.

[52] S. Hajforoosh, M. A. Masoum, and S. M. Islam, "Real-time charging coordination of plug-in electric vehicles based on hybrid fuzzy discrete particle swarm optimization," *Electric Power Systems Research*, vol. 128, pp. 19–29, 2015.

[53] A. Zaidi, K. Sunderland, and M. Conlon, "Impact assessment of high-power domestic ev charging proliferation of a distribution network," *IET Generation, Transmission & Distribution*, vol. 14, no. 24, pp. 5918–5926, 2020.

[54] Ö. Polat, O. H. Eyüboğlu, and Ö. Gül, "Monte carlo simulation of electric vehicle loads respect to return home from work and impacts to the low voltage side of distribution network," *Electrical Engineering*, 2020.

[55] L. Sun and D. Lubkeman, "Agent-based modeling of feeder-level electric vehicle diffusion for distribution planning," *IEEE Transactions on Smart Grid*, vol. 12, no. 1, pp. 751–760, 2021.

[56] H. Patil and V. N. Kalkhambkar, "Charging cost minimisation by centralised controlled charging of electric vehicles," *International Transactions on Electrical Energy Systems*, vol. 30, no. 2, p. e12226, 2020.

[57] F. L. Da Silva, C. E. H. Nishida, D. M. Roijers, and A. H. R. Costa, "Coordination of electric vehicle charging through multiagent reinforcement learning," *IEEE Transactions on Smart Grid*, vol. 11, no. 3, pp. 2347–2356, 2020.

[58] M. E. Kabir, C. Assi, H. Alameddine, J. Antoun, and J. Yan, "Demand-aware provisioning of electric vehicles fast charging infrastructure," *IEEE Transactions on Vehicular Technology*, vol. 69, no. 7, pp. 6952–6963, 2020.

[59] A. M. Sanchez, G. E. Coria, A. A. Romero, and S. R. Rivera, "An improved methodology for the hierarchical coordination of pev charging," *IEEE Access*, vol. 7, pp. 141 754–141 765, 2019.

[60] N. I. Nimalsiri, C. P. Mediwaththe, E. L. Ratnam, M. Shaw, D. B. Smith, and S. K. Halgamuge, "A survey of algorithms for distributed charging control of electric vehicles in smart grid," *IEEE Transactions on Intelligent Transportation Systems*, vol. 21, no. 11, pp. 4497–4515, 2020.

[61] K. Zhou and L. Cai, "Randomized phev charging under distribution grid constraints," *IEEE Transactions on Smart Grid*, vol. 5, no. 2, pp. 879–887, 2014.

[62] H. Xing, M. Fu, Z. Lin, and Y. Mou, "Decentralized optimal scheduling for charging and discharging of plug-in electric vehicles in smart grids," *IEEE Transactions on Power Systems*, vol. 31, no. 5, pp. 4118–4127, Sep. 2016.

[63] E. L. Karfopoulos and N. D. Hatziargyriou, "A multi-agent system for controlled charging of a large population of electric vehicles," *IEEE Transactions on Power Systems*, vol. 28, no. 2, pp. 1196–1204, May 2013.

[64] M. Liu, P. K. Phanivong, Y. Shi, and D. S. Callaway, "Decentralized charging control of electric vehicles in residential distribution networks," *IEEE Transactions on Control Systems Technology*, vol. 27, no. 1, pp. 266–281, 2019.

[65] L. Zhang, V. Kekatos, and G. B. Giannakis, "Scalable electric vehicle charging protocols," *IEEE Transactions on Power Systems*, pp. 1–1, 2016.

[66] IEEE, "IEEE guide for loading mineral-oil-immersed transformers and step-voltage regulators," *IEEE Std C57.91-2011 (Revision of IEEE Std C57.91-1995)*, pp. 1–123, 2012.

[67] M. H. Mobarak and J. Bauman, "Vehicle-directed smart charging strategies to mitigate the effect of long-range ev charging on distribution transformer aging," *IEEE Transactions on Transportation Electrification*, vol. 5, no. 4, pp. 1097–1111, 2019.

[68] P. Andrianesis and M. Caramanis, "Distribution network marginal costs: Enhanced ac opf including transformer degradation," *IEEE Transactions on Smart Grid*, vol. 11, no. 5, pp. 3910–3920, 2020.

[69] M. Soleimani and M. Kezunovic, "Mitigating transformer loss of life and reducing the hazard of failure by the smart ev charging," *IEEE Transactions on Industry Applications*, vol. 56, no. 5, pp. 5974–5983, 2020.

[70] M. Bunn, B. P. Das, B. Seet, and C. Baguley, "Empirical design method for distribution transformer utilization optimization," *IEEE Transactions on Power Delivery*, vol. 34, no. 4, pp. 1803–1813, 2019.

[71] R. Fonteijn, P. H. Nguyen, J. Morren, and J. G. Slootweg, "Demonstrating a generic four-step approach for applying flexibility for congestion management in daily operation," *Sustainable Energy, Grids and Networks*, vol. 23, p. 100378, 2020.

[72] The Department of Energy's Office of Electricity, "The Smart Grid," US Department of Energy, https://bit.ly/3uwO8tl, 2021.

[73] IEC, "Bringing intelligence to the grid," International Electrotechnical Commission, https://bit.ly/3l2KTGJ, 2018.

[74] IEEE, "About IEEE Smart Grid," Institute of Electrical and Electronics Engineers, https://bit.ly/3Fb8Cgc, 2015.

[75] ——, "IEEE recommended practice for network communication in electric power substations," *IEEE Std 1615-2007*, pp. 1–89, 2007.

[76] IEC, "Communication networks and systems for power utility automation — part 1: Introduction and overview," *PD IEC/TR 61850-1:2013*, 2013.

[77] BSI, "Communication networks and systems for power utility automation part 7-2: Basic information and communication structure — abstract communication service interface (acsi)," *BS EN 61850-7-2:2010*, 2010.

[78] IEEE, "IEEE standard for exchanging information between networks implementing iec 61850 and ieee std 1815(tm) [distributed network protocol (dnp3)]," *IEEE Std 1815.1-2015 (Incorporates IEEE Std 1815.1-2015/Cor 1-2016)*, pp. 1–358, Dec 2016.

[79] IEC, "Communication networks and systems in substations — part 2: Glossary," *PD IEC TS 61850-2:2019*, 2003.

[80] ——, "Communication networks and systems for power utility automation — part 90–4: Network engineering guidelines," *PD IEC/TR 61850-90-4:2020*, 2020.

[81] A. Al-Azzawi, *Fiber Optics : Principles and Advanced Practices, Second Edition*. Milton, UNITED KINGDOM: Taylor & Francis Group, 2017.

[82] Josell7, "Total internal reflection," Wikimedia Commons, https://bit.ly/3isstgT, 2015.

[83] FBGS, "FBG principle," FBGS International, https://bit.ly/3uyUatd, 2021.

[84] M. A. Awadallah, B. N. Singh, and B. Venkatesh, "Impact of ev charger load on distribution network capacity: A case study in toronto," *Canadian Journal of Electrical and Computer Engineering*, vol. 39, no. 4, pp. 268–273, Fall 2016.

[85] Q. Gong, S. Midlam-Mohler, V. Marano, and G. Rizzoni, "Study of pev charging on residential distribution transformer life," *IEEE Transactions on Smart Grid*, vol. 3, no. 1, pp. 404–412, March 2012.

[86] D. Susa, M. Lehtonen, and H. Nordman, "Dynamic thermal modelling of power transformers," *IEEE Transactions on Power Delivery*, vol. 20, no. 1, pp. 197–204, Jan 2005.

[87] M. K. Gray and W. G. Morsi, "On the role of prosumers owning rooftop solar photovoltaic in reducing the impact on transformer's aging due to plug-in electric vehicles charging," *Electric Power Systems Research*, vol. 143, pp. 563–572, 2017.

[88] D. Douglass and A.-A. Edris, "Real-time monitoring and dynamic thermal rating of power transmission circuits," *IEEE Transactions on Power Delivery*, vol. 11, no. 3, pp. 1407–1418, July 1996.

[89] S. Walldorf, J. Engelhardt, and F. Hoppe, "The use of real-time monitoring and dynamic ratings for power delivery systems and the implications for dielectric materials," *IEEE Electrical Insulation Magazine*, vol. 15, no. 5, pp. 28–33, Sep. 1999.

[90] M. Jalilian, H. Sariri, F. Parandin, M. M. Karkhanehchi, M. Hookari, M. A. Jirdehi, and R. Hemmati, "Design and implementation of the monitoring and control systems for distribution transformer by using gsm network," *International Journal of Electrical Power & Energy Systems*, vol. 74, pp. 36–41, 2016.

[91] M. Djamali and S. Tenbohlen, "Hundred years of experience in the dynamic thermal modelling of power transformers," *IET Generation, Transmission & Distribution*, vol. 11, no. 11, pp. 2731–2739, 2017.

[92] D. L. Alvarez, S. R. Rivera, and E. E. Mombello, "Transformer thermal capacity estimation and prediction using dynamic rating monitoring," *IEEE Transactions on Power Delivery*, vol. 34, no. 4, pp. 1695–1705, Aug 2019.

[93] Y. Liu, X. Li, H. Li, and X. Fan, "Global temperature sensing for an operating power transformer based on raman scattering," *Sensors*, vol. 20, no. 17, p. 4903, 2020.

[94] D. Tylavsky, Q. He, G. McCulla, and J. Hunt, "Sources of error in substation distribution transformer dynamic thermal modeling," *IEEE Transactions on Power Delivery*, vol. 15, no. 1, pp. 178–185, Jan 2000.

[95] D. Susa and M. Lehtonen, "Dynamic thermal modeling of power transformers: further development-part i," *IEEE Transactions on Power Delivery*, vol. 21, no. 4, pp. 1961–1970, Oct 2006.

[96] ——, "Dynamic thermal modeling of power transformers: further development-part ii," *IEEE Transactions on Power Delivery*, vol. 21, no. 4, pp. 1971–1980, Oct 2006.

[97] Z. Radakovic, M. Jevtic, and B. Das, "Dynamic thermal model of kiosk oil immersed transformers based on the thermal buoyancy driven air flow," *International Journal of Electrical Power & Energy Systems*, vol. 92, pp. 14–24, 2017.

[98] A. A. Taheri, A. Abdali, and A. Rabiee, "A novel model for thermal behavior prediction of oil-immersed distribution transformers with consideration of solar radiation," *IEEE Transactions on Power Delivery*, vol. 34, no. 4, pp. 1634–1646, Aug 2019.

[99] ——, "Indoor distribution transformers oil temperature prediction using new electro-thermal resistance model and normal cyclic overloading strategy: an experimental case study," *IET Generation, Transmission & Distribution*, vol. 14, no. 24, pp. 5792–5803, 2020.

[100] L. Wang, X. Zhang, R. Villarroel, Q. Liu, Z. Wang, and L. Zhou, "Top-oil temperature modelling by calibrating oil time constant for an oil natural air natural distribution transformer," *IET Generation, Transmission & Distribution*, vol. 14, no. 20, pp. 4452–4458, 2020.

[101] J. Ruan, Y. Deng, D. Huang, C. Duan, R. Gong, Y. Quan, Y. Hu, and Q. Rong, "Hst calculation of a 10 kv oil-immersed transformer with 3d coupled-field method," *IET Electric Power Applications*, vol. 14, no. 5, pp. 921–928, 2020.

[102] Y. Deng, J. Ruan, Y. Quan, R. Gong, D. Huang, C. Duan, and Y. Xie, "A method for hot spot temperature prediction of a 10 kV oil-immersed transformer," *IEEE Access*, vol. 7, pp. 107 380–107 388, 2019.

[103] K. S. T. R. Alves, M. Hell, F. L. Cyrino Oliveira, and E. P. de Aguiar, "An enhanced set-membership evolving participatory learning with kernel recursive least squares applied to thermal modeling of power transformers," *Electric Power Systems Research*, vol. 184, p. 106334, 2020.

[104] M. V. Gonçalves da Rocha, M. B. Hell, K. S. T. Rocha Alves, F. L. Cyrino Oliveira, and E. Pestana de Aguiar, "Power transformers thermal modeling using an enhanced set-membership multivariable gaussian evolving fuzzy system," *Electric Power Systems Research*, vol. 194, p. 107088, 2021.

[105] M. Zile, "Temperature analysis in power transformer windings using created artificial bee algorithm and computer program," *IEEE Access*, vol. 7, pp. 60 513–60 521, 2019.

[106] A. Y. Arabul and I. Senol, "Development of a hot-spot temperature calculation method for the loss of life estimation of an onan distribution transformer," *Electrical Engineering*, vol. 100, no. 3, pp. 1651–1659, 2018.

[107] D. Villacci, G. Bontempi, A. Vaccaro, and M. Birattari, "The role of learning methods in the dynamic assessment of power components loading capability," *IEEE Transactions on Industrial Electronics*, vol. 52, no. 1, pp. 280–290, Feb 2005.

[108] J. Yang, X. Bai, D. Strickland, L. Jenkins, and A. M. Cross, "Dynamic network rating for low carbon distribution network operation—a u.k. application," *IEEE Transactions on Smart Grid*, vol. 6, no. 2, pp. 988–998, March 2015.

[109] Y. Li, Y. Wang, and Q. Chen, "Optimal dispatch with transformer dynamic thermal rating in adns incorporating high pv penetration," *IEEE Transactions on Smart Grid*, vol. 12, no. 3, pp. 1989–1999, May 2021.

[110] M. Dong, A. B. Nassif, and B. Z. Li, "A data-driven residential transformer overloading risk assessment method," *IEEE Transactions on Power Delivery*, vol. 34, no. 1, pp. 387–396, 2019.

[111] I. Daminov, R. Rigo-Mariani, R. Caire, A. Prokhorov, and M.-C. Alvarez-Hérault, "Demand response coupled with dynamic thermal rating for increased transformer reserve and lifetime," *Energies*, vol. 14, no. 5, p. 1378, 2021.

[112] N. Viafora, K. Morozovska, S. H. H. Kazmi, T. Laneryd, P. Hilber, and J. Holbøll, "Day-ahead dispatch optimization with dynamic thermal rating of transformers and overhead lines," *Electric Power Systems Research*, vol. 171, pp. 194–208, 2019.

[113] A. Bracale, G. Carpinelli, and P. De Falco, "Probabilistic risk-based management of distribution transformers by dynamic transformer rating," *International Journal of Electrical Power & Energy Systems*, vol. 113, pp. 229–243, 2019.

[114] A. Bracale, P. Caramia, G. Carpinelli, and P. De Falco, "Smartrafo: A probabilistic predictive tool for dynamic transformer rating," *IEEE Transactions on Power Delivery*, vol. 36, no. 3, pp. 1619–1630, June 2021.

[115] Y. Gao, B. Patel, Q. Liu, Z. D. Wang, and G. Bryson, "Methodology to assess distribution transformer thermal capacity for uptake of low carbon technologies," *Iet Generation Transmission & Distribution*, vol. 11, no. 7, pp. 1645–1651, 2017.

[116] G. Rigatos and P. Siano, "Power transformers' condition monitoring using neural modeling and the local statistical approach to fault diagnosis," *International Journal of Electrical Power & Energy Systems*, vol. 80, pp. 150–159, 2016.

[117] G. C. Jaiswal, M. S. Ballal, P. A. Venikar, D. R. Tutakne, and H. M. Suryawanshi, "Genetic algorithm-based health index determination of distribution transformer," *International Transactions on Electrical Energy Systems*, vol. 28, no. 5, pp. 2050–7038, 2018.

[118] T. Rajakanthan, A. Meyer, and B. Dwolatzky, "Computer generated transformer zones as part of township electrification design software," *IEEE Transactions on Power Delivery*, vol. 15, no. 3, pp. 1067–1072, July 2000.

[119] M. A. Tsili, A. G. Kladas, P. S. Georgilakis, A. T. Souflaris, and D. G. Paparigas, "Advanced design methodology for single and dual voltage wound core power transformers based on a particular finite element model," *Electric Power Systems Research*, vol. 76, no. 9, pp. 729–741, 2006.

[120] M. A. Tsili, E. I. Amoiralis, A. G. Kladas, and A. T. Souflaris, "Optimal design of multi-winding transformer using combined fem, taguchi and stochastic-deterministic approach," *IET Electric Power Applications*, vol. 6, no. 7, pp. 437–454, 2012.

[121] C. Hernandez, M. A. Arjona, and S.-H. Dong, "Object-oriented knowledge-based system for distribution transformer design," *IEEE Transactions on Magnetics*, vol. 44, no. 10, pp. 2332–2337, Oct 2008.

[122] C. Hernandez and M. A. Arjona, "An intelligent assistant for designing distribution transformers," *Expert Systems with Applications*, vol. 34, no. 3, pp. 1931–1937, 2008.

[123] M. A. Tsili, A. G. Kladas, and P. S. Georgilakis, "Computer aided analysis and design of power transformers," *Computers in Industry*, vol. 59, no. 4, pp. 338–350, 2008.

[124] Z. R. Radakovic and M. S. Sorgic, "Basics of detailed thermal-hydraulic model for thermal design of oil power transformers," *IEEE Transactions on Power Delivery*, vol. 25, no. 2, pp. 790–802, April 2010.

[125] Y. Zhang, S. L. Ho, and W. Fu, "Applying response surface method to oil-immersed transformer cooling system for design optimization," *IEEE Transactions on Magnetics*, vol. 54, no. 11, pp. 1–5, Nov 2018.

[126] M. Yadollahi and H. Lesani, "Power transformer optimal design using an innovative heuristic algorithm combined with mixed-integer non-linear programming and fem technique," *IET Generation, Transmission & Distribution*, vol. 11, no. 13, pp. 3359–3370, 2017.

[127] L. Alhan and N. Yumuşak, "Discrete design optimization of distribution transformers with guaranteed optimum convergence using the cuckoo search algorithm," *Turkish Journal of Electrical Engineering & Computer Sciences*, vol. 25, no. 5, pp. 4409–4420, 2017.

[128] A. Soldoozy, A. Esmaeli, H. Akbari, and S. Z. Mazloom, "Implementation of tree pruning method for power transformer design optimization," *International Transactions on Electrical Energy Systems*, vol. 29, no. 1, p. e2659, 2019.

[129] ABB, "Total cost of ownership method: Basics of transformer tco calculation," ABB Ltd., http://bitly.ws/gnoK, 2015.

[130] L. P. Di Noia, D. Lauria, F. Mottola, and R. Rizzo, "Design optimization of distribution transformers by minimizing the total owning cost," *International Transactions on Electrical Energy Systems*, vol. 27, no. 11, p. e2397, 2017.

[131] S. Tamilselvi and S. Baskar, "Modified parameter optimization of distribution transformer design using covariance matrix adaptation evolution strategy," *International Journal of Electrical Power & Energy Systems*, vol. 61, pp. 208–218, 2014.

[132] S. Tamilselvi, S. Baskar, L. Anandapadmanaban, K. M. A. Kadhar, and P. R. Varshini, "Chaos-assisted multiobjective evolutionary algorithm to the design of transformer," *Soft Computing*, vol. 21, no. 19, pp. 5675–5692, 2017.

[133] S. Tamilselvi, S. Baskar, L. Anandapadmanaban, V. Karthikeyan, and S. Rajasekar, "Multi objective evolutionary algorithm for designing energy efficient distribution transformers," *Swarm and Evolutionary Computation*, vol. 42, pp. 109–124, 2018.

[134] S. Tamilselvi, S. Baskar, T. Sivakumar, and L. Anandapadmanaban, "Evolutionary algorithm-based design optimization for right choice of transformer conductor material and stepped core," *Electrical Engineering*, vol. 101, no. 1, pp. 259–277, 2019.

[135] M. A. Jarrahi, E. Roshandel, M. Allahbakhshi, and M. Ahmadi, "Cost-optimal as a tool for helping in designing distribution transformer using particle swarm optimization," *COMPEL - The international journal for computation and mathematics in electrical and electronic engineering*, vol. 38, no. 2, pp. 862–877, 2019.

[136] D. Martin, J. Marks, T. K. Saha, O. Krause, and N. Mahmoudi, "Investigation into modeling Australian power transformer failure and retirement statistics," *IEEE Transactions on Power Delivery*, vol. 33, no. 4, pp. 2011–2019, 2018.

[137] F. Weihui, J. D. McCalley, and V. Vittal, "Risk assessment for transformer loading," *IEEE Transactions on Power Systems*, vol. 16, no. 3, pp. 346–353, 2001.

[138] I. Dasgupta, *Design of transformers*. New York, N.Y.: McGraw-Hill Education, 2002.

[139] Time & Date AS, https://www.timeanddate.com/weather/new-zealand/auckland/climate, 2019.

[140] B. Das, S. Phadnis, and T. Syed, "Smart transformer kiosk for Australian and New Zealand utilities," in *EEA Conference and Exhibition 2016*. EEA, Conference Proceedings.

[141] ABB, "Txpert - the world's first digital distribution transformer," ABB Ltd., http://bitly.ws/gnoh, 2018.

[142] N. Lelekakis, D. Martin, and J. Wijaya, "Ageing rate of paper insulation used in power transformers part 1: Oil/paper system with low oxygen concentration," *IEEE Transactions on Dielectrics and Electrical Insulation*, vol. 19, no. 6, pp. 1999–2008, December 2012.

[143] "IEEE standard for requirements for distribution transformer tank pressure coordination," *IEEE Std C57.12.39-2017*, pp. 1–23, May 2018.

[144] L. J. Wang, X. Zhang, R. Villarroel, Q. Liu, Z. D. Wang, and L. J. Zhou, "Top-oil temperature modelling by calibrating oil time constant for an oil natural air

natural distribution transformer," *IET Generation, Transmission & Distribution*, vol. 14, no. 20, pp. 4452–4458, 2020.

[145] W. G. Chen and X. P. Su, "Application of kalman filter to hot-spot temperature monitoring in oil-immersed power transformer," *Ieej Transactions on Electrical and Electronic Engineering*, vol. 8, no. 4, pp. 322–327, 2013.

[146] D. Susa, M. Lehtonen, and H. Nordman, "Dynamic thermal modeling of distribution transformers," *IEEE Transactions on Power Delivery*, vol. 20, no. 3, pp. 1919–1929, 2005.

[147] B. Hampton and D. Medhunst, *The Vapotherm method of measuring directly the temperature of an EHV transformer winding*. CEGB, 1976.

[148] C. Bengtsson, "Status and trends in transformer monitoring," *IEEE Transactions on Power Delivery*, vol. 11, no. 3, pp. 1379–1384, July 1996.

[149] T. C. W. Lampe, B.G. Persson, "Hot-spot and top-oil temperatures proposal for a modified heat specification for oil immersed power transformers," in *International Conference on Large High Tension Electric Systems*. Cigre, Conference Proceedings.

[150] L. Pierce, "An investigation of the thermal performance of an oil filled transformer winding," *IEEE Transactions on Power Delivery*, vol. 7, no. 3, pp. 1347–1358, July 1992.

[151] W. CIGRE, "Direct measurement of the hot-spot temperature of transformers," *CIGRE Electra*, vol. 129, pp. 47–51, 1990.

[152] A. Emsley, "Degradation of cellulosic insulation in power transformers. part 4: Effects of ageing on the tensile strength of paper," *IEE Proceedings - Science, Measurement and Technology*, vol. 147, pp. 285–290(5), November 2000.

[153] T. Dao, "Effects of voltage harmonic on losses and temperature rise in distribution transformers," *IET Generation, Transmission & Distribution*, vol. 12, pp. 347–354(7), January 2018.

[154] IEEE, "IEEE recommended practice for establishing liquid-filled and dry-type power and distribution transformer capability when supplying nonsinusoidal load currents," *IEEE Std C57.110-2008 (Revision of IEEE Std C57.110-1998)*, pp. 1–52, 2008.

[155] B. P. Das and Z. Radakovic, "Is transformer kva derating always required under harmonics? a manufacturer's perspective," *IEEE Transactions on Power Delivery*, vol. 33, no. 6, pp. 2693–2699, Dec 2018.

[156] IEC, "Guide for the sampling of gases and of oil from oil–filled electrical equipment and for the analysis of free and dissolved gases." *IEC 60567:1992*, 1992.

[157] C. Wei-gen, L. Jun, W. You-yuan, L. Liu-ming, Z. Jian-bao, and Y. Yan-feng, "The measuring method for internal temperature of power transformer based on fbg sensors," in *2008 International Conference on High Voltage Engineering and Application*, Nov 2008, pp. 672–676.

[158] M. Kim, J.-H. Lee, J.-Y. Koo, and M. Song, "A study on internal temperature monitoring system for power transformer using pptical fiber bragg grating sensors," in *2008 International Symposium on Electrical Insulating Materials (ISEIM 2008)*, Sep. 2008, pp. 163–166.

[159] A. B. Lobo Ribeiro, N. F. Eira, J. M. Sousa, P. T. Guerreiro, and J. R. Salcedo, "Multipoint fiber-optic hot-spot sensing network integrated into high power transformer for continuous monitoring," *IEEE Sensors Journal*, vol. 8, no. 7, pp. 1264–1267, July 2008.

[160] J.-G. Deng, D.-X. Nie, B.-X. Pi, L. Xia, and L. Wei, "Hot-spot temperature and temperature decay rate measurement in the oil immersed power transformer through fbg based quasi-distributed sensing system," *Microwave and Optical Technology Letters*, vol. 59, no. 2, pp. 472–475, 2017.

[161] ABB, "ABB launches world's first digital distribution transformer," ABB Ltd., http://bitly.ws/gnoE, 2017.

[162] S. Talpur, T. T. Lie, R. Zamora, and B. P. Das, "Maximum utilization of dynamic rating operated distribution transformer (drodt) with battery energy storage system: Analysis on impact from battery electric vehicles charging," *Energies*, vol. 13, no. 13, 2020.